

**DESIGNING OF ENHANCED GAIN APERTURE  
COUPLED DIELECTRIC RESONATOR  
ANTENNA**

**A THESIS**

**SUBMITTED IN FULFILLMENT OF THE REQUIREMENT**

**FOR THE AWARD OF DEGREE OF**

**DOCTOR OF PHILOSOPHY**

**IN**

**ELECTRONICS AND COMMUNICATION ENGINEERING**

**BY**

**DEEPAK BATRA**

**SUPERVISORS**

**DR. SANJAY SHARMA**

**(PROFESSOR)**

**DR. AMIT KUMAR KOHLI**

**(ASSOCIATE PROFESSOR)**



**ELECTRONICS AND COMMUNICATION ENGINEERING DEPARTMENT**

**THAPAR UNIVERSITY, PATIALA-147004 (INDIA)**

**2015**

## CERTIFICATE

I, **Deepak Batra**, hereby declare that the thesis entitled, "**Designing of Enhanced Gain Aperture Coupled Dielectric Resonator Antenna**" submitted to Thapar University, Patiala, in partial fulfilment of the requirement for the award of the Degree of **Doctor of Philosophy in the Electronics and Communication Engineering** is a record of original and independent research work done by me during 2009-2015. This thesis has been conducted under the supervision and guidance of **Dr. Sanjay Sharma**, Professor and Head, Electronics and Communication Engineering Department, Thapar University and **Dr. Amit Kumar Kohli**, Associate Professor, Electronics and Communication Engineering Department, Thapar University. It has not formed the basis for the award of any Degree/Diploma/Associate-ship/Fellowship or other similar title to any candidate of any university.

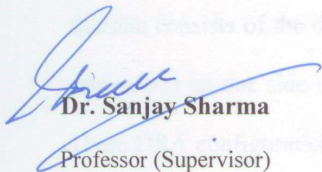


**Deepak Batra**

(Signature of Candidate)

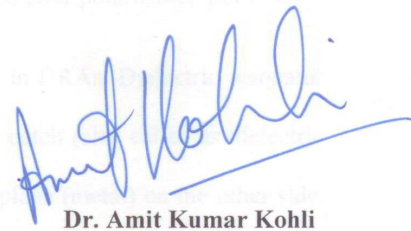
Date:

This is to certify that above statement made by the candidate is correct to the best of my knowledge.



**Dr. Sanjay Sharma**  
Professor (Supervisor)

Electronics and Communication Engg. Deptt.  
Thapar University, Patiala.



**Dr. Amit Kumar Kohli**

Associate Professor (Supervisor)  
Electronics and Communication Engg. Deptt.  
Thapar University, Patiala.

## **ABSTRACT**

Recent advances in the wireless communications have resulted in the development of antennas, which can be embedded into wireless products. For the last three decades, two classes of antennas i.e., the microstrip patch antenna (MPA) and the dielectric resonator antenna (DRA) have been under investigation for the modern wireless communication applications. MPA consists of a radiating patch on one side of the dielectric substrate with a ground plane on other side. MPAs are attractive due to their light-weight, low-profile planar configuration, conformability and low-cost as compared to the conventional antennas. These are highly compatible with embedded antennas in the handheld wireless devices, such as cellular phones and pagers etc. Another area, where the patch antennas have been used successfully, is satellite communication. MPAs radiate primarily because of the fringing fields between the patch edge and ground plane. For appropriate antenna performance, a thick dielectric substrate having a low dielectric constant is used to provide better efficiency, larger bandwidth (BW), and better radiation. But, such a configuration leads to a large antenna size. However, in order to design a compact MPA, higher dielectric constants are used, which are less efficient and result in narrower bandwidth. Moreover, MPAs have various limitations like narrow bandwidth, more metal losses (ohmic losses), low-gain, surface-wave excitation and poor polarization purity etc.

Most of the limitations of patch antenna are removed in DRAs. Dielectric resonator antenna consists of the dielectric materials in its radiating patch (also called as dielectric resonators) on one side of the substrate and has a ground plane (metal) on the other side. These DRA configurations have received great interest in the recent years for its potential applications in the microwave and millimeter-wave communication systems. These have been widely used as a tuning component in the shielded microwave circuits, such as filters, oscillators and cavity resonators. With an appropriate feed arrangement, these can

also be used as antennas, which offer efficient radiation patterns. These are easy to fabricate and offer more degree of freedom to control the resonant frequency as well as quality factor. These offer much wider impedance BW as compared to MPA because microstrip antenna radiates only through two narrow radiation slots, whereas DRAs radiates through its whole surface except the ground part. DRAs can have various three dimensional (3-D) shapes, but cylindrical, hemispherical, and rectangular DRAs (RDRAs) are the most commonly used.

In this research work, we first propose a combination of the slot antenna and the dielectric resonator antenna, which leads to the design of a dual-band dielectric resonator antenna. The resonance of slot and that of dielectric structure gets merged to obtain wide bandwidth over which the antenna polarization and the radiation patterns are preserved. In this design, neither the miniaturization nor the efficiency is compromised. However, the main focus is on the gain as well as bandwidth of the proposed antenna, while preserving the antenna polarization and radiation pattern. The antenna structure is simulated using Ansoft high frequency structure simulator (HFSS). The simulation and experimental results are presented to demonstrate that the proposed RDRA resonates at two frequencies, 5.8 Giga Hertz (GHz) and 8.0 GHz. It exhibits gain advantages of approximately 8.1 dBi and 9.05 dBi and the impedance BW of approximately 340 Mega Hertz (MHz) and 420 MHz, at the two resonance frequencies, 5.8 GHz and 8.0 GHz respectively. In addition, the effects of the size of slot on the radiation characteristics and antenna efficiency are also observed through simulation as well as experimentation. The proposed dual-band DRA has found applications in C- and X-band satellite wireless communication systems.

RDRAs have enormous advantages over the conventional DRA structures. These offer a second degree of freedom, which is one more than cylindrical shape and two more

than hemispherical shape, and these also facilitate the designer to have a greater design flexibility to achieve the desired profile and bandwidth characteristics for a given resonance frequency and dielectric constant. Therefore, these are preferred at millimeter-wave frequencies because of its simplicity in comparison to the cylindrical and hemispherical DRAs. However, the high-profile RDRA with length-to-height ratio less than two have restricted low-profile applications, as these antennas exhibit low bandwidth as well as gain. We next propose a high-gain dual-band DRA mounted with horn, which provides higher gain in comparison to the conventional DRA. Horn is an aperture type of antenna, which is excited by the proposed DRA in the presented work. By using the horn (fabricated using silver metal), the gain of the conventional RDRA is increased at the same resonance frequency, with reduced return loss. The simulation and experimental results are investigated to depict that the gain advantages of the proposed RDRA mounted with horn are approximately 8.95 dBi and 10.65 dBi and the impedance BW values are approximately 315 MHz and 375 MHz at the two resonance frequencies, 5.8 GHz and 8.0 GHz respectively. Therefore, the combination of surface mounted horn and DRA, results in the gain enhancement of approximately 0.85 dBi at 5.8 GHz frequency and approximately 1.6 dBi at 8.0 GHz frequency. However, the usage of horn results in increased cost of antenna fabrication. Therefore, other antenna configurations can also be investigated as an alternative.

We further present the DRA using the electromagnetic band-gap (EBG) technology. The EBG technology is based on the total internal reflection phenomenon of photonic crystal, which is realized by using the periodic structures. EBGs combat surface-waves in the printed antenna boards. A significant amount of energy gets trapped into the substrate resulting in the unwanted surface-wave loss, which if controlled can boost the gain of antenna. However, EBG blocks the surface-waves from propagating in a certain band-

gap. These do not allow the surface-waves to be reflected and interfere with desired radiated waves by grounding such spurious waves. The incorporation of EBG structure in DRA can substantially boost the gain and impedance BW. The simulation results are presented, to illustrate that the proposed hemispherical DRA resonates at 4.39 GHz, which provides a gain of 6.9 dBi and operates at a bandwidth of approximately 250 MHz. The simulation results also show that the hemispherical DRA with EBG structure provides improvement in the gain by approximately 3.7 dB (due to the suppression of related surface-waves). The bandwidth is also increased due to incorporation of EBG structure.

The efficiency and the efficacy of the aforementioned DRAs can be utilized by incorporating these structures in the modern broadband wireless communication systems. Future work includes the testing and performance evaluation of proposed DRA structures in the practical multiple input multiple output (MIMO) and fourth generation mobile communication systems.

## ACKNOWLEDGEMENT

First and foremost, I am beholden to the Almighty and I bow before Him for his umpteen blessings and bestowing in me the grit and confidence to carry out this research work.

I extend my thanks to our Hon'ble Director, **Dr. Prakash Gopalan** and **Dr. O. P. Pandey**, Distinguished Professor and Dean (Research and Sponsored Projects) for giving me this opportunity to undertake the Ph.D. I would like to put on record my heartfelt and sincere gratitude to my research guide **Dr. Sanjay Sharma**, Professor and Head of Department, Electronics and Communication Engineering Department, Thapar University, Patiala and **Dr. Amit Kumar Kohli**, Associate Professor, Electronics and Communication Engineering Department, Thapar University, Patiala. I feel bound to be grateful to both my guiding souls for their valuable and constant support, advice, and encouragement.

I am honor bound and profoundly thankful to the doctoral committee members **Dr. Rajesh Khanna**, Professor, Electronics and Communication Engineering Department, Thapar University, Patiala, **Dr. Kulbir Singh**, Associate Professor, Electronics and Communication Engineering Department, Thapar University, Patiala, and **Dr. Maninder Singh**, Associate Professor, Computer Science Engineering Department, Thapar University, Patiala for their consistent help.

I thank the management of Manav Rachna International University (MRIU), Faridabad, Haryana, India for countenancing me to pursue Ph.D. at Thapar University, Patiala. I am also thankful to **Dr. M. K. Soni**, Executive Director and Dean, FET, MRIU, **Dr. Naresh Grover**, Dean Academics, MRIU, **Dr. Dipali Bansal**, Professor and Head of Department, Electronics and Communication Engineering Department, FET, MRIU for their consistent guidance and support. I would like to extend special thanks to my colleagues and friends **Dr. Sunil Singla**, **Dr. Geeta Nijhawan**, **Dr. Rajeev Ratan**, **Dr.**

**Dharmvir Jain, Dr. Govind Patel, Mr. Tejbeer Singh, Dr. Pawan Kumar, Dr. Abhiruchi Passi and Mr.Yogesh Sachdeva** for their valuable suggestions, support, and encouragement.

It is great privilege to express my profound thankfulness, deep love, and fondness to my wife **Pooja** and my daughter **Lakshita**, who stood like a rock in my difficult times. Their love, patience, persistent encouragement, and good virtuous understanding enabled me to complete the research work successfully.

Finally, I will remain obligated to and filled with appreciation towards my parents **Sh. K. L. Batra** and **Smt. Ganesh Batra** for their love, affection, sacrifices, perseverance, and prayers all through my life.

**Thapar University**  
**Patiala, India.**

**Deepak Batra**

## TABLE OF CONTENTS

	PAGE NO.
<b>CERTIFICATE</b>	<b>(ii)</b>
<b>ABSTRACT</b>	<b>(iii)</b>
<b>ACKNOWLEDGEMENT</b>	<b>(vii)</b>
<b>TABLE OF CONTENTS</b>	<b>(ix)</b>
<b>LIST OF FIGURES</b>	<b>(xi)</b>
<b>LIST OF TABLES</b>	<b>(xiv)</b>
<b>ACRONYMS AND ABBREVIATIONS</b>	<b>(xv)</b>
<b>CHAPTER 1:- INTRODUCTION BASED ON LITERATURE REVIEW</b>	<b>1-32</b>
1.1 Introduction	(1)
1.2 Dielectric Resonator Antenna (DRA) with Various Coupling and Gain Enhancement Techniques	(4)
1.3 Aperture Coupled Rectangular Dielectric Resonator Antenna (RDRA)	(20)
1.4 DRA with Surface Mounted Horn (SMH)	(25)
1.5 DRA with Electromagnetic Band-Gap (EBG) Structures	(26)
1.6 Statement of Problem	(29)
1.7 Organization of Thesis	(31)
1.8 Summary of Chapter	(32)
<b>CHAPTER 2:- DUAL-BAND DIELECTRIC RESONATOR ANTENNA (DRA) FOR C- AND X- BAND APPLICATIONS</b>	<b>33-56</b>
2.1 Introduction	(33)
2.2 Design Model for Proposed Aperture Coupled Rectangular Dielectric Resonator Antenna (RDRA)	(37)
2.3 Formulation and Optimization of RDRA	(39)

2.4	Simulation and Experimental Results with Performance Analysis	(50)
2.5	Summary of Chapter	(56)

**CHAPTER 3:- HIGH-GAIN DUAL-BAND RECTANGULAR DRA (RDRA)**

	<b>WITH SURFACE MOUNTED SHORT HORN (SMSH)</b>	<b>57-81</b>
3.1	Introduction	(57)
3.2	Design Model for Proposed Aperture Coupled RDRA with SMSH	(65)
3.3	Design and Optimization of SMSH	(68)
3.4	Simulation and Experimental Results with Performance Analysis	(72)
3.5	Comparison of Experimental Results for Conventional RDRA and RDRA with SMSH	(78)
3.6	Summary of Chapter	(81)

**CHAPTER 4:- DESIGNING OF HIGH-GAIN HEMISPHERICAL DRA**

	<b>(HDRA) WITH ELECTROMAGNETIC BAND-GAP STRUCTURE</b>	<b>82-100</b>
4.1	Introduction	(83)
4.2	Design and Simulation of HDRA	(90)
4.3	Design and Simulation of HDRA with Cylindrical EBG Structure	(93)
4.4	Simulation Results with Performance Analysis	(96)
4.5	Summary of Chapter	(100)

**CHAPTER 5:- CONCLUDING REMARKS AND FUTURE SCOPE** **101-106**

5.1	Concluding Remarks	(101)
5.2	Future Scope	(105)

	<b>REFERENCES</b>	<b>(107)</b>
--	-------------------	--------------

## LIST OF FIGURES

FIG. NO.	CAPTION	PAGE NO.
Fig. 1.1	Dielectric Resonator Antennas of different geometries (cylinder-type, sphere-type, hemisphere-type, low-profile rectangle-type, triangle-type and circular disk-type DRAs)	(5)
Fig. 1.2	Advancement in shape of DRAs	(5)
Fig. 1.3	Hemispherical shaped DRA (one degree of freedom)	(6)
Fig. 1.4	Cylindrical shaped DRA (two degrees of freedom)	(7)
Fig. 1.5	Rectangular shaped DRA (three degrees of freedom)	(7)
Fig. 1.6	RDRA with microstrip line-feed	(9)
Fig. 1.7	RDRA with coaxial probe-feed	(10)
Fig. 1.8	CDRA with co-planar loop-feed	(11)
Fig. 1.9	RDRA with aperture coupled feed	(11)
Fig. 1.10	RDRA with SIW feed (a) SIW structure (b) Layout of RDRA fed by an aperture on SIW's wall	(13)
Fig. 2.1	Layered structure of proposed aperture coupled RDRA	(38)
Fig. 2.2	Dielectric waveguide (a) Infinite dielectric waveguide (b) Cross-sectional field distribution	(41)
Fig. 2.3	Dielectric waveguide modeled as DRA (a) Truncated dielectric waveguide (b) DRA on ground plane	(42)
Fig. 2.4	Fabricated model of aperture coupled RDRA (top view)	(49)
Fig. 2.5	Fabricated model of aperture coupled RDRA (bottom view)	(49)
Fig. 2.6	Frequency response of RDRA (near field measurement)	(50)
Fig. 2.7	Gain response of RDRA at 5.8 GHz (far field measurement)	(51)
Fig. 2.8	Gain response of RDRA at 8.0 GHz (far field measurement)	(52)

Fig. 2.9	Radiation pattern (E-plane) of RDRA at 5.8 GHz	(53)
Fig. 2.10	Radiation pattern (H-plane) of RDRA at 5.8 GHz	(53)
Fig. 2.11	Radiation pattern (E-plane) of RDRA at 8.0 GHz	(54)
Fig. 2.12	Radiation pattern (H-plane) of RDRA at 8.0 GHz	(54)
Fig. 2.13	Gain v/s frequency plot for RDRA	(55)
Fig. 3.1	RDRA with surface mounted short horn (a) Design model (b) Cross-sectional view	(67)
Fig. 3.2	Fabricated model of RDRA with SMSH (top view)	(71)
Fig. 3.3	Fabricated model of RDRA with SMSH (bottom view)	(71)
Fig. 3.4	Frequency response of RDRA with SMSH (near field measurement)	(72)
Fig. 3.5	Gain response of RDRA with SMSH at 5.8 GHz (far field measurement)	(73)
Fig. 3.6	Gain response of RDRA with SMSH at 8.0 GHz (far field measurement)	(74)
Fig. 3.7	Radiation pattern (E-plane) of RDRA with SMSH at 5.8 GHz	(75)
Fig. 3.8	Radiation pattern (H-plane) of RDRA with SMSH at 5.8 GHz	(75)
Fig. 3.9	Radiation pattern (E-plane) of RDRA with SMSH at 8.0 GHz	(76)
Fig. 3.10	Radiation pattern (H-plane) of RDRA with SMSH at 8.0 GHz	(76)
Fig. 3.11	Gain v/s frequency plot of RDRA with SMSH	(77)
Fig. 3.12	Measured gain response of RDRA with SMSH and without SMSH at 5.8 GHz	(79)
Fig. 3.13	Measured gain response of RDRA with SMSH and without SMSH at 8.0 GHz	(79)
Fig. 3.14	Measured gain v/s frequency plot of RDRA with SMSH and	(80)

without SMSH

Fig. 4.1	Geometry of proposed HDRA	(92)
Fig. 4.2	HDRA surrounded by a cylindrical (mushroom-like) EBG configuration (side view)	(94)
Fig. 4.3	HDRA surrounded by a cylindrical (mushroom-like) EBG configuration (top view)	(94)
Fig. 4.4	Frequency response of HDRA (near field measurement)	(96)
Fig. 4.5	Gain response of HDRA (far field measurement)	(97)
Fig. 4.6	Radiation pattern (E-plane) of HDRA	(98)
Fig. 4.7	Radiation pattern (H-plane) of HDRA	(98)
Fig. 4.8	Gain v/s frequency plot of HDRA	(99)

## LIST OF TABLES

Table 2.1	Parametric values of aperture coupled RDRA	(47)
Table 2.2	Simulation and measured results for RDRA	(55)
Table 3.1	Parametric values of SMSH	(70)
Table 3.2	Simulation and measured results for RDRA with SMSH	(77)
Table 3.3	Comparison of measured results for conventional RDRA and RDRA with SMSH	(80)
Table 4.1	Parametric values of HDRA	(92)
Table 4.2	Parametric values of cylindrical EBG structure	(95)
Table 4.3	Comparison of simulation results for conventional HDRA and HDRA with EBG structure	(99)

## ACRONYMS AND ABBREVIATIONS

2-D	:	Two Dimensional
3-D	:	Three Dimensional
AC-DRA	:	Aperture Coupled Dielectric Resonator Antenna
AC-MPA	:	Aperture Coupled Microstrip Patch Antenna
AC-RDRA	:	Aperture Coupled Rectangular Dielectric Resonator Antenna
BR	:	Back Radiation
BW	:	Bandwidth
CDR	:	Cylindrical Dielectric Resonator
CDRA	:	Cylindrical Dielectric Resonator Antenna
DR	:	Dielectric Resonator
DRA	:	Dielectric Resonator Antenna
DRP	:	Dielectric Resonator on Patch
DWM	:	Dielectric Waveguide Model
EBG	:	Electromagnetic Band-Gap
EM	:	Electromagnetic
EMCP	:	Electromagnetically Coupled Patch
F/B	:	Front-to-Back
GaAs	:	Gallium Arsenide
GHz	:	Giga Hertz
HDR	:	Hemispherical Dielectric Resonator
HDRA	:	Hemispherical Dielectric Resonator Antenna
HFSS	:	High Frequency Structure Simulator
MHz	:	Mega Hertz
MIC	:	Microwave Integrated Circuitry
MIMO	:	Multiple Input Multiple Output
MPA	:	Microstrip Patch Antenna

MSL	:	Microstrip Line
PCB	:	Printed Circuit Board
PIFA	:	Planar Inverted F Antenna
PVC	:	Poly Vinyl Chloride
RDR	:	Rectangular Dielectric Resonator
RDRA	:	Rectangular Dielectric Resonator Antenna
RL	:	Return Loss
SIW	:	Substrate Integrated Waveguide
SMH	:	Surface Mounted Horn
SMSH	:	Surface Mounted Short Horn
TL	:	Transmission Line
UPC-EBG	:	Uni-planar Compact Electromagnetic Band-Gap
UWB	:	Ultra-Wideband
VSWR	:	Voltage Standing Wave Ratio
WLAN	:	Wireless Local Area Network

**INTRODUCTION BASED ON LITERATURE REVIEW**

---

---

**1.1 INTRODUCTION**

Dielectric resonators (DRs) are important components for various communication systems operating at the frequencies in the microwave and millimeter-wave bands. For several years, dielectric resonators have primarily been utilized in the microwave circuitry like oscillators, filtering equipments etc., because of its high quality factor. DRs are usually manufactured using large dielectric constant material, possessing  $\epsilon_r > 20$  [1]. Due to such conventional utilities, dielectric resonators were normally considered as energy storage devices instead of radiating devices [2]. Though open DRs were observed to be radiating long back, but idea of incorporating dielectric resonator as antenna had not been broadly accepted until a formal investigation of DRs as radiating components was conducted in 1980s by Long *et al.* in [3]-[5], who investigated the properties of dielectric resonator antennas (DRAs) with various geometrical shapes like cylindrical, hemispherical and rectangular. Their innovative research demonstrated that the DRA could be considered as a fascinating alternative to the conventional small gain antenna components, like microstrip patches, monopoles as well as dipoles. During systematic study, it was inferred that desired frequency range for different communication systems had moderately progressed towards millimeter and near-millimeter range (100-300 GHz). In this frequency range, conductor loss of metal based antennas appears to be significant and the efficiency of antennas gets alleviated substantially. On the contrary, DRAs can incur only small losses due to the usage of imperfect dielectric material, in practice [2].

Dielectric resonator antenna has enticed many engineers and researchers [6]-[10] due to its innate beneficial properties of low-cost, low-losses, light-weight, compact size,

small surface-wave hazards, simple feeding arrangement and appreciable radiation efficiency because of possessing no conducting material. These can be easily integrated into the prevailing fabrication techniques and exhibit a flexible design procedure with different design attributes, like shape, size, aspect ratios and dielectric constant [11]-[15]. DRA can be fabricated in various shapes; these can be rectangular, cylindrical, hemispherical, etc., which permits more flexibility in the antenna design [16]. Moreover, DRAs can accommodate various types of feed structures. The DR antennas usually have comparatively small permittivity ( $\epsilon_r=10$ ) for radiation boosting. However, the low-profile dielectric resonator antennas of quite large  $\epsilon_r$  are also found to be effective radiating elements in [3]-[5].

DRAs can be easily modified by choosing the adequate dimensions and the appropriate permittivity value of resonating substance. These are simple in fabrication and also offer higher degree of freedom to control the resonance frequency as well as quality (Q) factor. The value of antenna Q parameter [17] is related to the resonating mode (excited) as

$$Q = 4\pi f_0 \left( \frac{\text{Stored Energy}}{\text{Radiated Power}} \right) = Cq \ 4\pi f_0 (\epsilon_r)^P \left( \frac{\text{Volume}}{\text{Surface}} \right)^S \quad (1.1)$$

where,  $f_0$  is resonance frequency and  $\epsilon_r$  is permittivity of resonating material, with  $P > S \geq 1$ . Here, Cq is the proportionality constant. It can be observed from Eq. (1.1) that the increasing value of dielectric constant enhances the value of Q-factor (which is a favourable outcome as far as the resonating material is concerned), but it results in very narrow bandwidth (BW), and therefore limits its usefulness as an antenna [17].

The size of a DR antenna, which is proportional to  $\epsilon_r^{-1/2}$ , decreases with the increasing value of dielectric constant ( $\epsilon_r$ ) of resonator. Hence, the small-size and low-cost antennas can be obtained by using DRs. However, the bandwidth of antenna also

decreases with an increase in the dielectric constant [18]-[19]. Therefore, it is commonly believed that DR antennas with a very high dielectric constant ( $\epsilon_r \geq 20$ ) are not very suitable for the antenna applications. While relatively small dielectric constant ( $\epsilon_r = 10$ ) is conventionally chosen for the DR antenna to enhance its radiation capability. Mongia *et al.* [6] have shown that the rectangular dielectric resonator antennas (RDRAs) of very high  $\epsilon_r$  can also be used as efficient radiators, but at the cost of reduced antenna BW. It is noteworthy that the dielectric constant is not the only factor determining BW of a DR antenna. The other factors influencing the bandwidth of a DRA are its shape and aspect ratio. For example, the numerical results presented in [20] depict that the radiation Q-factor of a cylindrical dielectric resonator (CDR) is approximately reduced by a factor of 4 (from  $\approx 40$  to 10 for a value of  $\epsilon_r = 38$ ), when its aspect ratio (height / diameter) is changed from 0.8 to 0.15. Similar results also hold true for the rectangular dielectric resonators (RDRs) [21]. A substantial improvement in its bandwidth can, therefore, be obtained by appropriately choosing the aspect ratio(s) of resonator. Numerical results reported in [6], [18] suggest that DRs with a very large or small aspect ratio have a smaller radiation Q-factor in comparison to maximum attainable value, which occurs for a moderate value of the aspect ratio. Therefore, the major focus is on the optimum choice of dielectric constant, design parameters and hybrid antenna configurations to improve gain without sacrificing bandwidth.

Next generation communication technology based equipments are tending towards high frequency ranges, which restrict the performance of metal based antennas, as these suffer due to acute conductor loss, weak radiation efficiency and narrower impedance BW. Under such conditions, DRA offers better outcomes. DRAs provide no excitation of surface-waves, decreased conductor loss, higher radiation efficiencies and increased

impedance BW in comparison to the metallic antennas [12], [22]. Hence, DRAs are potentially efficient antennas for the latest high data rate wireless systems.

## **1.2 DIELECTRIC RESONATOR ANTENNA (DRA) WITH VARIOUS COUPLING AND GAIN ENHANCEMENT TECHNIQUES**

DRA is a radio antenna widely utilized in the microwave as well as high frequency ranges, which contains a block of ceramic material of different geometries. This ceramic material, known as DR, is mounted over the metallic surface (ground plane). The microwave radiations are confined inside resonating material due to the sudden change in permittivity at the surface of resonator, which bounce back-and-forth in-between the walls of resonator, conceiving inevitable standing-waves. The walls of DR are partly transparent for radio waves, permitting radio power to get radiated in space. The dielectric constant of the dielectric resonators on DRAs can vary from 2 to 100. A large set of shapes of DRA have been explored in the past three decades, like hemispherical DRAs (HDRAs) [4], [23]-[26], cylindrical DRAs (CDRAs) [3], [27]-[29], RDRAs [5], [30]-[31], triangular DRAs [32]-[33] and other geometries [34]-[36] as shown in Fig. 1.1. However, among these different shapes, cylindrical, rectangular and hemispherical are the most common shapes. These shapes are simple in terms of mathematical formulations and mechanical fabrications. With the advent of time, there has been advancement in the variety of shapes of DRAs being used by the designers for various applications as shown in Fig. 1.2. Tunable dimensions for hemispherical, circular cylindrical and rectangular shapes are one, two and three respectively. For example, with a certain material, once the resonance frequency of an HDRA is determined by the radius, everything else is fixed, including the bandwidth.

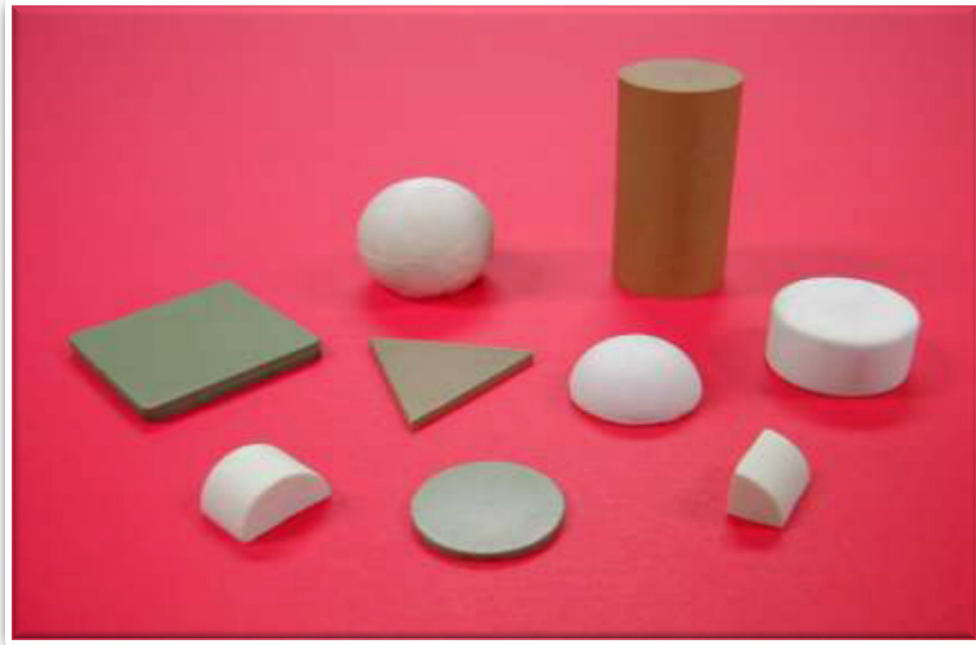
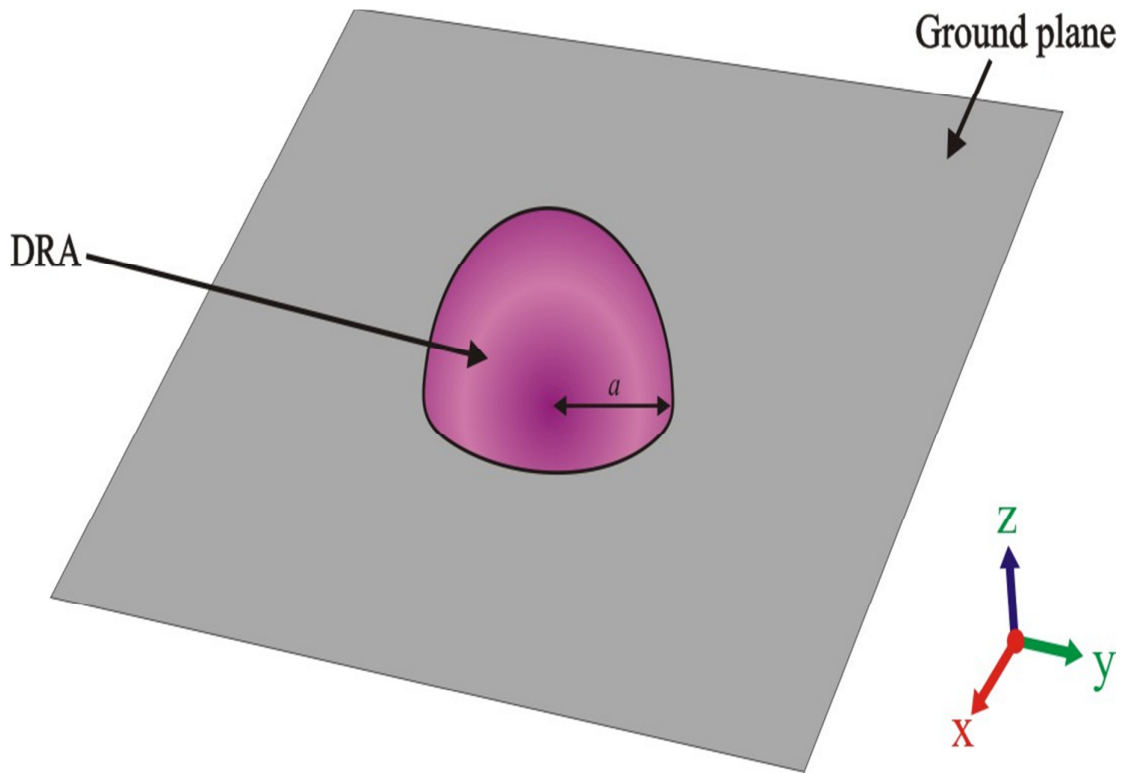


**Fig. 1.1: Dielectric resonator antennas of different geometries (cylinder-type, sphere-type, hemisphere-type, low-profile rectangle-type, triangle-type and circular disk-type DRAs)**



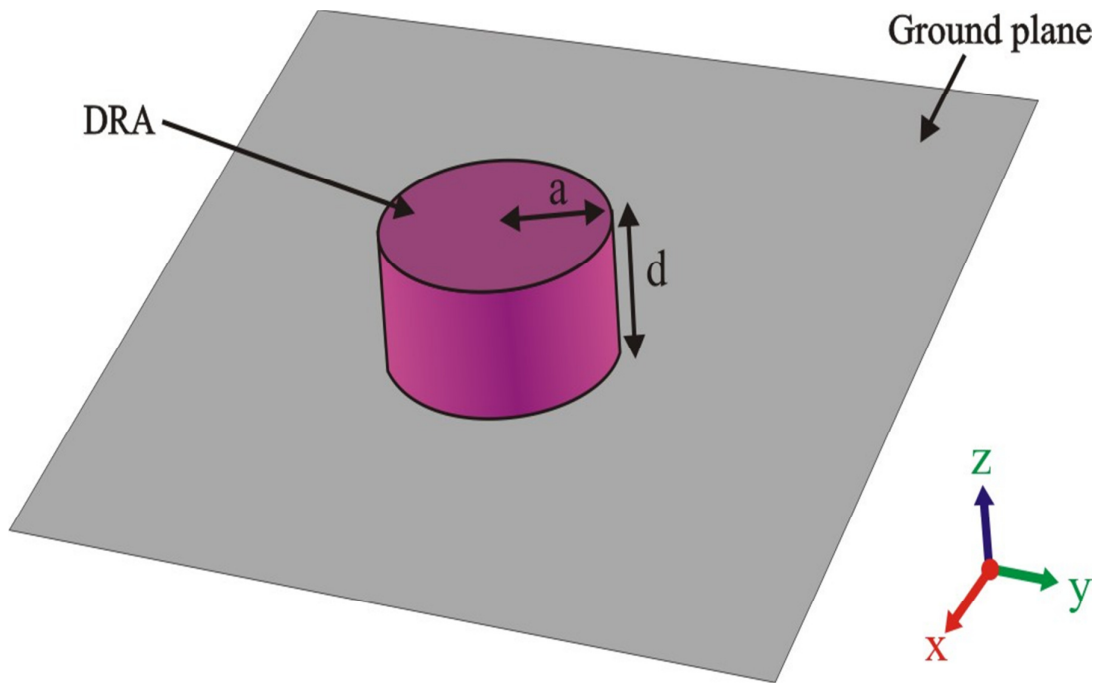
**Fig. 1.2: Advancement in shape of DRAs**

Fig. 1.3 shows the hemispherical shaped DRA. One-dimensional freedom makes HDRAs easy to design, but difficult to optimize for some particular requirements. As a result, HDRAs are, in practice, less frequently used.



**Fig. 1.3: Hemispherical shaped DRA (one degree of freedom)**

On the other hand, because of two degrees of freedom, a circular cylinder resonates at a certain frequency with a number of radius-height pairs. Different pairs may offer different values of bandwidth, directivity and volume occupations. Fig. 1.4 shows the cylindrical shaped DRA. The rectangular shaped DRAs have more benefits over cylindrical and hemispherical shaped dielectric resonator antennas.



**Fig. 1.4: Cylindrical shaped DRA (two degrees of freedom)**

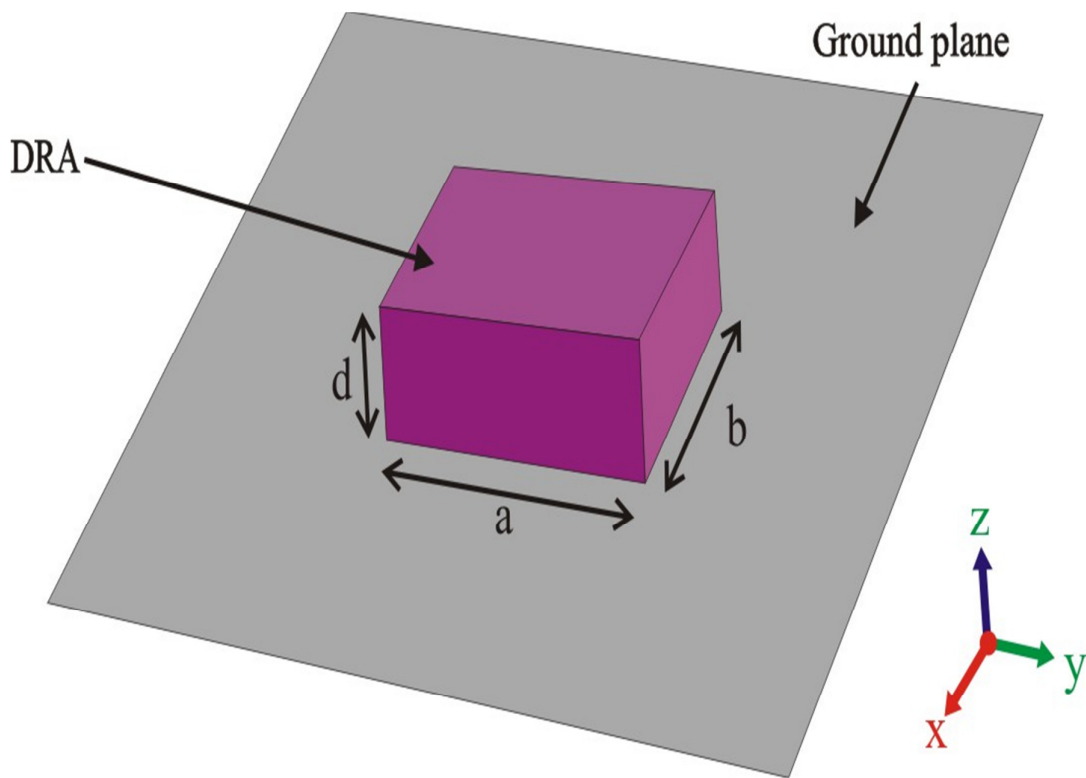


**Fig. 1.5: Rectangular shaped DRA (three degrees of freedom)**

RDRAs offer three degrees of freedom, that is one more than cylindrical and two more than hemispherical shaped DRAs. It provides the designer a greater design flexibility to achieve the desired profile and bandwidth characteristics for a given resonance frequency and dielectric constant. Fig. 1.5 shows the rectangular shaped DRA. Dielectric resonator antennas can be easily coupled to almost all types of transmission lines (TLs). These could be used for a large number of engineering applications as both independent elements and / or in discrete-element array. Dielectric resonator elements are recognized as effective antennas for the wireless communication equipments. DRAs can be simply implemented into the microwave integrated circuitry (MICs), as these are directly fabricated on the printed circuit board (PCB) of communication equipment.

Coupling techniques are required to energize the antenna i.e., to transfer the power into the antenna. Virtually every feeding scheme applicable to microstrip patch antenna (MPA) is compatible with DRA. However, DR antennas can be fed using variety of feed arrangements including coaxial probes [4], [37], microstrip-feed line [38], co-planar feeds [39]-[40] and aperture coupling [41]. Excitation of DRA by using a microstrip line (MSL) is the easiest method of feeding. Fig. 1.6 shows an RDRA coupled to an MSL. In this kind of feeding method, DR is fed by a conducting strip either directly connected to its edge or inserted under it. A common method of excitation with MSL is to use it by proximity coupling. The extent of coupling can be tuned by changing the lateral position of dielectric resonator antenna w.r.t. MSL. The dielectric constant of dielectric resonator antenna also affects the coupling. Higher the value of dielectric constant, higher will be the value of coupling. For the low values of dielectric constant (essential for DRAs demanding large bandwidth), the extent of coupling is usually small [2]. This feeding method is simple, easy to fabricate and provides simple impedance matching. The

spurious surface-waves get boosted with an increment in thickness of substrate of DRA, therefore the thickness of substrate must be kept small [38], [42].

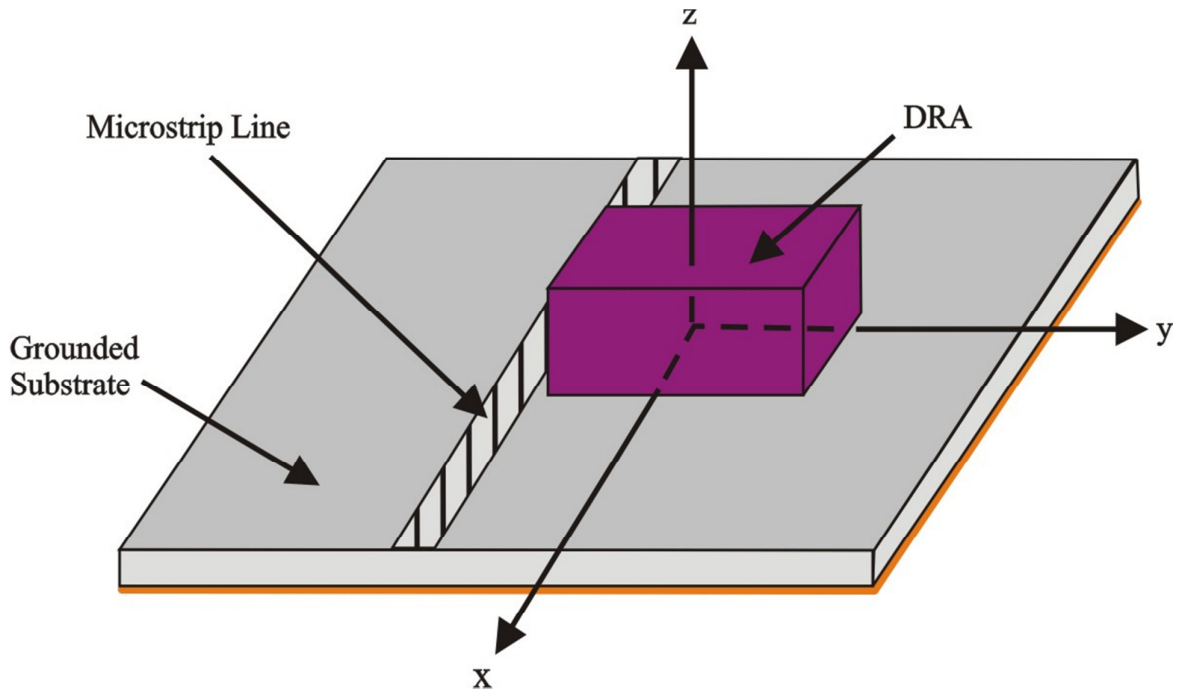


**Fig. 1.6: RDRA with microstrip line-feed**

Coaxial-probe is another commonly used coupling technique for DRA, as shown in Fig. 1.7. The coaxial-probe normally contains a centre pin of the coaxial TL, which extends via ground. However, probe is either located adjacent to DRA or embedded inside it. Coaxial probe adjacent to DRA is preferred, as drilling into DRA is not required in this case [2],[42]. The extent of coupling is optimized by varying height of the probe and location of dielectric resonator antenna. The length of probe is usually selected to be smaller in comparison to height of dielectric resonator antenna, to restrain the probe radiations. Different modes may be excited, which is based on the location of probe. The benefit of coaxial probe excitation is that it can be coupled directly to any 50- $\Omega$  equipment without requiring any matching circuitry [37], [43].

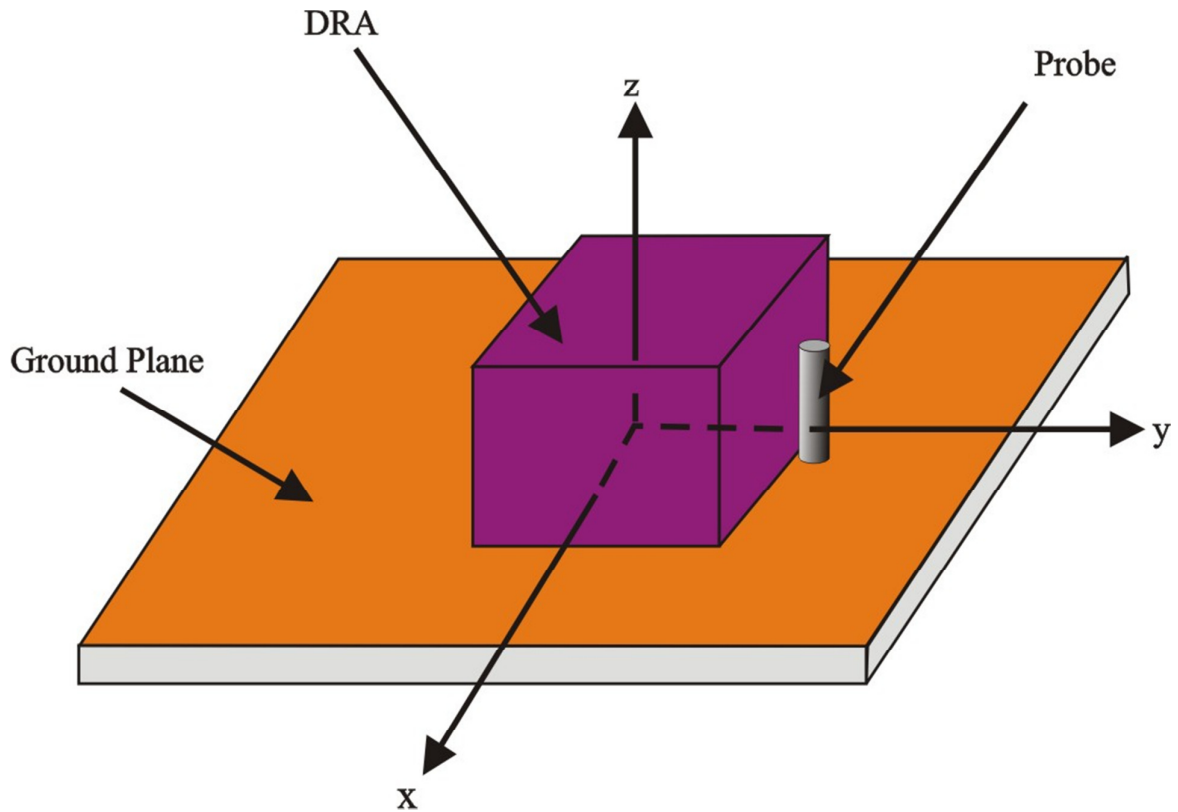


**Fig. 1.7: RDRA with coaxial probe-feed**

However, the coupling to dielectric resonator antennas may also be obtained by using the co-planar feeding technique. Open-circuited waveguides may be utilized to directly feed the dielectric resonator antennas. Moreover, supplementary governance of impedance matching may be obtained due to inclusion of stubs / loops at edge of MSL. Fig. 1.8 depicts a CDRA coupled with a co-planar loop. Further, the extent of coupling may be increased or decreased by adjusting the position of dielectric resonator antenna over the loop and also by adjusting loop position in between edge and centre of dielectric resonator antenna [2],[42]. The dimensions of co-planar feed must be selected quite large to ensure appropriate coupling, but at the same time, small enough to prevent excessive radiations in the back-lobe. The coupling behaviour of co-planar loop is similar to coaxial probe. However, loop provides merit of being non-obtrusive [30], [44].

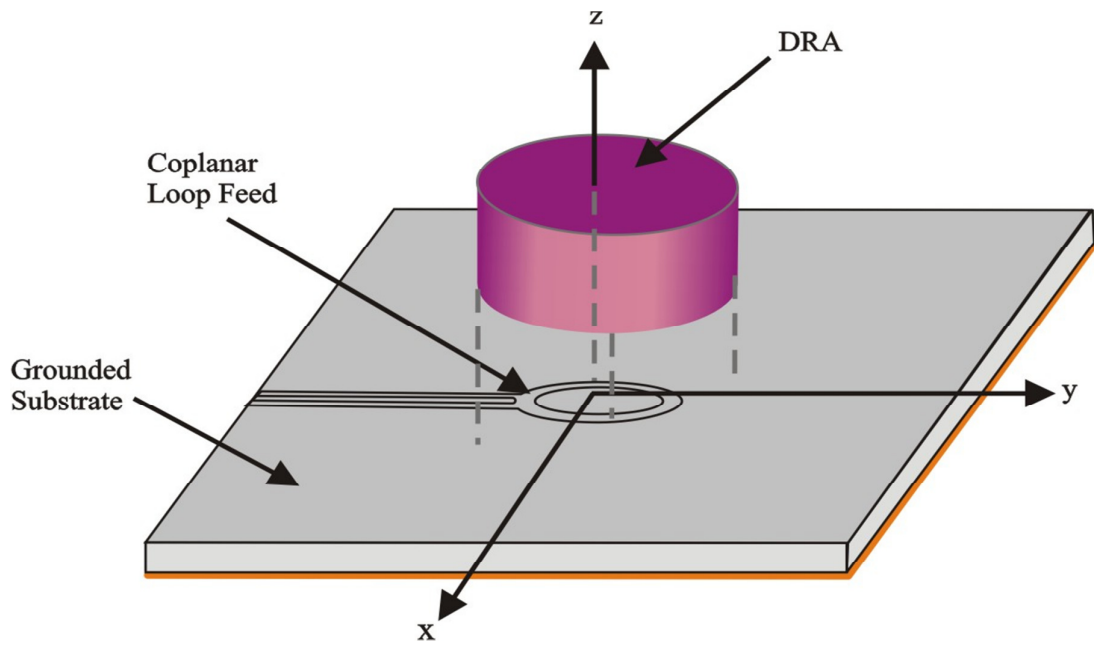


**Fig. 1.8: CDRA with co-planar loop-feed**

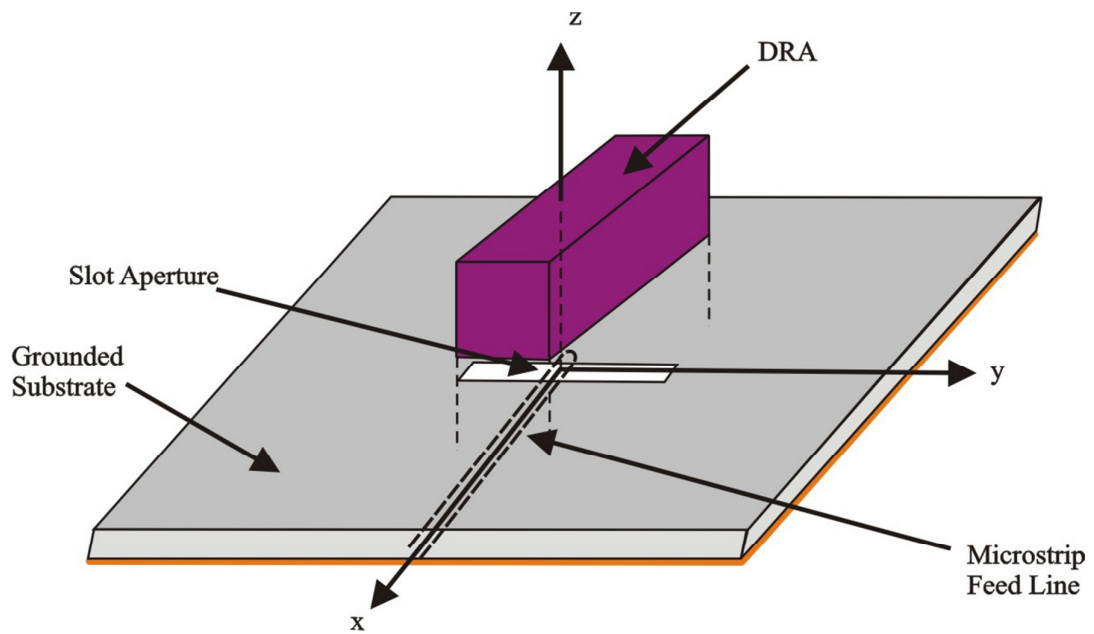


**Fig. 1.9: RDRA with aperture coupled feed**

Fig. 1.9 shows an RDRA fed by an aperture. Aperture coupling is a common technique to feed DRA. In this technique, DRA is excited via an aperture in ground plane. The aperture includes a slot etched in the ground, which is excited by an MSL below the ground plane. Small slot of rectangular shape is most commonly used aperture [42]. Electrically small slot dimensions minimize the radiations below the ground plane. However, substantial extent of impedance matching may be obtained by adjusting position of dielectric resonator antenna w.r.t. the slot. Feeding the aperture by using an MSL is the most popular method, as printed technology is simple to fabricate. Moreover, MSL also offers a degree of impedance tuning, which is unavailable in case of coaxial probes / waveguides [41]. As compared to other coupling schemes, aperture coupled feed has an advantage that physical contact does not exist between the feed and radiator. The feed network is placed beneath the ground plane, which isolates radiating element from undesired coupling and spurious radiations originating from the feeding circuitry [1], [45]. However, these feed techniques are applicable to DRAs of any shape.

Fig. 1.10a shows a substrate integrated waveguide (SIW) having structure similar to a rectangular dielectric-filled waveguide. Two rows of dense metallic vias of very small diameter  $d$  are formed in a substrate, which is metalized on both sides to make the SIW of width  $w$ . The distance between two neighbouring vias is  $s$ . The substrate acts as inner-filled dielectric of a waveguide. Two copper sheets on two sides of substrate are equivalent to two metallic broad walls of waveguide. Two integrated rows of metallic vias are equivalent to the narrow walls of waveguide. Therefore, a current loop is formed using the copper sheets and via holes. Thus, the loss and attenuation of SIW is negligible. The most important feature and unique mark of SIW is the distribution of current through vias. There is no specific direction of surface current on a traditional waveguide whereas

the flow of current in via holes surface is restricted to vertical direction. The side wall current in SIW cannot flow longitudinally because of discrete via holes in SIW [46].

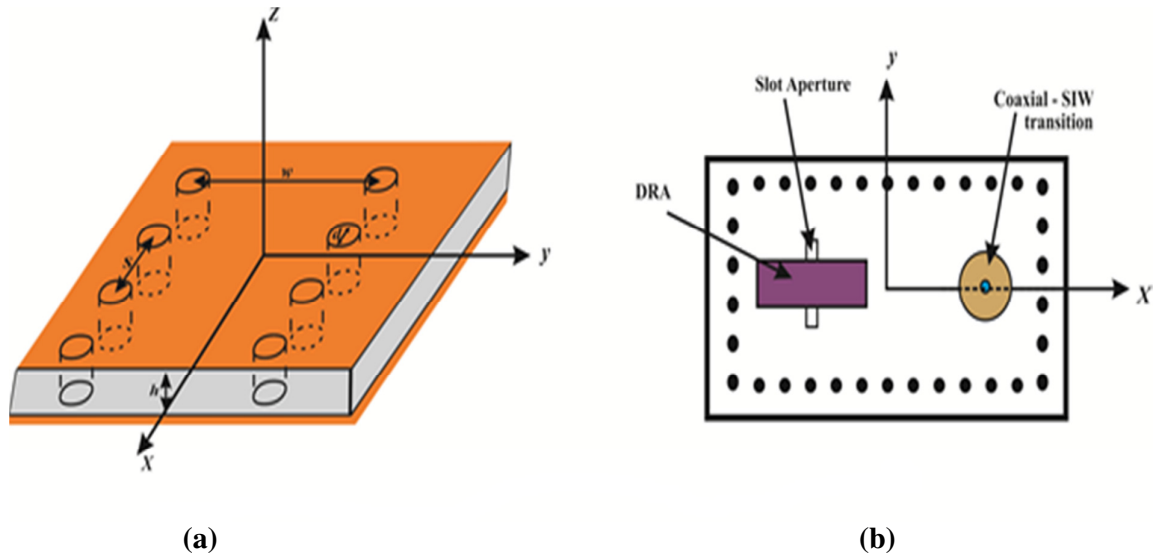


**Fig. 1.10: RDRA with SIW feed**  
**(a) SIW structure [46]**  
**(b) Layout of RDRA fed by an aperture on SIW's wall [47]**

Fig. 1.10b shows an RDRA fed by an SIW. The antenna is excited by introducing a coaxial to SIW transition. SIW feeds the DRA normally by cutting a slot on the SIW wall. The SIW forms transmission lines which are similar to planar printed transmission lines and have performance similar to solid waveguide. Therefore, parasitic radiation and radiation loss can be minimized and a low-profile, low-cost, and compact solution can be obtained at the millimetre frequency range [47].

Since metal is used to cover the SIW and the substrate has restricted number of feeding fields, the shielding of the SIW is brilliant between external and internal surfaces. Therefore, SIW minimizes the parasite radiation and radiation loss of the feeding structure. In addition, Q-factors of the SIW are large and the loss of DRA is minimum in the millimetre frequency range. Thus, communication systems can prominently utilize the SIW-fed DRA for low-loss millimetre frequency range. Moreover, this feeding scheme is

becoming popular because of ease in fabrication, low-profile, and less cost. This feeding scheme has been used by many researchers in designing of dielectric resonator antennas at millimetre wave frequency range [48]-[50].

DRAs are mainly fabricated for high frequency applications. But its gain needs to be enhanced further, as it is not sufficient in many of the engineering applications. Over the years, various techniques have been proposed to modify gain of dielectric resonator antennas. Anybody may utilize two or more uniformly distributed elements to form the antenna-array [51]. These arrays have been successfully incorporated in different communication equipments for long time, though these still suffer due to a few fundamental hazards. Most prominent drawback is their complex and lossy feeding structures. But, mutual coupling phenomena have restricted their applications to some extent [52]-[54].

Another technique for gain enhancement is to reduce the back radiations (BRs) of the antenna. Back radiations are the unwanted radiations, which antenna radiates in backward direction (opposite to the desired direction) in addition to radiations in the desired direction. Targonski *et al.* [55] have presented a broadband eight-element aperture coupled microstrip patch antenna (AC-MPA) linear array by utilizing reflecting elements. Patterns for these two configurations, a single element as well as full array, at 5.3 GHz are demonstrated with reflector elements in place and also for reflector elements out of place. The back-lobe reduction effect is illustrated to be more significant in antenna-array configuration as compared to single element. In the absence of reflecting elements, good amount of back-lobe radiations exist, but these are substantially lowered due to incorporation of these reflecting elements. However, analogous lowering in amount of BR occurs across whole bandwidth. The front-to-back (F/B) ratio more than 20 dB is obtained in frequency range 5.2 GHz - 6.8 GHz.

Targonski *et al.* [55] have successfully reduced the back radiations, but the enhancement in the gain is not reported. Kirov *et al.* [56] have proposed a three-layer configuration with a screen to enhance antenna gain by decreasing backward radiations. A wideband circularly polarized AC-MPA is detailed in [56]. The higher BR level is restricted due to a metal screen. The metallic screen is found to reflect antenna back radiations in the direction of primary EM energy flux i.e., in desired direction of radiation, improving its gain. Consequently, BR of antenna gets alleviated by approximately 12 dB, while its gain is enhanced by approximately 1.3 dB, in comparison to traditional double-layer AC-MPA. This antenna is designed to work in frequency range of Ku-band. A comparison of three similar circularly polarized antennas with resonant slots is accomplished. First antenna is a two-layer AC-MPA, second antenna is a three-layer AC-MPA with a screen and the third antenna is a three-layer AC-MPA in combination with a reflecting patch. This reflector with square geometrical shape is centered below the radiation patch. However, three substrates are utilized in this structure: a) patch substrate, b) feed substrate and c) screen or reflector substrate. The gain of two-layer AC-MPA is 4.9 dBi. The patch reflector boosts antenna gain by approximately 0.3 dB (from 4.9 dBi to 5.2 dBi). At the same time, screen enhances antenna gain by approximately 1.3 dB (from 4.9 dBi to 6.2 dBi).

Kirov *et al.* have enhanced the gain of microstrip antenna by using a reflector and a screen in [56], but the gain enhancement is only 1.3 dB. Waterhouse *et al.* [57] have proposed a wideband millimeter-wave MPA array with low back radiations by making use of a reflector. The proposed technique uses an MPA element on the back side of MSL-fed aperture, which acts like a reflecting element. This antenna contains eight-element linear antenna-array of aperture-stacked patches and corresponding eight back patches. The reflecting element is deliberately made to work at a frequency higher than its

resonating frequency. The printed antenna encompasses a slot in ground plane excited by an MSL along with stacked-patch structure. A reflector patch is positioned on feeding side of ground plane of antenna. The reflecting patch is segregated from MSL by using a substrate of low permittivity. The incorporation of reflecting patches not only modifies F/B ratio to approximately 30 dB over complete  $Ka$ -band, but also enhances antenna gain by 2 dB. This concept of metallic reflector (used by the researchers Targonski *et al.* [55], Kirov *et al.* [56] and Waterhouse *et al.* [57] to increase the gain of MPA by decreasing the back radiations) is equally applicable for the DRAs as well.

In [55]-[57], significant efforts have been made to enhance the antenna gain by reducing backward radiations with the help of metallic reflector. But the gain enhancement using this method is not very high (at the most 2 dB). An alternative method to achieve higher gain is to use composite layer DRs. A hike in the value of DR permittivity reduces the antenna radiation efficiency [58]. The loss in radiation efficiency of antenna (in case of high dielectric constant) may be recovered by coating it with single layer of high permittivity substance. This scheme of using high dielectric constant substance for gain improvement is demonstrated by Hwang *et al.* in [59] for a planar inverted F antenna (PIFA). Enhanced gain of a PIFA loaded with a very high permittivity substrate has been demonstrated. Three antennas are designed for the comparison purpose. The first antenna is a conventional air PIFA, and it is used as a reference. The second antenna is a loaded PIFA with a single-layered substrate of  $\epsilon_r = 38$  without a covered superstrate. In third antenna, which is the proposed one, the planar element on a substrate of  $\epsilon_r = 38$  is covered by a superstrate of  $\epsilon_r = 80$ . The authors have demonstrated that a DRA, which is normally designed for the microwave and millimeter-wave frequency applications, can be extended for the use in lower frequency bands. All three antennas are designed at 1.8 GHz frequency band (allocated to the personal

communication networks). It is shown that the size of planar element loaded with a very high permittivity substrate is reduced by approximately four times. The measured impedance BWs are 90 MHz for the conventional air-filled antenna, 19.5 MHz for the simple loaded antenna and 18 MHz for the proposed antenna. The loading of PIFA with a high permittivity material has reduced the impedance BW from 5% to 1%. The proposed PIFA has a net relative power increment of 10.2 dBm in comparison to the simple dielectric-loaded PIFA.

The concept of usage of large dielectric constant substance for gain improvement of PIFA is extended to DRA gain enhancement by Antar *et al.* in [60]. The proposed structure is designed to resonate at 1.8 GHz frequency. Here, two aperture coupled dielectric resonator antennas (AC-DRA) are designed, manufactured as well as tested. One antenna consists of single-layer configuration of large dielectric constant ( $\epsilon_r = 38$ ) substance, whereas other consists of two-layer structure fabricated using large dielectric constant ( $\epsilon_r = 38$  and 80) substances. The heights of concerned DRs are 7.62 mm and 5.71 mm for single- and two-layer antennas respectively. Further, rectangular slot is utilized to couple energy from an MSL to RDR. The resonance frequency of both DRs is measured to be 1.796 GHz. The impedance BW measurement is 57.5 MHz (3.2%) for antenna consisting of single-layer. But, it is alleviated to 46.3 MHz (2.7%) for two-layered antenna. It provides 1.2 dB gain advantage and 25% height decrement in comparison to aperture coupled rectangular dielectric resonator antennas (AC-RDRA) with single-layer of large dielectric constant ( $\epsilon_r = 38$ ) substance. The gain measurement is 5 dBi for DRA with single-layer and 6.2 dBi for DRA with two layers. It is demonstrated that DRA with two layers provides not only height lessening, but it also provides gain enhancement.

However, attempts are put to enhance gain of dielectric resonator antenna using the composite layer DRs in [60]. But it has been noticed that impedance BW is decreased with an increasing value of the gain of antenna. An alternative method to increase the gain of DRA without any adverse effect on impedance BW is to use the concept of stacked DRs. This concept was originally used by Luk *et al.* in [61] to enhance gain as well as bandwidth of an MPA, in which properties of dual-patch rectangular AC-MPA with an air-gap in-between substrates supporting two patches are analysed practically. Leung *et al.* [62] have investigated experimentally offset dual-disk AC-DRA with large dielectric constant [7]. Authors have used concept of offset dual-antenna to modify gain and bandwidth of low-profile circular disk-type DRA of large  $\epsilon_r$  in [62]. It is apparent that this structure provides an impedance BW 4.6 times larger than that of antenna with one element. The DRA resonates at 4.36 GHz, and it is excited using slot-coupling. The effects of the offset and air-gap in-between fed and parasitic elements have been explored further. A rectangular slot couples energy from an MSL to two similar circular dielectric resonator disks of dielectric constant  $\epsilon_r = 82$ . There is air-gap with thickness 's' between fed and parasitic elements. Impedance BW and maximum antenna gain are measured at three dissimilar values of s i.e., s = 2 mm, s = 3 mm and s = 5 mm. For s = 2 mm, the impedance BW is modified from 3.9% (one element) to 6% and maximum antenna gain has increased from 5 dBi (one element) to 7.4 dBi. For s = 3 mm, impedance BW is increased to 12% and maximum antenna gain has increased to 7.4 dBi. For s = 5 mm, the impedance BW is increased to 18% and maximum antenna gain has increased to 7.7 dBi.

Leung *et al.* have made the attempts to increase the gain of DRA without any adverse effect on bandwidth, using the concept of stacked DR, in which two identical circular DR disks of high dielectric constant are used [62]. Using this concept, gain enhancement is

higher in comparison to the aforementioned two methods (using reflector on the back side of antenna [55]-[57] and using composite layer DRs [59]-[60] to enhance gain of DRA. Moreover, high-gain is achieved without any adverse effect on the impedance BW. But, this structure is not suitable for the high-gain requirements because the separation between fed and parasitic elements (which is an air-gap) should be large to achieve high-gain. Consequently, the overall thickness of antenna becomes large and the antenna structure is no longer planar. An alternative scheme to enhance gain of DRA is to use parasitic overlays. It is noteworthy that Lee *et al.* [63] and Afzalzadm [64] have reported substantial enhancement in the gain of bare MPAs with parasitic overlays, which has encouraged authors for this study and research. In [63], Lee *et al.* have proposed two different rectangular microstrip antennas:

- a) with one overlaying parasitic patch (two layers of electromagnetically coupled patches (EMCPs)),
- b) with two overlaying parasitic patches (three layers of EMCPs).

For comparison purpose, the gain and radiation patterns of a single microstrip patch without any parasitic patch is also measured. Teflon spacers are used to vary the element spacing between each of the two layers. The measured gain for the single patch is 4.7 dBi, as compared to 8.4 dBi for the two-layer and 10.6 dBi for the three-layer EMCP antennas. There is a gain improvement of 3.7 dB with single parasitic patch and 5.9 dB with the two parasitic patches. Further increase in gain is possible with additional parasitic directors. Using the concept of Lee *et al.* [63] and Afzalzadm [64] for the gain enhancement in microstrip antennas, Hakkak *et al.* [65] have presented an experimental study for the gain enhancement of DR loaded probe-fed circular waveguide antennas using overlapping parasitic disks (dielectric directors). The dielectric disk is selected to have  $\epsilon_r = 8$  and also fix the physical attributes corresponding to the resonating frequency of 11 GHz.

Here, disk is fed through probe-feed. When parasitic element is located over the waveguide aperture, a significant enhancement in forward gain is achieved. When another parasitic element is added, marginal modification in gain is further noticed. However, it may be inferred from the results that when appropriately spaced, single overlay can modify gain by 6 dB; and gain modification of approximately 7 dB can be achieved in bandwidth of at least 10%, when the directors are used.

An effort has been made to boost gain of DRA with the help of parasitic overlays with single director and two directors in [65]. But this configuration is quite long, and hence unsuitable for the compact antenna applications. As an alternative, two techniques can be used, which are commonly incorporated for the gain enhancement of antennas without any adverse effect on bandwidth. First technique is to use electromagnetic band-gap (EBG) structures. EBG configurations help in reducing the losses due to the presence of surface-wave propagation, which can generate ripples in radiation patterns [66]-[67]. The removal of surface-waves results in modification in peak gain, when DRA or an MPA is placed above one of these EBG surfaces. Second method for the antenna gain enhancement is by using surface mounted horn (SMH), which confines the EM field on / in the vicinity of radiating antenna and it also provides isolation of antenna-array elements [11]. Both of these techniques are discussed in subsequent sections in detail.

### **1.3 APERTURE COUPLED RECTANGULAR DIELECTRIC RESONATOR ANTENNA (RDRA)**

Latest wideband communication equipments and radars need light weight small antennas exhibiting large-gain and broad bandwidth. MPA is a famous choice for the microwave scanned antenna-array equipments. These provide low-profile, light-weight, and low-cost designs, which may be easily incorporated in the microwave circuitry. But, disadvantages

of patch antennas are severe ohmic losses and narrow impedance BW at the microwave frequencies [68]. DRAs are being used as an alternative to the MPAs at microwave frequencies (where ohmic losses become a severe problem for traditional metal antennas) because these provide low conductor losses, significant improvement in mechanical simplicity, wider range of dielectric materials, higher power capabilities and increased impedance BW [12], [22]. Dielectric resonator antennas possess relatively higher bandwidth (approximately 10% at  $\epsilon_r \approx 10$ ), however MPAs exhibit bandwidth of only 1% to 3%. DRA can be versatile in shape and supports a variety of feeding techniques. The different antenna characteristics like input impedance, bandwidth as well as beam patterns may be controlled through adjustment of permittivity value, physical attributes of DR and feed techniques [69].

Different geometries of DRAs have been explored in the last three decades, like hemispherical, cylindrical, rectangular and triangular etc. In comparison to other geometries, the rectangular resonators are more attractive for its fabrication advantages and also because of the existence of two independent aspect ratios (height / length and width / length) for better design flexibility to meet the impedance and radiation requirements. Its two dimensions may be tuned independently for a selected value of resonance frequency and for a particular material permittivity [70]. In case of RDRA, the resulting antenna characteristics like bandwidth, resonance frequency and radiation pattern may be conveniently controlled through adjustment of aspect ratios [71]. Moreover in RDRAs, mode degeneracy can be precluded by appropriately selecting its three dimensions. However, the mode degeneracy comes into picture in case of spherical-type DRA and in hybrid modes of CDRAs, which results in the lower cross polarization, and hence limits the antenna performance [70], [72]. CDRAs have been widely used in most of the applications at the microwave frequencies. However at millimeter-wave

frequencies, it becomes difficult to fabricate the CDRAAs owing to its small-size. Therefore at these frequencies, RDRAAs are preferred over the CDRAAs [73].

The DRA is usually presented as a better alternative to an MPA, but for a fair comparison, the DRA has to have a low-profile. However to have a low-profile, DRA is to be made out of very high-permittivity material. In [74], Esselle has presented a very low-profile RDRA with a length-to-height ratio of about six using a medium permittivity material of  $\epsilon_r=10.8$ . Rezaei *et al.* [75] have analysed a novel two-segment RDRA for the size reduction and broadening of the impedance BW. This structure consists of two rectangular dielectric sections separated by a metal plate. As compared to a DRA, this configuration offers a substantial size alleviation of approximately 41.5% in volume because of the extra metallic plate, which behaves like the electric wall. In addition to size reduction, designed antenna illustrates more than 76.8% impedance BW at 3.32 GHz - 7.46 GHz frequency band.

Although the bandwidth offered by DRA is large as compared to an MPA, but still there is a need to enhance its bandwidth, as required in many applications. The inclusion of lateral parasitic DRs improve the antenna BW [76], but at the cost of increased area. On the other hand, the antenna BW can be significantly increased, without significant change in the area, by replacing the DRA with a dielectric resonator on patch (DRP) element [77]. The DRP encompasses microstrip patch resonating element and DR. The DRP antenna exhibits a large bandwidth because of two resonances: a) resonance of dielectric resonator, b) resonance of patch. The pair of two resonating materials, that resonate at different frequencies, provides large impedance BW. With DRP antenna configuration, which has a symmetrical vertically stacked resonator arrangement, the same performance can be achieved without significantly increasing the footprint. Esselle *et al.* used this special type of a hybrid-resonator antenna (DRP antenna) in [78] to extend

the bandwidth of DR. The patch resonator and dielectric resonator are coupled by a slot (upper slot) in the microstrip patch. The rectangular hybrid-resonator structure is fed by an MSL through a second (lower) slot in its ground. The dielectric constants of the patch and feed substrates are 2.2 and 10.2 respectively. The results indicate a very wide bandwidth 23.5% (5.14 GHz - 6.51 GHz) because of DRP antenna.

The feeding technique for any antenna is an important parameter because it affects the bandwidth and other parameters. DRAs are fed through various feeding techniques, which include coaxial probes, MSL feed, aperture coupled feed and co-planar feed [44]. Aperture coupling is an indirect feeding technique for antenna systems. Here, MSL is coupled with microstrip slot antenna via an aperture. The energy of MSL is coupled through a slot in its ground plane, which excites the radiating element. If an appropriate combination of the shape of feeding element and slot is selected and adjusted efficiently, it provides an optimum impedance BW with a modified radiation pattern. There are two coupling mechanisms, which take place: a) between MSL and slot, b) between slot and radiating antenna [79]. The aperture coupling scheme was pioneered by Pozar in [80] for patch antennas, and then it was used by Martin in [41] for a CDRA. The aperture coupled feed has the advantage that feed and radiator have no physical contact in-between both. Hence, it isolates the dielectric resonator antenna from active circuitry, and meanwhile completely makes use of the feed substrate for the active circuit integration. It can broaden the impedance BW considerably by isolating the spurious feed radiations from the antenna component and providing much space to a feeding network. The single layer probe or MSL-fed elements are particularly restricted to bandwidths of 2% to 5%. On the other hand, the results in [81]-[86] illustrate that the aperture coupled elements possess bandwidths up to 10% to 15% for a single layer structure and up to 30% to 50% for a stacked patch structure. For optimum coupling, feed line must be centered across the

aperture and the radiating element must be centered over aperture. The geometrical shape of coupling aperture has a substantial impact on the level of coupling between MSL and radiating element. However, thin rectangular-type coupling slots have been utilized in a large number of aperture coupled antennas, because these provide relatively more coupling than round apertures. The coupling strength is mainly determined by slot length. Therefore, slot must not be made larger than, which is needed for impedance matching. The coupling strength is also affected by the width of slot, which is very low in comparison to the slot length [45].

Neshati *et al.* [87] have investigated numerically and experimentally a microstrip slot-coupled RDRA. In this, results are presented to demonstrate that size of slot substantially affects the radiation characteristics of RDRA. The rectangular dielectric resonator antenna consists of a DR with dimensions  $19 \times 19 \times 9.5 \text{ mm}^3$  and dielectric constant  $\epsilon_r = 38$ , which is located on a ground plane of an MSL and fed via a narrow slot. The rectangular slot is etched on ground plane of MSL. Effects of slot size on antenna beam pattern are investigated. Here, coupling slot is centered below resonator, which gives rise to symmetric coupling between DR and slot. Further, slot length is varied from 6 mm to 14 mm, and the slot width is varied between 0.2 mm to 1.8 mm. It is observed that for every value of slot width, there is optimum length for critical coupled system. For slot width  $\geq 1$  mm, the peak level of coupling comes into picture at the slot length of 9 mm. Hence, optimum coupling may be achieved through adjustment of slot size. Salameh *et al.* [30] have undertaken a theoretical and experimental study in order to investigate the coupling from co-planar waveguide to DR. This structure includes a rectangular dielectric resonator (RDR) placed over a linear slot in ground plane of co-planar waveguide. Here, the slot is centered below DR. The slot indicates coupling phenomenon between resonator and co-planar waveguide line. Further, slot length is optimized to provide optimum

coupling. The computed resonance frequency is 4.52 GHz and measured resonance frequency is 4.635 GHz. The gain of antenna is 5.05 dBi, its bandwidth is 6% and the F/B radiation ratio is 15 dB.

#### **1.4 DRA WITH SURFACE MOUNTED HORN (SMH)**

A lot of research activities have been conducted so far to improve the gain of dielectric resonator antenna. These contain stacking parasitic dielectric resonator with air-gap in-between driven and parasitic dielectric resonators [88]-[92], incorporating an offset dual-disk DR [62] and employing composite layered dielectric resonator of high dielectric constant [58]. But, the gain enhancement of approximately 2.7 dB in comparison to a DR element has been achieved by the above mentioned DRA gain boosting techniques. A gain of 7 dBi is obtained from a DR loaded waveguide antenna with parasitic dielectric directors in [65]. But, it is too large configuration, and therefore unsuitable for small-size antenna applications. Moreover, all aforementioned gain improvement schemes use two or more dielectric elements, resulting in large-size, high-cost and more weight. An alternative method to boost the gain of DRA is to use an surface mounted short horn (SMSH) over the radiating element. In past two decades, various researchers have designed microstrip patch antennas (MPAs) as well as DRAs with SMSH for gain enhancement [93]-[102]. Initially, Rahman *et al.* [94] proposed a design to modify radiation properties of MPA arrays by using the artificial horn structures resulting in increased gain of the individual patches. Authors have reported an improvement of minimum 3 dB in the gain of designed MPA (working at 11 GHz) over a wide bandwidth due to the usage of artificial horn structure. An improvement in the gain of two-element probe-fed microstrip antenna-array by 3 dB is noted because of inclusion of quasi-planar SMSH in [95]. The gain with large bandwidth of four- and eight-element patch antenna-arrays has been enhanced with SMSH in [96]. It is observed that the application of quasi-

planar SMSH to four- and eight-elements patch array enhances gain of MPA array by 4 dB. However, gain enhancement of an ultra-wideband (UWB) slot antenna through the usage of an SMSH has been reported in [97]. An average gain improvement of 2.03 dB is observed in comparison to mean gain of corresponding bare slot radiating antenna. A large-gain and wideband AC-MPA with an SMH for 60GHz communication system has been proposed in [98]. However, Nasimuddin *et al.* [99] were the first to integrate a quasi-planar SMSH with a DRA for its performance improvement. The gain of rectangular slot-coupled DRA is enhanced by 3.2 dB because of the addition of SMSH. A gain enhancement of 4.9 dB for a low-profile AC-RDRA with a quasi-planar SMSH has been reported in [11]. It is demonstrated that by adjusting the slant angle and position of the horn for a fixed horn height, the gain of DRA can be optimized. Also, the gain can be further enhanced, if the SMSH is supported on a foam structure. An in depth exploration of the effects of horn material on antenna characteristics has been conducted in [102]. It is found that the horn material substantially affects antenna gain. Horn made of thin copper strips supported by itself / foam provides larger gain as compared to other horn materials.

### **1.5 DRA WITH ELECTROMAGNETIC BAND-GAP (EBG) STRUCTURES**

Another technique to enhance gain of antenna is to alleviate losses due to surface-wave propagation, which may conceive ripples in radiation pattern [71]. Surface-waves are unwanted waves, which get trapped in substrate. Because of these confined EM radiations, efficiency as well as gain of antenna get substantially reduced [103]. A substantial volume of radiations with EM energy gets confined in substrate, which leads to undesired surface-wave losses. If these losses are controlled, it may boost antenna gain [51]. Different techniques have been explored to alleviate the losses due to surface-waves [104]-[110]. One such technique is synthesized substrate, which reduces the effective permittivity of substrate under and around the patch [104]-[105]. Other techniques

include the usage of parasitic elements [106]-[107] or reduced surface-wave antenna [108]-[110]. Electromagnetic band-gap substrates, also called photonic crystals [111], are commonly utilized to improve the performance of antenna [112]-[118]. The surface-waves can be suppressed by creating EBG structures in the substrate. These configurations are capable of opening a band-gap, which is the frequency band in which travelling of EM waves is prohibited i.e., EBG blocks the surface-waves from travelling in a particular band-gap. Alleviation of mutual coupling as well as co-site interference are additional advantages of electromagnetic band-gap structures [67], [119]. By appropriately using these artificial materials (EBG structures), antenna aperture efficiency is substantially modified without effecting the antenna size. Various investigations have demonstrated that electromagnetic band-gap configurations, when incorporated with MPAs [120]-[124] or DRAs, may substantially improve its characteristics like directivity, gain, bandwidth, RL as well as size reduction etc. [103]. Due to incorporation of resonant artificial materials, the surface-waves are generated by antenna and added in antenna gain. Within the band-gap, in the neighbourhood of the resonance frequency of antenna, these artificial materials prevent surface-waves from travelling in the substrate. Consequently, these surface-wave radiations travel in the vertical direction and boost antenna gain [103], [125]. In every design using EBG structure, the antenna is designed with its resonance frequency falling in the band-gap of electromagnetic band-gap structure [126]. Various MPAs as well as DRAs have been designed by the researchers in past few years with EBG substrates for the gain enhancement. The literature about MPAs designed with EBG substrates and DRAs designed with EBG substrates is explored further.

Initially, Boutayeb *et al.* proposed a circularly periodic EBG structure for gain improvement of a circular MPA in [119]. A gain modification of 2.9 dB has been

observed because of significant excision of surface-waves excited in dielectric substrate, due to the inclusion of EBG structure. The gain of a single-layer coaxial probe-fed MPA has been improved by 3.4 dB by surrounding the patch resonator with three rows of EBG unit cells (mushroom-like EBG structure) in E-plane as well as H-plane directions [67]. However, back radiations are also observed to be reduced due to the usage of EBG structure. Three different EBG configurations have been proposed to improve radiation characteristic of an MPA operating at 11 GHz by suppressing surface-waves [103]. First EBG structure uses partial substrate removal technique, second EBG structure uses a mushroom-like EBG configuration and third EBG structure is based on a double-grid configuration. Among three proposed EBG structures, the gain enhancement is maximum in case of mushroom-like EBG structure. But at the same time, its design is most complex among all. Although partial substrate removal scheme is simplest in design among three techniques, but the gain enhancement by using this technique is least. Grid-type EBG structure exhibits average gain improvement and is simple to design. The performance of an aperture coupled millimeter-wave DRA has been improved by including a uni-planar compact EBG (UPC-EBG) configuration in [127]. The designed antenna exhibits increased radiation efficiency, marginally increased gain and reduction in BR because of the cancellation of surface-waves. However, gain of a cylindrical DRA (CDRA) is improved by 3 dB by integrating it within a cylindrical EBG substrate in [128].

Most of the gain enhancement techniques for DRA use two or more dielectric elements. These techniques lack in mechanical stability and are quite large in size. Therefore, these are unsuitable for individual compact antennas and antenna-array elements. Both, the quasi-planar surface mounted horn and the EBG structures seem to be the good options for the gain enhancement of DRA without any adverse effect on impedance BW.

## 1.6 STATEMENT OF PROBLEM

The latest next generation wireless communication equipments are shifting towards high frequency bands, while restricting the performance of metal based antennas. MPAs have been undeniably the most extensively used antennas for the low-gain microwave applications. MPA encompasses a metallic patch on the top of a grounded substrate, and it is coupled through a coaxial probe or an aperture. The large popularity of MPAs is due to its low-profile, compatibility with microwave integrated circuit designs and mechanical robustness. In addition, MPAs are compatible with planar as well as non-planar surfaces, and these are also economical to manufacture using the latest printed-circuit techniques. However, the disadvantages of MPAs are reflected in its applications, where high antenna efficiency and / or a wide impedance BW are required. These disadvantages limit the scope of MPAs. Under these circumstances, the performance of DRA offers better results in comparison to MPAs.

DRAs not only provide most of the advantages of MPAs, but also overcome most of the disadvantages of MPAs. DRAs are open resonating structures, made of high-permittivity low-loss dielectric materials. DRAs are characterized by high radiation efficiency, compact size and wide operational bandwidth as compared to the other resonating antennas. The excited modes, resonance frequencies and radiation characteristics of DRAs are determined by its geometry, dielectric constant and coupling mechanism. This great versatility of the DRAs in terms of its shape and feeding scheme, in combination with its other advantageous inherent properties, make it suitable candidate for many commercial applications.

In spite of having advantages over MPAs, two of the most significant challenges in the design of DRA, are its gain and bandwidth response. Latest communication systems keep the gain and / or bandwidth necessities quite high, and the antenna systems require

to cope up with these requirements. The dielectric resonator antenna BW may be enhanced through the reduction of dielectric constant. However, for a dielectric resonator antenna with small dielectric permittivity ( $\epsilon_r = 10$ ), bandwidth response does not cross 10 - 15%, that is not always ample for various industrial applications. A reduction in value of  $\epsilon_r$  however, results in an elevation of the dielectric resonator antenna dimensions, that is unwanted in different industrial applications. A trade-off between dielectric resonator antenna BW and size leads to a challenging situation as far as the design and optimization are concerned. Moreover, dielectric resonator antenna designer might encounter a lot of challenges emerging due to requirements of stable patterns and good polarization purity.

Presently, the investigations on bandwidth and gain enhancement of DRAs have been of main interest. The major problem in communication systems for satellite communication, which operate on C- and X-band, is the size of antenna that can provide optimum gain and bandwidth. These systems require a simple structure and compact size with stable gain. The variations in the aspect ratio of DRA have not been explored to obtain dual-mode operation of DRA with high-gain and reasonable bandwidth. DRAs have been designed for different frequency ranges, but there is still a strong need to design DRA for C- and X-band to provide optimum performance with compact size.

Different approaches have been presented to enhance gain of DRA by using metallic reflectors, composite layer DRs, stacked DRs and parasitic overlays. In case of reflector and offset dual-disk DRAs, the gain enhancement is moderate. In the domain of composite layer DRs, it has been observed that the impedance BW reduces with the increasing value of gain of the antenna. Due to the usage of parasitic overlays, gain is enhanced, but this configuration is quite long and therefore unsuitable for small antenna applications. As an alternative, the surface mounted horn and EBG structures can be used to modify the DRA gain without compromising impedance BW. However, the high-

profile rectangular DRAs with length-to-height ratio of two or less are unsuitable for the low-profile applications due to lower usable bandwidth and poor gain of DRAs. An improvement is required in effective bandwidth as well as gain of DRA, which can be accomplished by aperture coupling and mounting a quasi-planar horn over the RDRA, and by incorporating an EBG structure with an HDRA.

And the problem (P), as treated in this research work, may be broken up into three main parts as follows:

- P1) Designing of aperture coupled dual-band rectangular dielectric resonator antenna, which operates in C- and X-bands with high gain.
- P2) Mounting of a quasi-planar short horn on rectangular dielectric resonator antenna for its gain enhancement without compromising its bandwidth.
- P3) Incorporation of a mushroom-like EBG structure with an hemispherical rectangular dielectric resonator antenna for its gain enhancement without compromising its bandwidth.

## **1.7 ORGANIZATION OF THESIS**

### **Chapter 2:- “Dual-band Dielectric Resonator Antenna (DRA) for C- and X-Band Applications”**

In this chapter, we first provide the details about dielectric waveguide model (DWM) to get the initial dimensions of an RDRA [72]-[73]. Subsequently, the designing and simulation of RDRA are discussed. The simulation results for the designed RDRA are provided and these results are then compared with the corresponding measured results (with fabricated antenna). Finally, summary of chapter is given to illustrate the significant contributions in this chapter.

### **Chapter 3:- “High-Gain Dual-Band Rectangular (RDRA) with Surface Mounted Short Horn (SMSH)”**

In this chapter, first the design and simulation of RDRA mounted with a quasi-planar short horn over its surface are discussed. Subsequently, the simulation results for RDRA mounted with horn have been illustrated and are also compared with corresponding measured results. Then, the results of conventional RDRA (without horn) are compared with RDRA mounted with horn. Finally, summary of chapter is given to illustrate the significant contributions in this chapter.

### **Chapter 4:- “Designing of High-Gain Hemispherical DRA (HDRA) with Electromagnetic Band-Gap Structure”**

In this chapter, first the design and simulation of HDRA are discussed. Subsequently, the design and simulation of HDRA incorporated with mushroom-type EBG configurations are discussed. Then, simulation results of traditional HDRA (without EBG structure) and HDRA with EBG structure have been illustrated and are also compared. Finally, summary of chapter is given to demonstrate significant contributions in this chapter.

### **Chapter 5:- “Concluding Remarks and Future Scope”**

We conclude the thesis with a summary of the important results and suggestions for the future work.

## **1.9 SUMMARY OF CHAPTER**

This chapter acts as a capsule for the motivation of thesis. An exhaustive literature survey has been presented about various shapes, coupling techniques and gain enhancement techniques for DRAs. Based on this, objectives of the thesis have been identified, in which the main motive is to enhance the gain of DRAs without any adverse effect on its bandwidth.

**DUAL-BAND DIELECTRIC RESONATOR ANTENNA  
(DRA) FOR C- AND X- BAND APPLICATIONS**

---

In recent years, the antenna design engineers have shown great interest in the DRAs due to the prospect of shrinking down the size of antennas for satellite phone operations, the potential in the cost reduction, and ease of manufacturing. DRA is one of the latest progresses in antenna design techniques, taking its place at par among the more common antennas, such as wired antennas and microstrip antennas etc. It is such a recent development that, there is still much room for development and improvement in the performance of DRAs. In this chapter, a technique has been suggested to augment effective bandwidth of DRA, so that it can be used in C- and X-band communication systems. First, a combination of the slot antenna and DRA is proposed, which leads to the design of a dual-band DRA. The resonance of slot as well as dielectric structure is combined to obtain the large BW, in which antenna polarization and beam patterns are conserved. However, in this design, neither miniaturization nor the efficiency is compromised. The main focus is on the gain as well as bandwidth optimization of the proposed antenna. In this chapter, simulation results are elaborated and these results are compared with the measurement outcomes (with fabricated antenna). It is apparent that there is a decent harmony between the measured results and simulation results.

**2.1 INTRODUCTION**

DRA is a radio antenna utilized at microwave and as well as at high frequencies, which includes a block of ceramic material i.e. DR, mounted on ground plane. EM waves are propagated interior to resonating material using a transmitter circuitry, which propagate back and forth in-between DR walls, generating standing-waves. Here, DR walls are

partly transparent for radio wave propagation, permitting electromagnetic power to be radiated in space. A benefit of DRAs is that DR exhibits no inherent conductor loss. These lack in metal parts, which are responsible for the dissipation of energy in high frequency bands. Therefore, these antennas offer low-losses and are highly efficient as compared to metallic antennas in higher frequency range, where conductor loss is proportional to the frequency. This results in improved radiation efficiency of antenna. This DRA characteristic can be exploited in the millimeter-wave satellites, where DRAs can be used for satellite-to-satellite communication. The earth atmosphere is opaque to the electromagnetic spectrum at millimeter frequencies due to the absorption by  $O_2$  and  $N_2$  molecules in the atmosphere. This means that the information transmitted from one satellite to another satellite via millimeter-waves will have increased security, due to the impossibility to tap such signals from earth.

Also, there is much room for flexibility in DRA designs to optimize the bandwidth. On the manufacturing side, DRA can be easily tuned to its resonant frequency, by using a tuning screw attached above DRA. The large degree of freedom means the design is difficult, because a lot of variables interplay with each other. However, if the physics is well understood, it is possible to design DRA to operate at nearly any rational input impedance, thus eliminating the need of a matching circuitry. Hence, the performance of dielectric resonator antenna may be easily optimized through experimental setup. The operating bandwidth of dielectric resonator antenna can be changed over a large range by appropriately selecting the values of parameters of DR. The bandwidth of lower order modes of dielectric resonator antenna may be simply changed from a fraction of 1% to 20%, by an appropriate selection of permittivity of substance and / or by strategic shaping of DR. Dielectric resonators, used in DRAs, are simple to manufacture and provide high degree of freedom to adjust resonating frequency as well as Q-factor. Every mode of

dielectric resonator antenna has a particular internal and associated external field distribution. Hence, various radiation properties can be achieved by exciting various modes in DRA.

Size of DRA is proportionate to  $\epsilon_r^{-1/2}$ , in which  $\epsilon_r$  is permittivity of resonating material. Therefore, by selecting large value of  $\epsilon_r \approx 10-100$ , size of dielectric resonator antenna may be substantially alleviated. The permittivity of the resonating material not only affects the size of DRA, but also affects its bandwidth. An increase in the dielectric constant results in the reduction in bandwidth of DRA. Due to this constraint, the design engineers are reluctant to use high dielectric constant material ( $\epsilon_r \geq 20$ ) for high bandwidth antenna applications. The permittivity of the resonating material is not the only factor determining the bandwidth of DRA. The other factors, which affect the bandwidth of DRA, are the shape and aspect ratio of resonating material. A substantial improvement in the bandwidth can, therefore, be obtained by appropriately selecting aspect ratio(s) of resonator. Further, radiation capability of DRA also depends on the dielectric constant of the resonating material. DRA with relatively low permittivity value ( $\epsilon_r = 10$ ) has better radiation capability than a DRA with high dielectric constant. However, the low-profile dielectric resonator antennas with large value of  $\epsilon_r$  have also been found to be excellent radiating elements in [3]-[5], but at the cost of bandwidth.

Like most good things in life, DRAs come in many forms of shapes and sizes. DRAs in cylindrical, rectangular and hemispherical shapes are most commonly used in the modern communication systems. The rectangular shaped DRA can be designed more easily with flexibility to achieve the desired profile and bandwidth than the hemispherical shaped DRAs. This is because the rectangular shaped DRA offers three degrees of freedom, as compared to two degrees of freedom in CDRA and one degree of freedom in HDRA.

Another significant parameter, which affects the bandwidth of DRAs, is the feeding technique. Dielectric resonator antennas provide easy coupling methods for almost every transmission line (TL) utilized in microwave as well as millimeter-wave frequency ranges. This makes it compatible to be integrated into various planar strategies. However, coupling between dielectric resonator antenna and planar TLs can be adjusted merely by changing location of dielectric resonator w.r.t. line. Commonly used coupling schemes are coaxial probe, microstrip feed line, co-planar feed and aperture coupled feed. In comparison to other coupling schemes, the aperture coupled feed is advantageous, as it does not require a physical contact between the feed and radiator. In aperture coupling, the energy of the microstrip line (MSL) is coupled through an aperture in ground plane and it feeds radiating element. Since, the feed network is positioned beneath ground plane, therefore radiating element gets isolated from undesired coupling / spurious radiations emerging from feeding system. The aperture coupled feed can provide optimum impedance BW along with modified radiation pattern, if the shape of feeding structure and aperture are selected optimally and adjusted appropriately. The coupling between dielectric resonator and feed line may be optimized by variation in position and shape of coupling aperture. The rectangular shaped coupling apertures provide better coupling than the round apertures. The extent of coupling is decided by dimensions of coupling aperture. Therefore, maximum coupling can be achieved through tuning of aperture size. The tuned aperture coupled elements have been demonstrated to provide much wider bandwidths in comparison to other coupling schemes.

The antenna source is modeled as a magnetic or electric current while coupling to a dielectric resonator antenna. The extent of coupling, which evolves between fields within dielectric resonator antenna and source, is expressed as  $\chi$ . Apart from transfer of power, the coupling mechanism to dielectric resonator antennas induces a loading effect. It

affects the Q-factor of dielectric resonator antenna. Here,  $Q_{ext}$  is external Q- factor, and it is denoted in terms of coupling factor  $\chi$  as

$$Q_{ext} = \frac{Q}{\chi} \quad (2.1)$$

$Q_L$  is the loaded Q-factor of dielectric resonator antenna, and it is indicated as

$$Q_L = \frac{Q \cdot Q_{ext}}{Q + Q_{ext}} = \frac{Q}{1 + \chi} \quad (2.2)$$

where,  $Q$  is unloaded Q-factor. When value  $\chi$  is one, then there is maximum power transfer between the coupling port and dielectric resonator antenna. This physical situation is called critical coupling. If  $\chi < 1$ , then dielectric resonator antenna is under-coupled, and when  $\chi > 1$ , DRA is over-coupled.

This chapter is organized as follows. Design model of proposed antenna is presented in section 2.2. Section 2.3 demonstrates the design and simulation of rectangular DRA (RDRA). The simulation and measured results (with fabricated antenna) are illustrated and compared in section 2.4. This chapter is concluded in section 2.5.

## **2.2 DESIGN MODEL FOR PROPOSED APERTURE COUPLED RECTANGULAR DIELECTRIC RESONATOR ANTENNA (RDRA)**

This section presents a design model of the proposed antenna. Geometry of the AC-DRA is shown in Fig. 2.1, where an aperture of length  $l_s$  and width  $W_s$  are utilized to couple energy from MSL to RDR of length  $a$  and width  $d$ . Here, dielectric resonator is located above a thin ground plane, in which inductive rectangle-type aperture is incorporated.

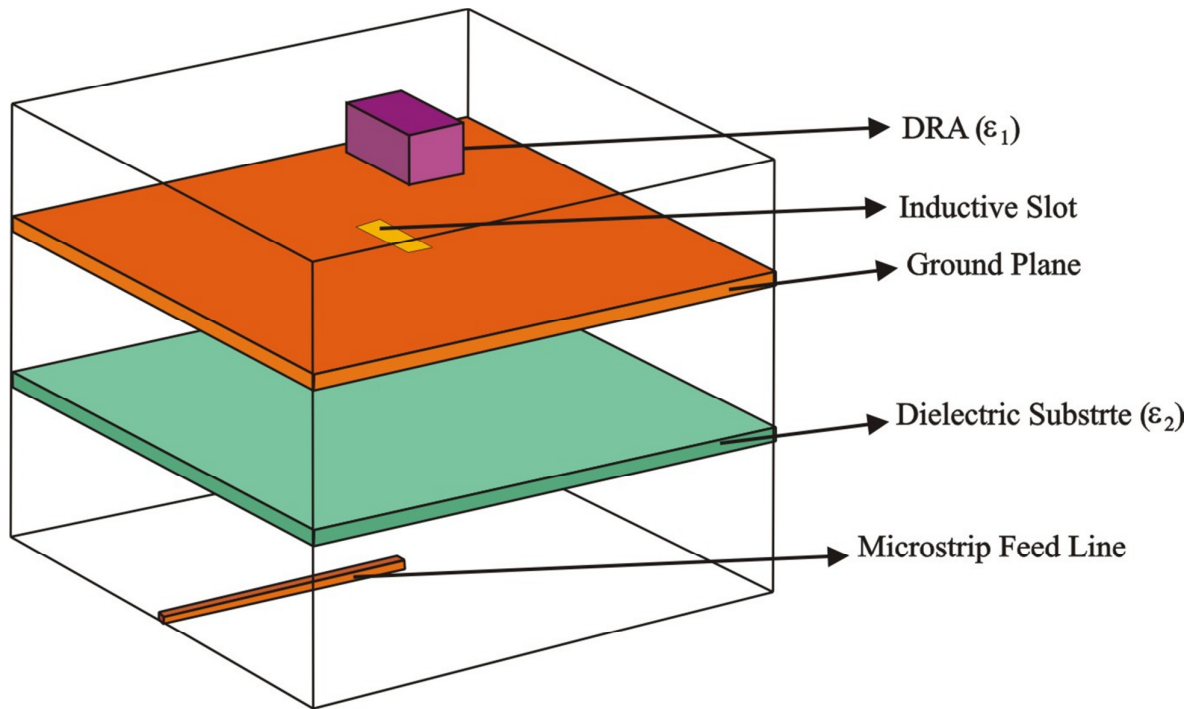


**Fig. 2.1: Layered structure of proposed aperture coupled RDRA**

Dielectric resonator antenna is fed indirectly by an MSL feed via this rectangle-type aperture (in the ground plane), while maintaining location of dielectric resonator above the center of rectangular slot. However, resonator and slot in the designed antenna are symmetrically coupled (MSL is centered below aperture, and DR is centered over aperture) to provide good coupling. Further, the tuning of slot dimensions provides optimum coupling. The major advantage of the aperture coupled feed is that it eliminates the requirement of a physical contact between the feed and radiator. Thus, aperture coupled feed not only isolates DRA from the active circuitry, but at the same time, it also integrates the active circuitry by fully utilizing the whole feed substrate. Another advantage of the aperture coupled feed is that it isolates the spurious feed radiations from the antenna components, which results in significant enhancement of the impedance BW. Below the ground plane, there is a dielectric substrate. In the presented design, the materials used for DRA and dielectric substrate are Gallium Arsenide (GaAs) and Gil

GML 1034, which exhibit permittivity of 12.94 and 3.38 respectively. However, permittivity of dielectric resonator ( $\epsilon_1$ ) is taken more than that of dielectric segment ( $\epsilon_2$ ). Dielectric segment of lower permittivity ( $\epsilon_2$ ), which is placed between the ground plane and the microstrip feed line, exhibits same surface dimensions as for the ground plane ( $60\text{mm}\times 60\text{mm}$ ). The formulation and optimization of the RDRA has been presented in next section.

### 2.3 FORMULATION AND OPTIMIZATION OF RDRA

In this section, design procedure of RDRA and its fabricated model are presented. The proposed RDRA for C- and X-band has been designed by using dielectric waveguide model (DWM) and manipulating aspect ratios of DR. A dual-mode operation of DR is obtained, such that both the operating modes have a voltage standing wave ratio (VSWR) lower than two, and also possess similar radiation patterns. The proposed AC-DRA is designed with HFSS software using closed form of the design equations. First, the preliminary dimensions of RDRA are calculated for a given resonance frequency, using DWM. Then, these dimensions are optimized to provide good impedance matching. The aspect ratios of RDRA are manipulated to achieve dual-band operation.

DWM was first proposed by Marcatili [129] to find out the guided wavelength in rectangular cross-section dielectric guides. Subsequently, it has been used in [72]-[73] for the analysis of RDRAs. The design equations (based on DWM) given by Mongia *et al.* in [72] are very useful for designs of the RDRAs. In the proposed design, the preliminary values of dimensions of RDRA are calculated using equations derived in [72]. Any DR can have two types of modes: a) confined modes, b) non-confined modes. Following condition must be fulfilled by both confined as well as non-confined modes, at each surface of resonator

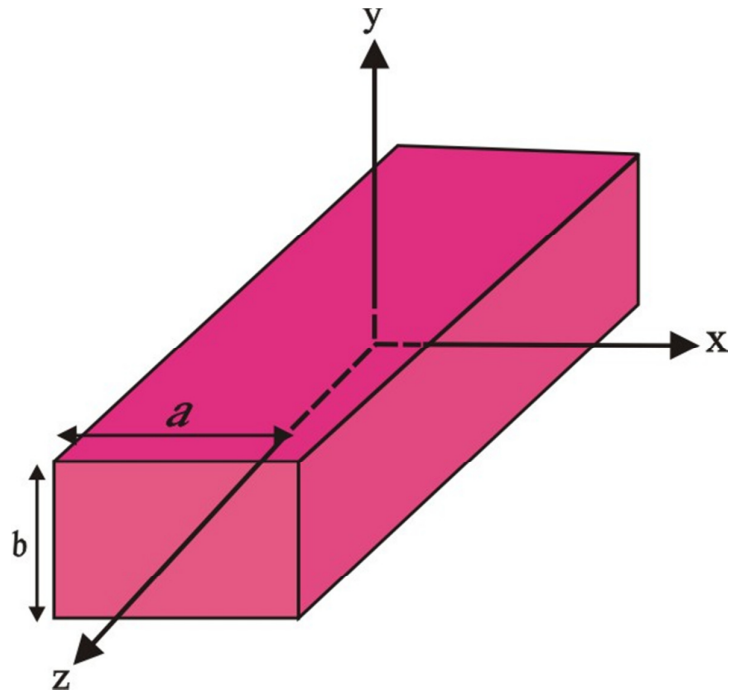
$$E \cdot \hat{n} = 0 \quad (2.3)$$

where, E signifies electric field intensity and  $\hat{n}$  signifies normal to the surface of the DR. Equation (2.3) is one of the conditions, which fields satisfy at the magnetic wall. Another magnetic wall condition, specified in Eq. (2.4), may or may not be satisfied at every surfaces of dielectric resonator each mode.

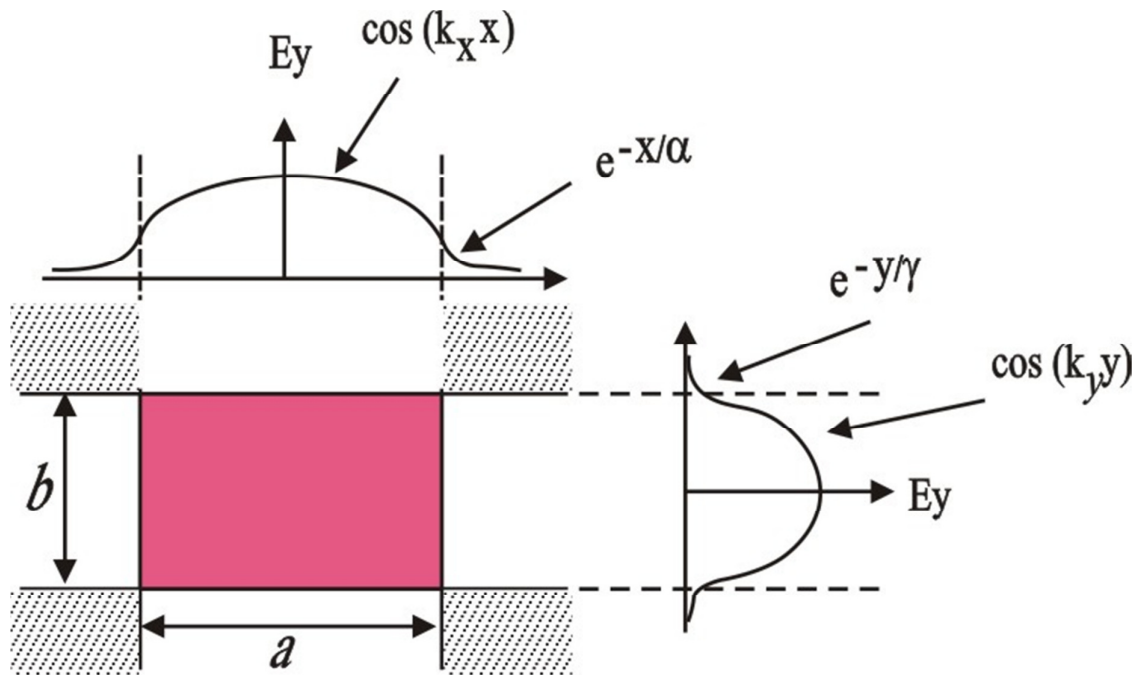
$$\hat{n} \times H = 0 \quad (2.4)$$

where, H signifies the magnetic field intensity. The modes of a dielectric resonator, which satisfy both Eq. (2.3) and Eq. (2.4), are called as confined modes. Whereas the modes, which satisfy only Eq. (2.3), are known as non-confined modes. Bladen has shown in [130] that only the bodies of revolution, like sphere-type and cylinder-type dielectric resonators, can support confined modes.

As rectangle-type dielectric resonator is not a body of revolution, therefore it supports only non-confined modes. When DWM is utilized to explore the fields of lowest order TM modes, these don't satisfy Eq. (2.3) [73]. Hence, the existence of TM modes seems to be doubtful in RDRs. Whereas, existence of lowest order TE modes is significantly established [131]. The dielectric guide has been shown in Fig. 2.2a, which has rectangle-type cross-section of length 'a' along x-direction, height 'b' along y-direction and waves propagate in z-direction. Fields within guide are considered to change in sinusoidal trend, whereas fields outside guide are considered to decrease in exponential fashion [73]. If fields in shaded regions of Fig. 2.2b are considered to be zero, then the analysis of underlying antenna problem becomes simple.



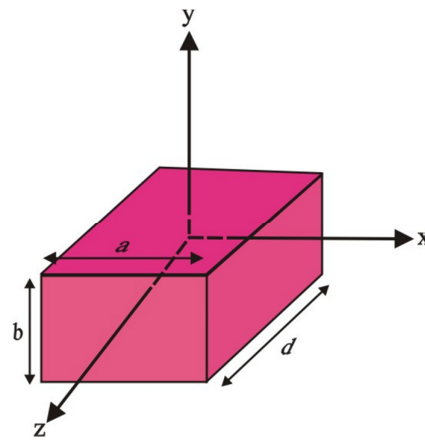
(a)



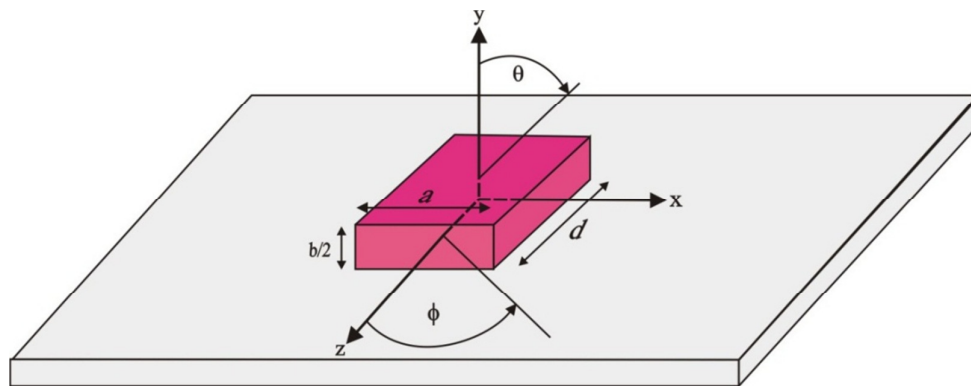
(b)

**Fig. 2.2: Dielectric waveguide**  
**(a) Infinite dielectric waveguide**  
**(b) Cross-sectional field distribution**

In order to model DRA, the waveguide is truncated along z-direction at  $\pm d/2$ , as depicted in Fig. 2.3a, with magnetic walls. This paradigm is utilized in case of an isolated dielectric resonator antenna in free space (exhibiting physical attributes  $a$ ,  $b$ , and  $d$ ). It may be utilized in practical applications in case of dielectric resonator antenna (exhibiting physical attributes  $a$ ,  $h = b/2$ , and  $d$ ) placed on a ground plane, which is demonstrated in Fig. 2.3b. However in practice, the image theory is utilized for elimination of ground plane and to increase height of dielectric resonator antenna (approximately double). For an RDRA with physical attributes  $a$ ,  $b > d$ , lowest order mode can be  $TE_{11\delta}^z$ .



(a)



(b)

**Fig. 2.3: Dielectric waveguide modeled as DRA**  
**(a) Truncated dielectric waveguide**  
**(b) DRA on ground plane**

The usage of DWM [72] results in following fields within dielectric resonator antenna

$$H_x = \frac{k_x k_z}{j\omega\mu_0} B \sin(k_x x) \cos(k_y y) \sin(k_z z) \quad (2.5)$$

$$H_y = \frac{k_y k_z}{j\omega\mu_0} B \cos(k_x x) \sin(k_y y) \sin(k_z z) \quad (2.6)$$

$$H_z = \frac{(k_x^2 + k_y^2)}{j\omega\mu_0} B \cos(k_x x) \cos(k_y y) \cos(k_z z) \quad (2.7)$$

$$E_x = B k_y \cos(k_x x) \sin(k_y y) \cos(k_z z) \quad (2.8)$$

$$E_y = -B k_x \sin(k_x x) \cos(k_y y) \cos(k_z z) \quad (2.9)$$

$$E_z = 0 \quad (2.10)$$

Here, B is an arbitrary constant. The wave propagation numbers;  $k_x$ ,  $k_y$  and  $k_z$  along x-, y-, and z-directions respectively (for  $|x| \leq a/2$  and  $|y| \leq b/2$ ) are derived by substituting

the boundary condition (2.3) at the surfaces of DR i.e., at  $x = \pm \frac{a}{2}$  and  $y = \pm \frac{b}{2}$

$$k_x = \frac{\pi}{a} \quad (2.11)$$

$$k_y = \frac{\pi}{b} \quad (2.12)$$

For  $k_z$ , the following transcendental equation is obtained by using the DWM [73]

$$k_z \tan(k_z \frac{d}{2}) = \sqrt{(\epsilon_1 - 1)k_0^2 - k_z^2} \quad (2.13)$$

However, above approximation is comparable to the consideration that magnetic walls

happen to be there at  $x = \pm \frac{a}{2}$  and  $y = \pm \frac{b}{2}$ . Here,  $\epsilon_1$  is relative permittivity of DR (GaAs).

By substituting boundary condition at surfaces of DR i.e., at  $x = \pm \frac{a}{2}$  and  $y = \pm \frac{b}{2}$ ,

attenuation constants in x- and y-directions ( $\alpha, \gamma$ ) (for  $|x| \geq a/2$  and  $|y| \geq b/2$ ) are given as

$$\alpha = \frac{1}{\sqrt{(\varepsilon_1 - 1)k_0^2 - k_x^2}} \quad (2.14)$$

$$\gamma = \frac{1}{\sqrt{(\varepsilon_1 - 1)k_0^2 - k_y^2}} \quad (2.15)$$

where,  $\varepsilon_1$  is the permittivity of dielectric resonator,  $k_x$  and  $k_y$  are wave numbers along x- and y-directions respectively, and  $k_0$  is free space wave number, which is related to resonance frequency ( $f_0$ ) by following equation

$$k_0 = \frac{2\pi f_0}{c} \quad (2.16)$$

where,  $c$  is speed of light in space. Three wave numbers in x-, y- and z-directions satisfy following equation

$$k_x^2 + k_y^2 + k_z^2 = \varepsilon_1 k_0^2 \quad (2.17)$$

The dimensions of RDR are  $a$ ,  $b$  and  $d$  along x-, y- and z-directions respectively. The length of DR is given as

$$a = \frac{\lambda_g}{2} \quad (2.18)$$

where  $\lambda_g$  is the guided wavelength, which is expressed as

$$\lambda_g = \frac{\lambda_0}{\sqrt{\varepsilon_2}} \quad (2.19)$$

Here  $\lambda_0$  is wavelength at the resonance frequency and  $\varepsilon_2$  is permittivity of substrate (GIL GML 1034). The value of  $\lambda_0$  is given as

$$\lambda_0 = \frac{c}{f_0} \quad (2.20)$$

where,  $f_0$  is the resonance frequency of the proposed antenna. By substituting values of  $c$  and  $f_0$  in Eq. (2.20), the value of  $\lambda_0$  can be calculated. Then by substituting value of  $\lambda_0$

and  $\epsilon_2$  in Eq. (2.19), the value of  $\lambda_g$  can be calculated. Further, by substituting value of  $\lambda_g$  in Eq. (2.18), the preliminary value of length of DR  $a$  can be obtained. The preliminary value of width of DR  $d$  can be calculated using following equation by putting value of  $a$  in it

$$d = \frac{a}{AR} \quad (2.21)$$

where,  $AR$  is the aperture ratio (length / width) of the RDR, whose value is greater than one. In our design, we take the value of  $AR = 1.75$ . Then, the preliminary value of height of RDR  $b$  is determined from the Eqs. (2.11) - (2.13) and Eqs. (2.16) - (2.17). By substituting value of  $c$  and  $f_0$  in Eq. (2.16), the value of  $k_0$  can be obtained. The value of wave number in x-direction  $k_x$  can be calculated from Eq. (2.11) by substituting value of  $a$  in it. Then, by substituting values of  $k_0$ ,  $d$  and  $\epsilon_1$  in Eq. (2.13), the value of wave number in z-direction  $k_z$  can be obtained. Further, by substituting the values of  $k_0$ ,  $k_x$ ,  $k_z$  and  $\epsilon_1$  in Eq. (2.17), the value of wave number in y-direction  $k_y$  can be determined. Finally, by substituting value of  $k_y$  in Eq. (2.12), the preliminary value of height of RDR  $b$  is obtained.

The following guidelines are used for designing the rectangle-type slots

(1) Slot length  $l_s$  is selected to be quite large to achieve satisfactory level of coupling between dielectric resonator antenna and MSL. At the same time, it must be reasonably small, such that it must not resonate at a frequency lying in effective bandwidth which generally results in a significant BR. The slot length  $l_s$  is given as

$$l_s = \frac{0.4 \lambda_0}{\sqrt{\epsilon_e}} \quad (2.22)$$

$$\varepsilon_e = \frac{\varepsilon_1 + \varepsilon_2}{2} \quad (2.23)$$

where,  $\varepsilon_1$  and  $\varepsilon_2$  are the permittivity values of DR and substrate respectively. By substituting the values of  $\lambda_0$ ,  $\varepsilon_1$  and  $\varepsilon_2$  in Eq. (2.22) and Eq. (2.23), the values of slot length  $l_s$  can be calculated.

2) A reasonably slender slot width is generally selected to prevent high BR. Therefore, a genuine parameter setting is according to

$$W_s = 0.2 l_s \quad (2.24)$$

where,  $W_s$  is the width of slot. At high frequencies, narrow  $W_s$  may lead to slender slot, which is tough to manufacture because of etching restrictions. At such frequencies, a broader slot width may be considered.

As dielectric permittivity values are considered to be constant, physical attributes like length, width and height of dielectric resonator are utilized to obtain operational bandwidth of DRA. However, parameters like length and width of slot are used for fine-tuning of operational bandwidth and / or to obtain fair impedance tuning in required frequency band. Once the initial dimensions for DR and slot have been calculated, these are optimized using full-wave techniques (Ansoft HFSS). The optimized dimensions of DR are found to be  $13.2\text{ mm} \times 7.1\text{ mm} \times 6.5\text{ mm}$  and dimensions of slot are found to be  $W_s = 1.2\text{ mm}$  and  $l_s = 6.4\text{ mm}$ . These dimensions of slot maximize the coupling of energy between feed line and DR.

Size of dielectric substrate is  $60\text{ mm} \times 60\text{ mm}$ . Table 2.1 shows the parametric values of RDRA obtained after optimization. All the antenna parameters are optimized except width of the feed line and size of substrate. It is observed that resonance frequency is mainly affected by length of DR, height of DR, length of slot and position of slot. By

varying width of DR, width of slot and length of microstrip feed line, the resonance frequency is not affected, but the return loss (RL) is affected.

**TABLE 2.1**  
**PARAMETRIC VALUES OF APERTURE COUPLED RDRA**

Parameter	Value
Permittivity of DR (GaAs), $\epsilon_1$	12.94
Length of DR, $a$	13.2 mm
Width of DR, $d$	7.1 mm
Height of DR, $b$	6.5 mm
Permittivity of substrate (GIL GML 1034), $\epsilon_2$	3.38
Thickness of substrate, $h$	0.5 mm
Slot Length, $l_s$	6.4 mm
Slot Width, $W_s$	1.2 mm
Length of 50 $\Omega$ MSL, $l_f$	31.5 mm
Width of 50 $\Omega$ MSL, $W_f$	1.15 mm
Resonance Frequency of DR	5.8 GHz

The radiation Q-factor of dielectric resonator antenna is obtained using following equation [72]

$$Q = \frac{2\omega W_e}{P_{rad}} \quad (2.25)$$

where,  $W_e$  and  $P_{rad}$  are the stored energy and radiated power respectively. These quantities are given by

$$W_e = \frac{abd\epsilon_0\epsilon_1}{32} \left( 1 + \frac{\sin(k_z d)}{k_z d} \right) (k_x^2 + k_y^2) \quad (2.26)$$

$$P_{rad} = 10k_0^4 |P_m|^2 \quad (2.27)$$

where,  $P_m$  is magnetic dipole moment of dielectric resonator antenna

$$P_m = \frac{-j\omega 8\epsilon_0(\epsilon_r - 1)}{k_x k_y k_z} \sin\left(\frac{k_z d}{2}\right) \hat{z} \quad (2.28)$$

The impedance BW of dielectric resonator antenna can be obtained using Q-factor as

$$BW = \frac{S-1}{Q\sqrt{S}} \quad (2.29)$$

where,  $S$  is peak suitable VSWR. Therefore, above equations can be used to generate the graphs for Q-factor for different values of permittivity and different values of  $a/b$ . Here, normalized Q-factor is denoted as

$$Q_e = \frac{Q}{\epsilon_1^{3/2}} \quad (2.30)$$

Fig. 2.4 shows the top view of the fabricated paradigm of RDRA. Fig. 2.5 portrays bottom view of the fabricated paradigm of RDRA. In this section, the dimensions of various antenna parameters have been found by using the DWM equations and optimization functions of HFSS. Various simulation results and measured results (with fabricated antenna) are presented in the next section.

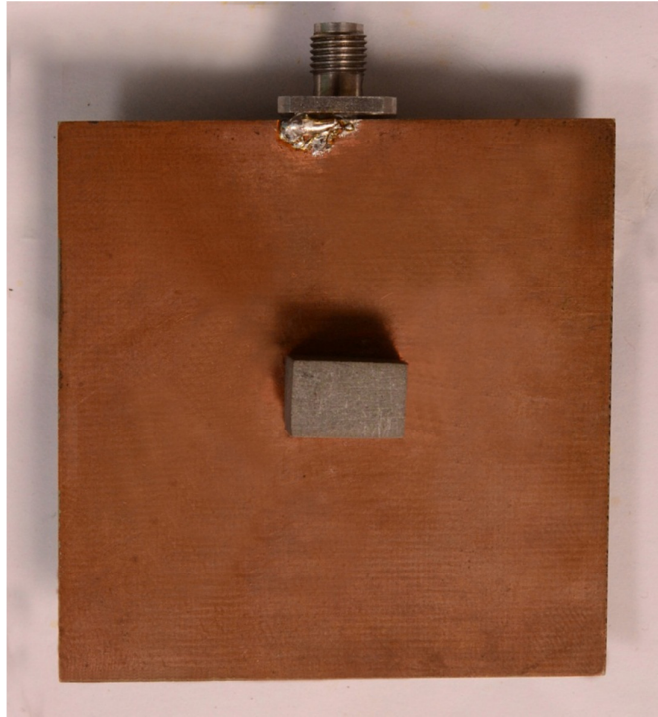


**Fig. 2.4: Fabricated model of aperture coupled RDRA (top view)**

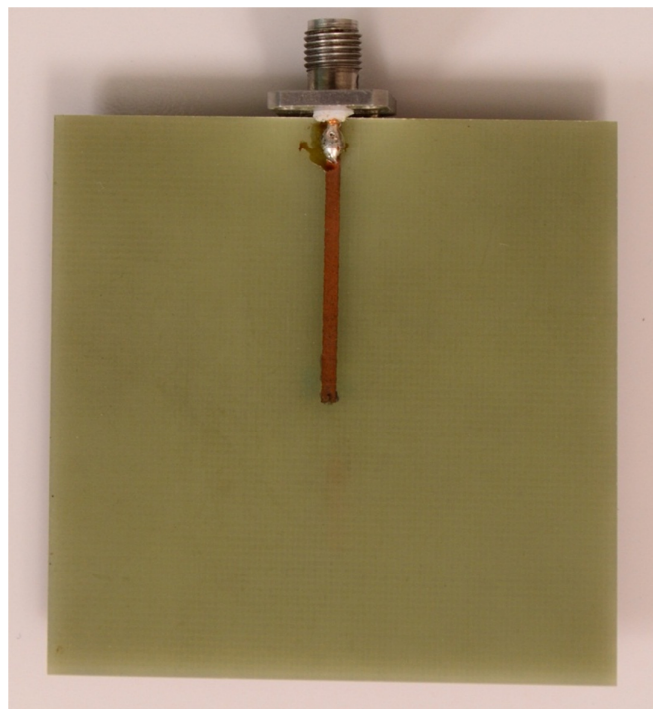


**Fig. 2.5: Fabricated model of aperture coupled RDRA (bottom view)**

## 2.4 SIMULATION AND EXPERIMENTAL RESULTS WITH PERFORMANCE ANALYSIS

This section presents various simulation results and measured results (with fabricated antenna) of the dual-band RDRA. Fig. 2.6 illustrates the measured (with fabricated model) RL and the RL observed through simulation of the dual-band antenna. It is observed that resonance frequency of dielectric resonator antenna changes by varying slot and dielectric resonator dimensions. It has been observed that the designed dual-band DRA resonates at two frequencies. The simulation resonance frequencies are 5.8 GHz and 8.0 GHz, whereas the measured resonance frequencies are 5.8 GHz and 7.95 GHz. The impedance BW obtained through simulation is approximately 6.5 % (380 MHz) at resonating frequency of 5.8 GHz, and this is approximately 5.6 % (450 MHz) at resonating frequency of 8.0 GHz.

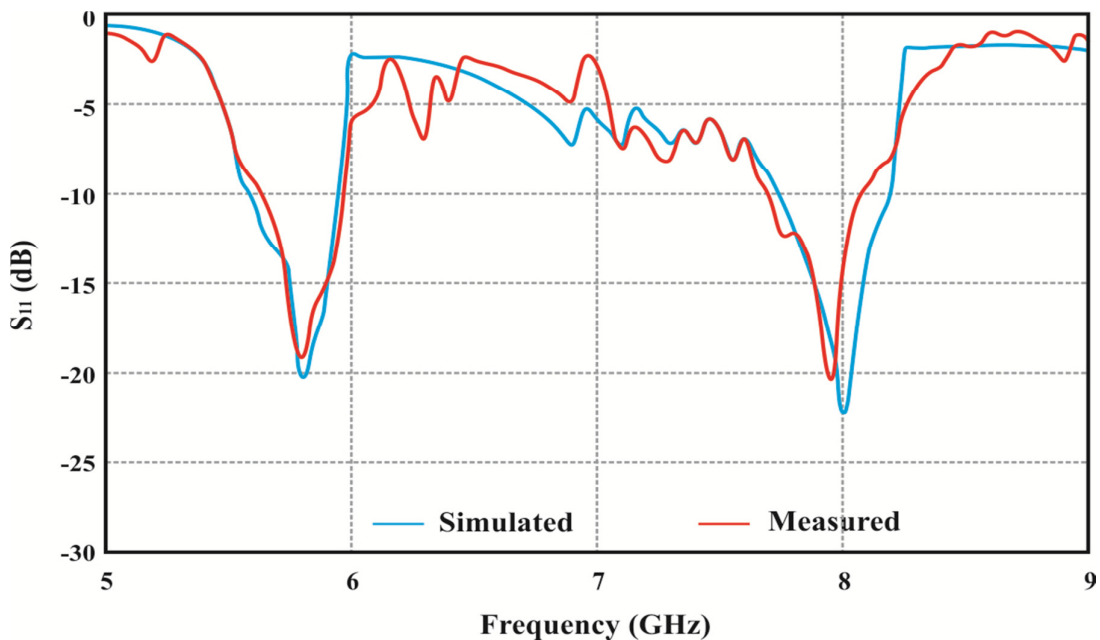


**Fig. 2.6: Frequency response of RDRA (near field measurement)**

However, the measured (with fabricated antenna) impedance BW is approximately 5.8 % (340 MHz) at resonating frequency of 5.8 GHz, and this is approximately 5.2 % (420 MHz) at resonating frequency of 7.95 GHz. However, return loss values observed through simulation are -20.5 dB and -22.5 dB at these two resonating frequencies respectively i.e., at 5.8 GHz and 8.0 GHz respectively. Whereas, the measured RL values (with fabricated antenna) are -19 dB and -20.5 dB at 5.8 GHz frequency and 7.95 GHz frequency respectively. The RL observed through simulation and measured return loss is plotted together in same figure for comparison purpose, and a fair accord is observed among both outcomes with -10 dB return loss. However, gain achieved through simulation are 8.5 dBi and 9.6 dBi at 5.8 GHz frequency and 8.0 GHz frequency respectively. The measured gain (with fabricated antenna) achieved are 8.1 dBi and 9.05 dBi at 5.8 GHz frequency and 7.95 GHz frequency respectively.

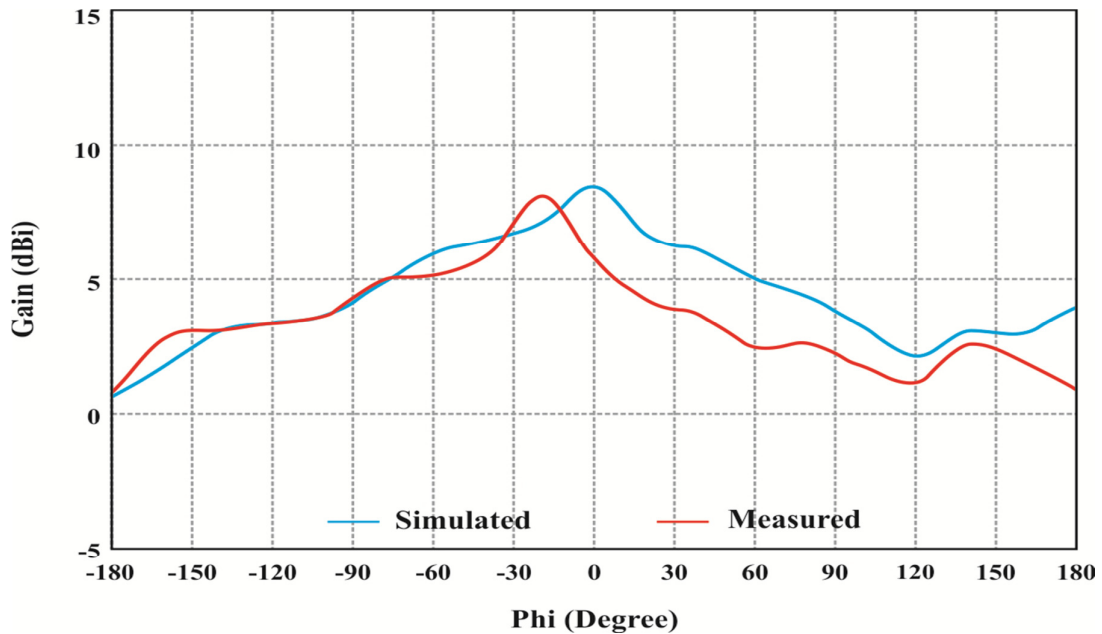


**Fig. 2.7: Gain response of RDRA at 5.8 GHz (far field measurement)**

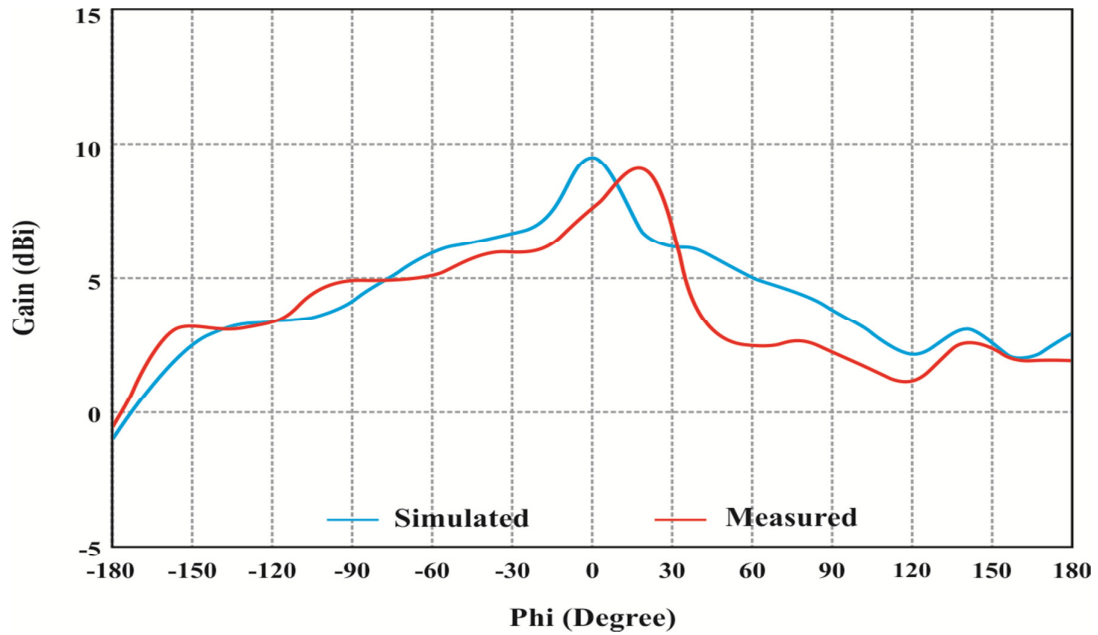


**Fig. 2.8: Gain response of RDRA at 8.0 GHz (far field measurement)**

For comparison purpose, gain achieved through simulation and measured gain is plotted together in Fig. 2.7 and Fig. 2.8. It is observed that measured gain is marginally lower as compared to gain achieved through simulation. Fig. 2.9 illustrates the radiation pattern of RDRA in E-plane, whereas Fig. 2.10 illustrates the radiation pattern of RDRA in H-plane observed through simulation as well as through measurement (with fabricated antenna) at lower resonating frequency 5.8 GHz. Fig. 2.11 illustrates the radiation pattern of RDRA in E-plane, whereas Fig. 2.12 illustrates the radiation pattern of RDRA in H-plane observed through simulation as well as through measurement (with fabricated antenna) at higher resonating frequency 8.0 GHz.

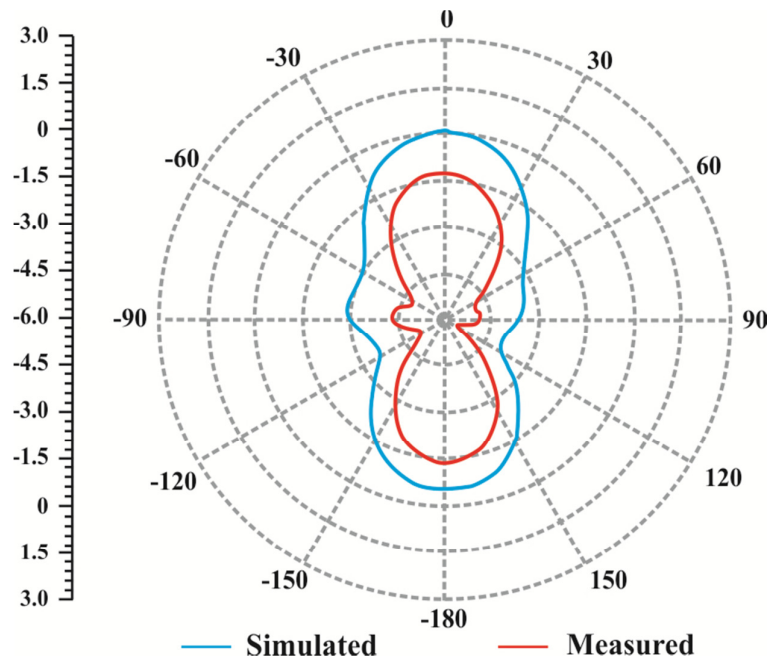


**Fig. 2.9: Radiation Pattern (E-Plane) of RDRA at 5.8 GHz**

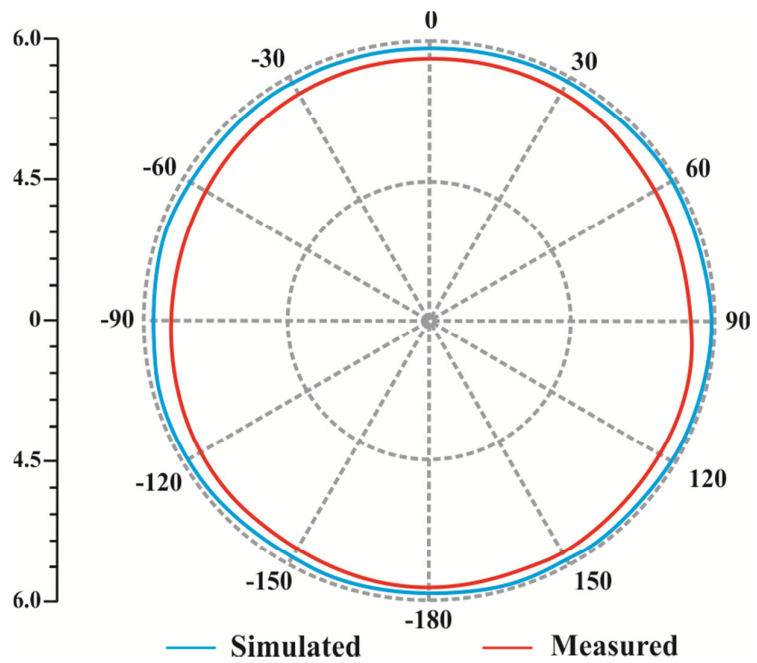


**Fig. 2.10: Radiation Pattern (H-Plane) of RDRA at 5.8 GHz**

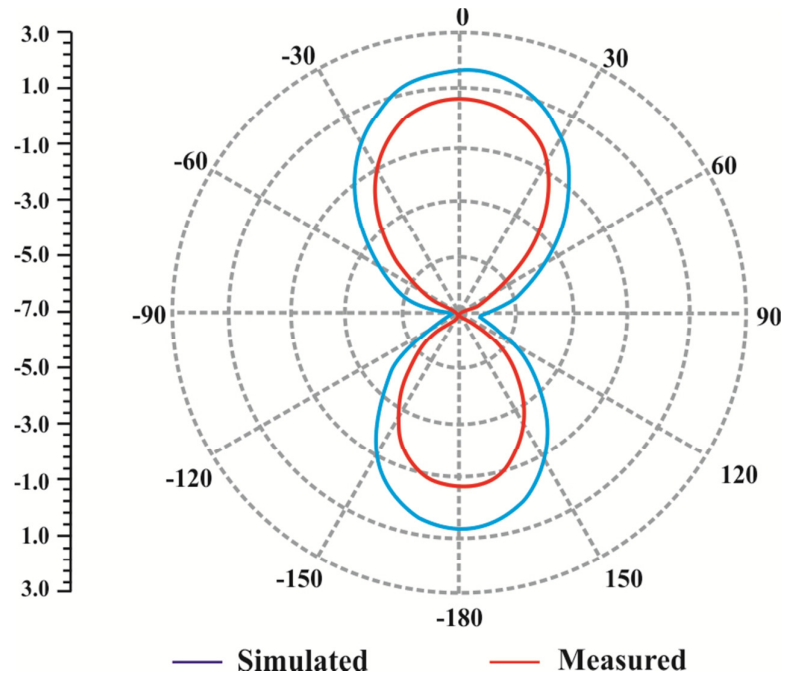


**Fig. 2.11: Radiation Pattern (E-Plane) of RDRA at 8.0 GHz**

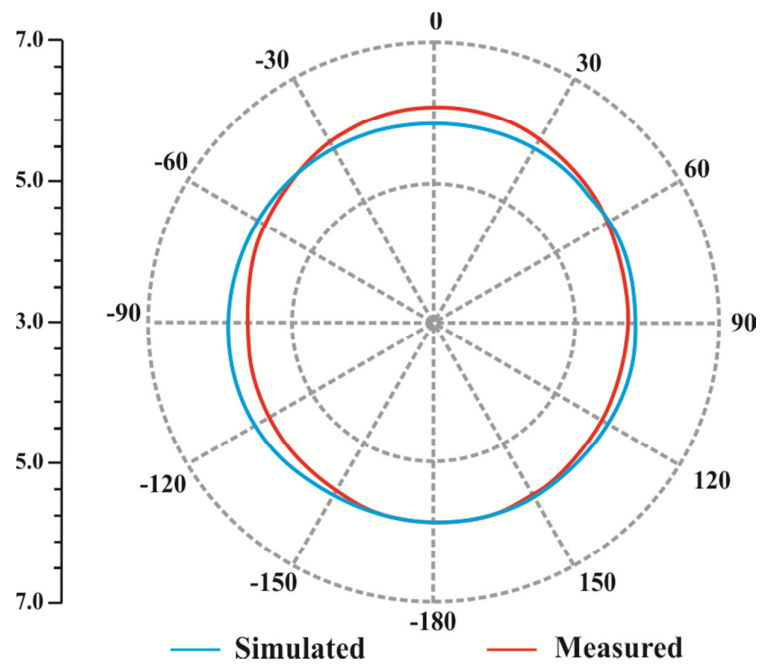


**Fig. 2.12: Radiation Pattern (H-Plane) of RDRA at 8.0 GHz**

In Fig. 2.13, gain achieved through simulation as well as measured gain is depicted as the function of frequency in range 5 GHz to 9 GHz. Simulation results and measured results (with fabricated antenna) for RDRA are shown in Table 2.2.

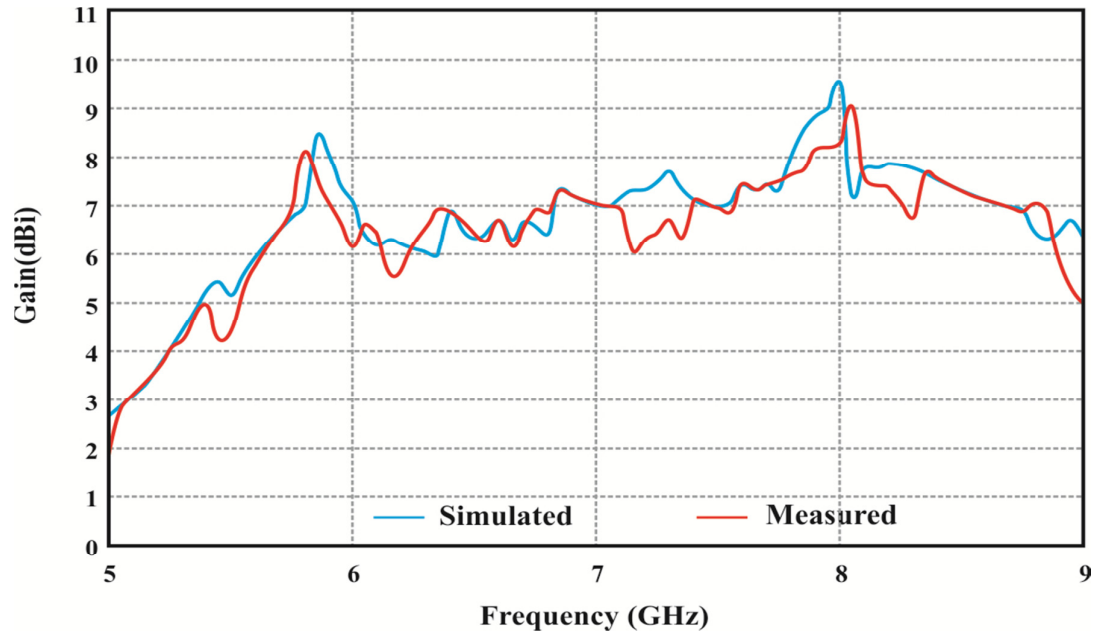


**Fig. 2.13: Gain v/s frequency plot for RDRA**

**TABLE 2.2**

**SIMULATION AND MEASURED RESULTS FOR RDRA**

ATTRIBUTE	SIMULATION RESULT		MEASURED RESULT	
	5.8 GHz	8.0 GHz	5.8 GHz	7.95 GHz
<b>RESONANCE FREQUENCY</b>	5.8 GHz	8.0 GHz	5.8 GHz	7.95 GHz
<b>GAIN</b>	8.5 dBi	9.6 dBi	8.1dBi	9.05 dBi
<b>BANDWIDTH</b>	380 MHz	450MHz	340 MHz	420 MHz
<b>RETURN LOSS</b>	-20.5 dB	-22.5 dB	-19 dB	-20.5 dB

From Table 2.2, marginal differences between the simulation results and measured results (with fabricated antenna) can be observed for the proposed antenna, which might be

because of proximity effects, fabrication errors, and effects due to connector utilized to feed antenna. However, measured gain and bandwidth are slightly lower as compared to corresponding simulation results. At lower resonance frequency (5.8 GHz) as well as at higher resonance frequency (8.0 GHz), the measured RL (with fabricated antenna) is slightly more than the RL observed through simulation.

## **2.5 SUMMARY OF CHAPTER**

In this chapter, a dual-band AC-RDRA has been designed with simple structure, compact size, and low-loss. This presented configuration has been manufactured as well as tested. Simulation outcomes have been confirmed by conducting experimentation on fabricated antenna. The objectives are to obtain dual-band operation with reasonable gain and bandwidth. The simulation and measured results (with fabricated antenna) illustrate that the proposed antenna provides reasonable gain at both resonance frequencies. It possesses high power handling capability as compared to patch antenna. The major advantages of the presented AC-RDRA are that it is simple to manufacture and found to be mechanically stable. Moreover, the presented AC-DRA has optimized shape and size. This dual-band DRA has found applications in C- as well as X-band based communication systems, like in satellite communication systems. In this chapter, the dual-band aperture coupled RDRA is designed, and in the next chapter, performance of the dual-band AC-RDRA is modified by mounting a horn over the designed DRA structure.

**HIGH-GAIN DUAL-BAND RECTANGULAR DRA (RDRA) WITH  
SURFACE MOUNTED SHORT HORN (SMSH)**

---

---

The application of quasi-planar SMSH to attain significant gain of RDRA has been investigated in this chapter. Design and fabrication of a dual-band aperture coupled RDRA have been discussed in chapter 2, where the simulation as well as measured results (with fabricated antenna) have been compared. In this chapter, we present the integration of an SMSH with the earlier designed AC-RDRA for gain improvement. In the presented work, SMSH of rectangular base is manufactured using silver metal. The horn height is a fraction of wavelength. So, antenna size is not significantly increased due to the inclusion of horn. Full height of the antenna is only 14 mm ( $0.27\lambda_0$ ), therefore whole antenna structure is quasi-planar in nature. It is found that by using the SMSH, the gain of conventional RDRA (RDRA without horn) is enhanced significantly at both resonance frequencies, with marginally decreased impedance BW. Various horn parameters such as slant length, slant angle and horn position (separation distance between horn and edge of the broader dimension of an RDRA), have been optimized for peak gain at resonating frequency of antenna. Simulation results are demonstrated, and these results are also compared with the measured results. The simulation and measured outcomes are observed to be in a fair accord. HFSS software has been employed for simulation of proposed antenna structure.

**3.1 INTRODUCTION**

Dielectric resonator antennas (DRAs) offer numerous benefits over MPAs. The major advantages of DRA are compact design and negligible dissipation loss because of

insignificant conducting parts [74], [132]-[136]. But, the disadvantage of DRA is that it provides low antenna gain. Various methods have been presented to enhance gain of DRA by using metallic reflector [55]-[57], composite layer DRs [60], stacked dielectric resonators [62], parasitic overlays [65], superstrate on top of DRA [137]-[138] and by exciting higher order modes [139]-[141]. In case of reflector and offset dual-disk DRAs, the gain enhancement is not very high. With composite layer DRs, it has been observed that the impedance BW reduces with increasing gain of the antenna. Due to the usage of parasitic overlays, gain is enhanced, but this configuration is quite long, and therefore unsuitable for small antenna applications. As an alternative, the SMH can be used to modify the antenna gain without sacrificing antenna BW [93]. Fortunately, radiating element and the SMH can be designed separately. In past few years, various researchers have designed MPAs as well as DRAs with SMH for the gain enhancement. Further, the literature about MPAs designed with SMH and the DRAs designed with SMH is explored.

Rahman *et al.* [94] have proposed a technique to modify radiation properties of antenna-arrays by trapping EM field on / in vicinity of microstrip patch, by utilizing the artificial horn configuration resulting in increased gain of independent patch. It also provides isolation between antenna-array elements. Increased gain of independent patch elements results in reduced number of antenna-array elements, which in turn reduces the size as well as cost of the whole array. The gain of the antenna is boosted by guiding patch's fringing fields by utilizing surface mounted horn. Horn wall gives contribution in concentrating fringing field at edges. It also suppresses mutual coupling in-between neighbouring antenna-array elements. However, the antenna impedance matching has been modified due to the addition of artificial horn. However, scattering parameter  $S_{11}$  for this antenna shows good matching at approximately 11 GHz. Both simulation and

measurement results indicate enhancement of at least 3 dB in gain and 4 dB in broadband matching properties of designed MPA.

Using their own idea from [94] for antenna gain enhancement, Rahman *et al.* [95] have proposed a novel probe-fed compact square MPA with quasi-planar SMH, achieving higher gain than results presented in previous work in this regard. Horn in this new design, has the slant length  $L_s = \lambda_0 / 4 = 0.875 \text{ cm}$ , where  $\lambda_0$  is wavelength at resonating frequency. Horn is constructed from plastic sheet and painted using silver epoxy. This patch antenna resonates at 8.77 GHz. An MPA designed on thin substrate gives slender bandwidth of approximately 2%. Authors have investigated MPA with and without horn for substrates of different thickness (h, 2h, 3h and 4h). Two different horn positions ( $d = \lambda_0 / 4$  and  $\lambda_0 / 8$ ) are taken while examining the antenna, where d is distance in-between patch and inner edge of horn. Two-element array with / without horn is also designed. Here, antenna thickness involving horn is approximately 6.94 mm. Gain of 11.5 dBi is obtained for two-element array with horn and 8.5 dBi for same array without horn. Thus, horn enhances gain of two-element array by approximately 3 dB. It reduces RL from -22 dB to -35 dB. Bandwidth procured is approximately 9.0 % for this configuration, which may be further enhanced by the usage of relatively thick substrate. Horn also modifies isolation in-between elements of array by 10 dB.

Rahman *et al.* [93] have extended their previous work in [95], to improve gain of a compact AC-MPA, designed to work in the Ku-band, with quasi-planar SMH with slant length  $\lambda_0 / 4$ . The rectangle-type patch is designed to feed the horn at 11.78 GHz frequency. Horn is fabricated using plastic sheet, and it is placed on substrate of an AC-MPA, which feeds horn. Horn surface is painted using silver epoxy. Variations in directive gain is examined for  $d = \lambda_0 / 8$ ,  $\lambda_0 / 4$  and  $\lambda_0 / 2$ , where d is the separation distance between horn and patch edge. Directive gain of 10.1 dBi is achieved for

$d = \lambda_0 / 4$  . For  $d = \lambda_0 / 8$  , 8.6 dBi direction gain is achieved. SMH modifies not only gain of presented antenna configuration by approximately 4.2 dB, but it also minimises BRs. This structure has bandwidth 12.4% (11.08 GHz - 12.5 GHz).

Rahman *et al.* [96] have extended the work presented in [93], to enhance the gain with large bandwidth of four-element and eight-element patch antenna-arrays with the SMH. The horn is fabricated by using a thick polyvinyl chloride (PVC) sheet and painted with conductive silver epoxy paint. The four-element patch antenna-array with corporate feed is designed to resonate at 11.45 GHz frequency. The short horn with slant length,  $L_s = \lambda_0 / 4$  was selected in [93], but in [96], it is chosen to be  $3\lambda_0 / 4$ , where  $\lambda_0$  is the wavelength at the resonance frequency. The horn position  $d$ , which is the distance in-between horn and patch edge, is taken to be  $\lambda_0 / 4$ , which is same as in previously reported work in [93]. The separation between patches is taken to be  $0.85 \lambda_0$ . For the four-element square array, 15 dBi gain is measured and for the eight-element ( $2 \times 4$ ) array, 18 dBi gain is observed. Application of the quasi-planar SMH to the four- and eight-elements patch array enhances the gain of array by 4 dB. However, about 9 dB enhancement in side lobe level is observed because of SMH. The horn does not degrade RL.

The gain of MPA array has been successfully enhanced with reasonable bandwidth by Rahman *et al.* in [93], [96]. Further, Ranga *et al.* [97] have reported gain modification of an ultra-wideband (UWB) slot antenna by using SMSH. Horn having slant angle  $\theta = 45^\circ$  is mounted on slot to modify directivity as well as gain. SMSH has marginal effects on impedance BW. The mean gain of the slot radiating antenna is 5.67 dBi, while maximum gain change is 1.1 dB and the impedance BW is 149%. The peak gain of slot antenna combined with a SMSH is 11 dBi. However, its mean gain modification over mean gain

of bare slot radiating antenna is approximately 2.03 dB. This antenna exhibits a 10 dB RL bandwidth of 145% i.e., 15.48 GHz (2.9 GHz - 18.38 GHz).

Subsequently, Albino *et al.* [66] have proposed an antenna design, which utilizes a ferrite ring to modify antenna gain without sacrificing impedance BW. Ferrite ring is incorporated at a certain distance from circumference of circular patch. The ferrite ring enhances the gain by forcing constructive interference in-between incident and reflected fields inside substrate. Results of MPA in combination with traditional dielectric substrate (without ferrite ring) and in combination with presented substrate (with ferrite ring) are appraised in [66]. Former is referred to as traditional substrate and latter (dielectric-ferrite) as the hybrid substrate. Design that utilizes hybrid substrate shows peak gain of 10.9 dBi in frequency band of 5.5 - 6 GHz, with mean gain of 9.28 dBi. However, traditional substrate shows a peak gain of 6.37 dBi in same frequency band, and mean gain is observed to be 4.4 dBi. Hence, proposed hybrid configuration exhibits maximum gain modification of 4.53 dB. In most of the cases, the impedance BW is reduced with the increasing value of gain. But in presented structure, it is not alleviated, rather it is observed to be enhanced. Bandwidth of 8.62% is obtained using hybrid substrate, whereas only 6.7% is obtained for traditional substrate. Therefore by utilising new design, a modification of approximately 2% in impedance BW is obtained.

Sethi *et al.* [98] have proposed large-gain and wideband AC-MPA with SMSH for 60 GHz communication systems. The waveguide component of horn is fabricated on FR4 substrate. Then, antenna is adjusted to operate in a wideband of frequencies at 60 GHz. However, inclusion of FR4 has no other effect on the antenna performance, except to give support to mounting horn. Horn has a significant effect on modification of overall antenna gain without influencing resonating frequency / operational bandwidth. Gain as well as directivity of structure without horn are 5.6 dBi and 6.68 dBi respectively.

Simulated antenna satisfies less than -10 dB RL bandwidth of 8.3% (57.437 - 62.426 GHz) around 60 GHz. Gain as well as directivity of structure with horn are 11.65 dBi and 12.51 dBi respectively. Moreover, addition of horn results in enhancement of directivity and gain of presented antenna and it does not affect bandwidth and RL. Its estimated efficiency is 82%.

Nasimuddin *et al.* [99] were the first to propose novel method to boost gain of the DR antenna by incorporating quasi-planar SMH. An RDRA with dielectric constant 9.8 has been used in this design. This slot-coupled RDRA behaves as feeding system for SMH. DRA is located at center of rectangle-type coupling slot in ground plane. Consequently, proposed technique is physically stable and simple in fabrication. The proposed antenna is designed to resonate at 6.05 GHz. The simulation results show that with conventional DRA (without SMH), maximum gain achieved is 5.8 dBi and the impedance BW is approximately 3.7% (based on 10 dB RL). Whereas for the DRA with surface mounted horn, maximum gain obtained is 9.0 dBi and the impedance BW is approximately 4% (5.94 - 6.18 GHz). Hence, the maximum antenna gain is enhanced by 3.2 dB because of the surface mounted horn.

Nasimuddin *et al.* [11] have extended their own work in [99], to propose a low-profile and high-gain AC-RDRA with quasi-planar SMH. By adjusting slant angle and position of horn for a fixed horn height, the gain of DRA is optimized. Full height of this fabricated configuration is  $0.172 \lambda_0$  i.e. 8.61 mm at 6.0 GHz. Therefore, total antenna structure is quasi-planar in nature. SMH is constructed from copper sheet. The DRA is fed by a 50- $\Omega$  MSL. This antenna may be utilized for low-profile, high-gain, and antenna-array applications. The measured gain of the conventional DRA (without horn) is 3.6 dBi, and with SMH, it is 8.5 dBi at 6.0 GHz frequency. Thus, SMH improves the gain of DRA by 4.9 dB. The simulation depicts that the gain may be further enhanced by

approximately 1 dB, if SMH is supported on a foam structure. The impedance BW achieved is approximately 3.6%.

Nasimuddin *et al.* [100] have further extended the work presented in [11] to achieve very large bandwidth along with high-gain and low-profile. A broadband hybrid DRP element [77] has been integrated with a quasi-planar SMSH for gain as well as bandwidth enhancement. Full height of this antenna is approximately 8.6 mm. Moreover, proposed hybrid element includes a cross DR aperture coupled to a metallic patch. The patch resonator and dielectric resonator are coupled by a slot (upper slot) in the microstrip patch. The hybrid element is coupled to an MSL via a second (lower) slot. In this configuration, hybrid dielectric resonator patch element behaves as a feeding source for the SMSH. The simulated results indicate an impedance BW of 26% (6.03 GHz - 7.88 GHz) and an antenna gain of approximately 9.0 dBi over entire bandwidth. Whereas, the measured results show 21.3% (6.07 GHz - 7.52 GHz) 10 dB RL bandwidth and an antenna gain of approximately 9.0 dBi over complete bandwidth. Initially, the hybrid DRP element is designed for large impedance BW. Subsequently, it is combined with SMSH for gain improvement, without adversely affecting the impedance BW. The patch as well as DR contributes to the radiation [77]. Gain of dielectric resonator on patch is enhanced, while maintaining height of surface mounted short horn approximately same as height of DRP. SMSH is made of copper strips, and it is placed on a manufactured aperture coupled hybrid DRP element by using metal screws. It is apparent that cross dielectric resonator on patch improves antenna gain by approximately 0.5 dB in comparison to corresponding RDR on patch. Moreover, inclusion of SMSH to DRP has also enhanced the extent of back-lobe by approximately 5 dB. It is inferred that the surface mounted short horn fabricated from copper strips has more gain in comparison to an SMSH fabricated from a copper block [101] or from a PVC block [95].

Nasimuddin *et al.* [102] have shown the effects of horn material on the antenna performance. For this purpose, the horns made with four different materials are investigated: (a) copper strips, (b) copper block, (c) copper film on PVC substrate ( $\epsilon_r = 2.2$ ) and (d) copper film on epoxy glass substrate ( $\epsilon_r = 4.4$ ). In the presented structure, the AC-DRA works as a feeding source for a surface mounted short horn. The horn slant angle of  $45^\circ$  is selected because of its fabrication simplicity. For comparison purpose, DRA without SMSH is also designed. Its gain is found to be 3.7 dBi and the 10 dB RL bandwidth is found to be 3.2% (5.85 GHz - 6.03 GHz). Then an elaborated analysis of effects of horn material on the antenna characteristics is performed. It is apparent that antenna gain is substantially affected due to horn material. A foam / self-supported horn made of thin copper strips exhibits largest gain (9.7 dBi). However, a horn made of PVC substrate coated with copper film possesses least gain (7.3 dBi) at 6.0 GHz. But, value of gain of the horn fabricated from copper block (8.7 dBi) is in-between. After this theoretical discussion, an SMSH is constructed from thin copper strips and is mounted on dielectric resonator antenna. At 6 GHz, measurement gain is observed to be approximately 9.8 dBi, which is akin to theoretically analysed gain of 9.7 dBi. Then, the effect of SMSH material on the radiation pattern has been studied. The larger beam-width is observed with the usage of PVC / epoxy as supporting substance. It illustrates reduction in antenna gain in these materials. It is also inferred that horn made of copper strips delivers slender beam, enhanced antenna gain as well as fair polarization clarity.

Subsequently, the authors have demonstrated that how antenna BW may be substantially improved, without any adverse effect on its gain, by replacing dielectric resonator antenna in earlier antenna with a wideband element. This wideband element chosen here is a rectangle-type DRP element [77]. The measured 10 dB RL bandwidth is approximately 24.7% (6.10 GHz - 7.82 GHz). The average gain alteration in impedance

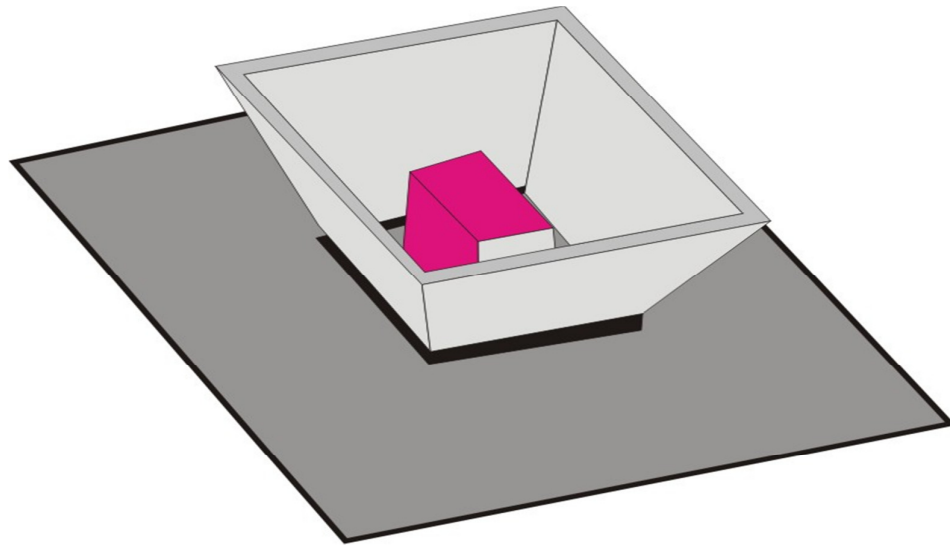
BW is approximately 1 dB. However, antenna gain is approximately 8.5 dBi over whole impedance BW. Height of horn is approximately same as the height of feed element (DR or DRP). Therefore, there is insignificant enhancement in the profile of antenna due to its combination with horn. Here, optimum slant angle of SMSH is  $45^{\circ}$ . Horn fabricated from thin conducting films, which is supported by using low permittivity material like foam, has least beam-widths and largest gains. The strength of surface mounted horn as broadband large-gain antenna is showcased in [102], where a DRP antenna is used to feed.

This chapter is organized as follows. Design paradigm of presented structure has been discussed in section 3.2. Section 3.3 demonstrates the design and simulation of RDRA with SMSH. The simulation and measured results (with fabricated horn) have been illustrated and compared in section 3.4. The measured results of RDRA and RDRA with SMSH have been compared in section 3.5. This chapter is concluded in section 3.6.

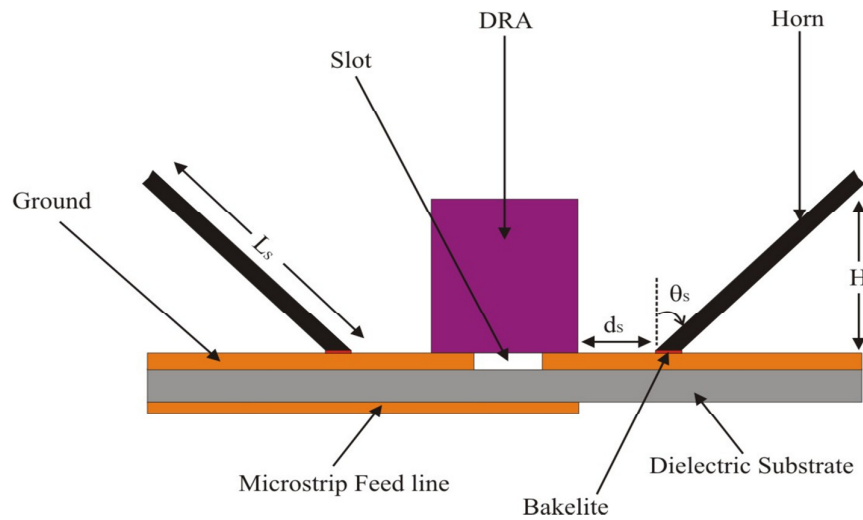
## **3.2 DESIGN MODEL FOR PROPOSED APERTURE COUPLED RDRA WITH SMSH**

RDRAs are more attractive as compared to other geometries, for its fabrication advantages and also because of the existence of two independent aspect ratios. The antenna characteristics such as resonance frequency, radiation pattern and bandwidth can be conveniently controlled through adjustment of its aspect ratios [142]. Its two dimensions can be adjusted independently for a particular resonance frequency and for a material with particular permittivity. Cylindrical DRAs (CDRAs) have also been widely used in many of applications [143]-[148] at microwave frequencies. But, it becomes difficult to fabricate the CDRAs at millimeter-wave frequencies owing to its small-size. Therefore at these frequencies, RDRAs are preferred over the CDRAs. Aperture coupling

is a technique of feeding the antenna, in which energy of microstrip line (MSL) is coupled via a slot in ground plane that feeds radiating element. Aperture acts as magnetic current flowing parallel to length of slot that stimulates magnetic fields in dielectric resonator antenna. This aperture contains a slot cut in the ground plane, which is fed through an MSL below ground plane. In aperture coupled feed, no physical contact exists between feed and radiator, as feeding network is positioned beneath ground plane. Therefore, impedance BW is enhanced significantly due to isolation of the spurious feed radiations from the antenna component. The aperture coupled elements have been shown to possess much wider bandwidths as compared to coaxial probe or microstrip strip line-fed elements [81]-[86]. The shape and size of coupling aperture controls the extent of coupling between feed line and radiating element. Thin rectangle-type slots offer better coupling than round apertures. Further, optimum tuning of the dimensions of slot gives improved radiation characteristics for the designed antenna. The extent of coupling is usually tuned by changing position of DRA w.r.t. slot. The symmetric positions of feed line, aperture and the radiating element offer maximum coupling. To provide symmetry, the coupling aperture should be centered between radiating element and feed line. Moreover, slot coupling is an attractive scheme for combining dielectric resonator antennas with printed feed configurations.



(a)



(b)

**Fig. 3.1: RDRA with surface mounted short horn**

(a) Design model

(b) Cross-sectional view

This section presents the design model of the presented antenna. The design model is demonstrated in Fig. 3.1a. The cross-section of presented antenna structure is depicted in Fig.3.1b, where a short rectangular horn with slant length  $L_s$ , slant angle  $\theta_s$  and height  $H$  is used in combination with an RDRA to increase its gain. As illustrated in Fig. 3.1b,

slant length of horn makes angle  $\theta_s$  (slant angle) w.r.t. vertical-axis to DR. In this configuration, aperture coupled RDRA (AC-RDRA) is not primary radiating element. This is a feeding source for SMSH. In this, horn is fabricated using silver metal, and it is placed on surface of AC-RDRA. The designing and simulation of RDRA with SMSH is presented in the next section.

### **3.3 DESIGN AND OPTIMIZATION OF SMSH**

The horn is an aperture type of antenna, which is fed by an RDRA in presented work. Horn aperture can have various shapes. Most common aperture shapes are square, rectangular and conical. The objective of using horn is to direct the radiated electromagnetic waves in a desired direction. Horn confines the EM field on / in vicinity of radiating antenna. The increased directivity in turn enhances its efficiency as well as gain. In other words, the horn can also be called as wave director. When used in arrays, in addition to improving the gain of array elements, the horn also provides isolation between these elements. Gain enhancement of elements results in reduced number of array elements, which in turn reduces the size as well as cost of entire array. When horn is used in combination with MPA, the horn walls contribute in concentrating fringing fields at edges. It also alleviates mutual coupling among neighboring elements. However, antenna matching is improved by adding this artificial horn [94]. The implementation of horn has a significant positive impact on the enhancement of antenna gain, which doesn't influence the operating frequency and effective bandwidth [98]. However, radiating element and horn can be designed separately.

In this section, the design procedure of SMSH (integrated with RDRA) and its fabricated model are presented. First, the preliminary dimensions of SMSH are calculated for the lower resonance frequency [96], and then these dimensions are optimized by

parametric optimization to achieve the maximum gain at both operating frequencies of antenna. While designing an RDRA with SMSH, the parametric values of RDRA are observed to be similar as used in chapter 2 (in the design of AC-RDRA, which operates in C- and X-band). A bakelite layer of thickness 1.5 mm is inserted between the ground plane and horn to provide insulation. The thickness of horn  $t_h$  is 2 mm. The preliminary value of slant angle  $\theta_s$  is considered to be  $45^\circ$ . The preliminary values of slant length  $L_s$  and horn position  $d_s$  are calculated from following relations [96]

$$L_s = \frac{\lambda_0}{4} \quad (3.1)$$

$$d_s = \frac{\lambda_0}{8} \quad (3.2)$$

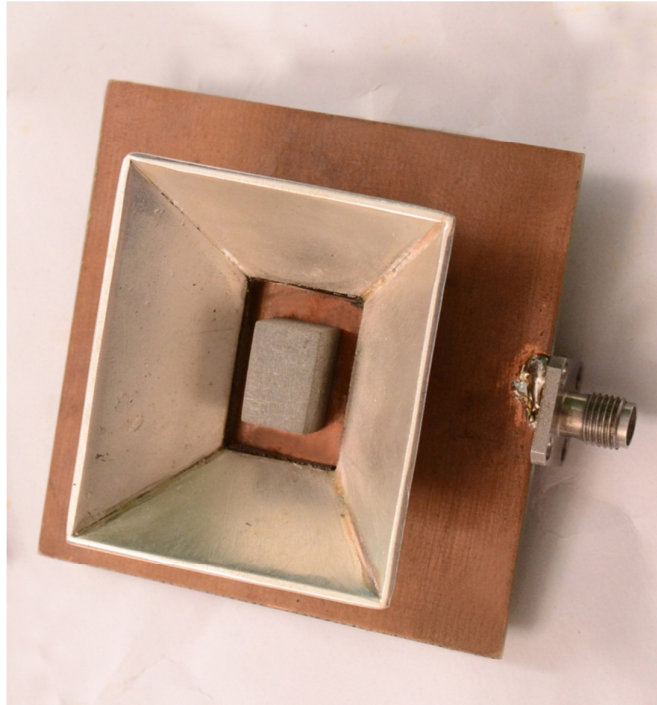
where,  $\lambda_0$  is wavelength at resonating frequency and  $d_s$  is separation distance in-between horn and edge of RDRA. After getting the initial values of slant length and horn position from Eq. (4.1) and Eq. (4.2), these two parametric values are optimized along with horn slant angle  $\theta_s$ , to achieve the maximum gain at its operating frequency.

Table 3.1 shows the final parametric values (after optimization) of SMSH with rectangular base. The maximum antenna gain is achieved at the center frequencies 5.75 GHz and 7.95 GHz, with the values of  $L_s$ ,  $d_s$  and  $\theta_s$  fixed as 16.8 mm, 3.2 mm and  $44.5^\circ$  respectively. The height of SMSH is 12 mm, whereas the full height of antenna is 14 mm ( $0.27 \lambda_0$ ). The horn position (separation distance) is 3.2 mm. The horn bottom aperture (at substrate level) is  $19.6mm \times 13.5mm$ , whereas the horn top aperture is  $43.2mm \times 37.1mm$ .

**TABLE 3.1**  
**PARAMETRIC VALUES OF SMSH**

Parameter	Value
Horn slant length, $L_s$	16.8 mm
Horn slant angle, $\theta_s$	$44.5^\circ$
Horn position, $d_s$	3.2 mm
Horn height, $H$	12 mm
Horn thickness, $t_h$	2 mm
Horn bottom aperture (substrate level)	$19.6mm \times 13.5mm$
Horn top aperture	$43.2mm \times 37.1mm$
Bakelite height, $h_b$	1.5 mm

Fig. 3.2 portrays the top view of fabricated model of AC-RDRA with SMSH. Whereas, its bottom view is illustrated in Fig. 3.3. In this section, dimensions of different horn parameters have been found by using the optimization functions of HFSS. Various simulation results and measured results (with fabricated antenna) are presented in the next section.



**Fig. 3.2: Fabricated model of RDRA with SSMH (top view)**

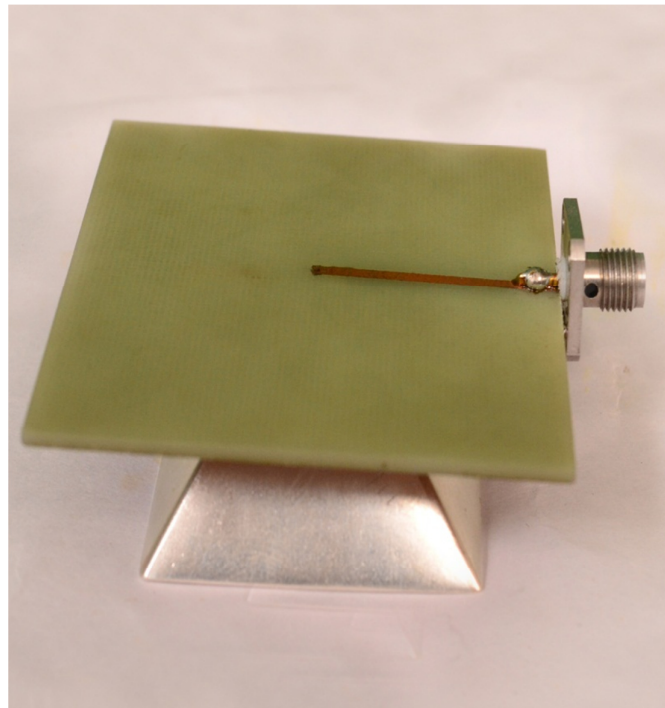


**Fig. 3.3: Fabricated model of RDRA with SSMH (bottom view)**

### 3.4 SIMULATION AND EXPERIMENTAL RESULTS WITH PERFORMANCE ANALYSIS

This section presents various simulation results and measured results (with fabricated antenna) of the AC-RDRA with SMSH. Fig. 3.4 illustrates the return loss (RL) observed through simulation and the measured (with fabricated model) RL of aperture coupled RDRA mounted with short horn. It is observed that the resonance frequency of proposed structure is not affected by changing various horn parameters.

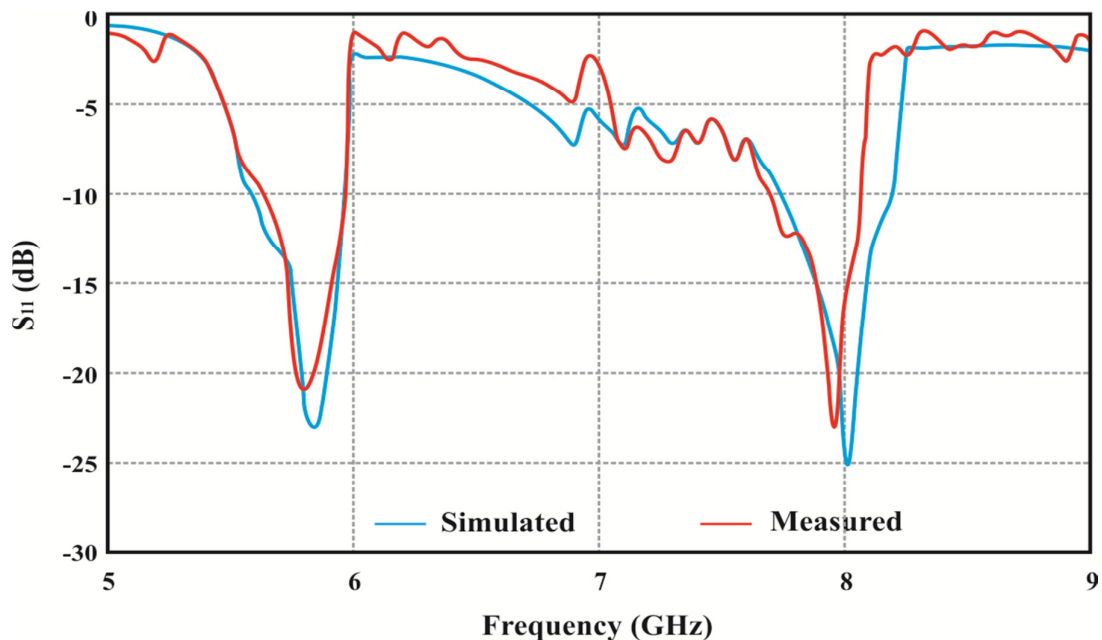


**Fig. 3.4: Frequency response of RDRA with SMSH (near field measurement)**

It has been observed that the designed dual-band RDRA with SMSH resonates at two frequencies. The simulation resonance frequencies are 5.8 GHz and 8.0 GHz, whereas the measured resonance frequencies are 5.75 GHz and 7.95 GHz. The impedance BW obtained through simulation is approximately 6.5 % (380 MHz) at 5.8 GHz, and approximately 5.5 % (440 MHz) at 8.0 GHz. Whereas, the measured (with fabricated antenna) impedance BW is approximately 5.4 % (315 MHz) at 5.78 GHz, and

approximately 4.7 % (375 MHz) at 7.95 GHz. However, RL observed through simulation is -23 dB at the lower resonance frequency (5.8 GHz) and -25 dB at upper resonance frequency (8.0 GHz). Whereas, the measured RL values (with fabricated antenna) are -21 dB and -23 dB at 5.75 GHz and 7.95 GHz frequency respectively. For comparison purpose, the RL observed through simulation and measured RL are plotted together in the same figure, and a good harmony is observed between both results with RL less than -10 dB. However, gain advantages achieved through simulation are 9.3 dBi and 11.1 dBi at 5.8 GHz and 8.0 GHz frequency respectively. Whereas, the measured gain advantages (with fabricated antenna) achieved are 08.95 dBi and 10.65 dBi at 5.75 GHz frequency and 7.95 GHz frequency respectively. The gain achieved through simulation and the measured gain at lower resonating frequency (5.8 GHz) are plotted together in Fig. 3.5. Whereas, its gain achieved through simulation and measured gain at upper resonance frequency (8.0 GHz) are depicted in Fig. 3.6.

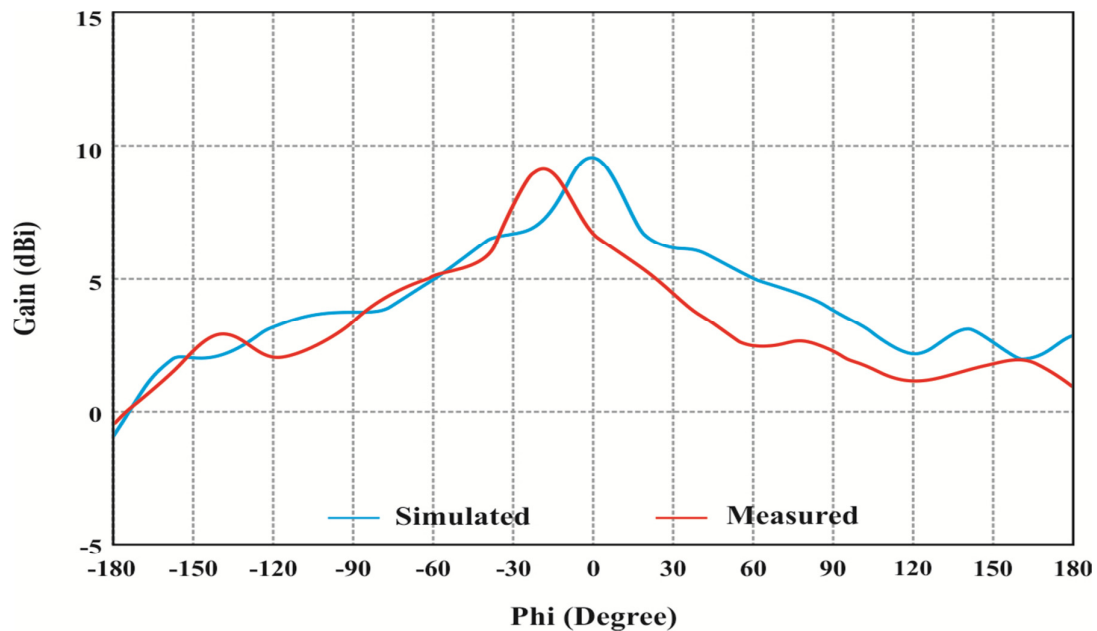


**Fig. 3.5: Gain response of RDRA with SMSH at 5.8 GHz (far field measurement)**

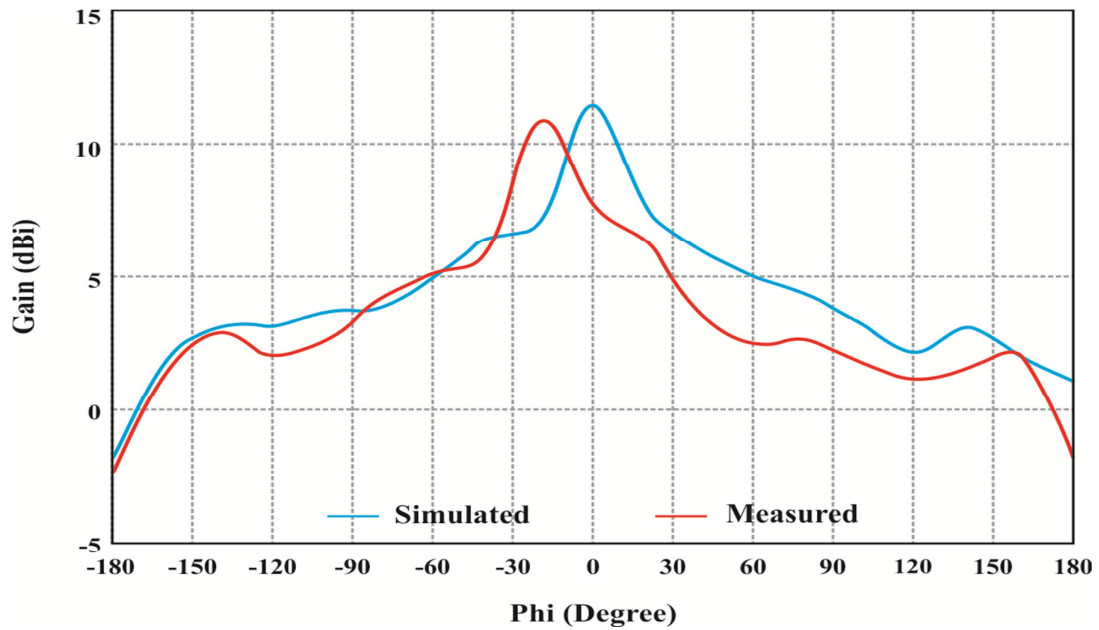


**Fig. 3.6: Gain response of RDRA with SMSH at 8.0 GHz (far field measurement)**

The measured gain is marginally lower as compared to gain achieved through simulation. Fig. 3.7 illustrates the radiation pattern (E-plane) of RDRA with SMSH, whereas Fig. 3.8 illustrates the radiation pattern (H-plane) of RDRA with SMSH observed through simulation as well as through measurement (with fabricated antenna) at resonating frequency 5.8 GHz. Fig. 3.9 illustrates the radiation pattern (E-plane) of RDRA with SMSH, whereas Fig. 3.10 illustrates the radiation pattern (H-plane) of RDRA with SMSH observed through simulation as well as through measurement (with fabricated antenna) at resonating frequency 8.0 GHz.

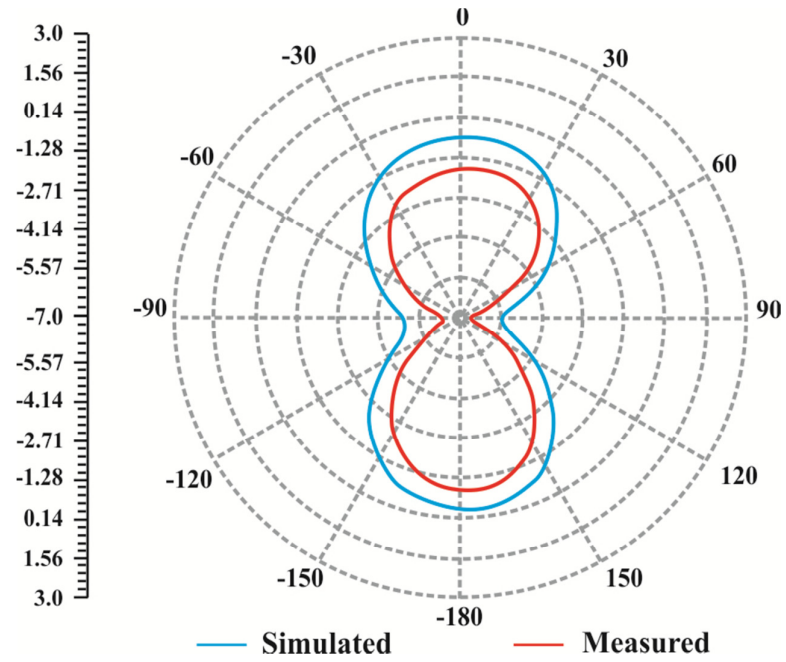


**Fig. 3.7: Radiation Pattern (E-Plane) of RDRA with SMSH at 5.8 GHz**

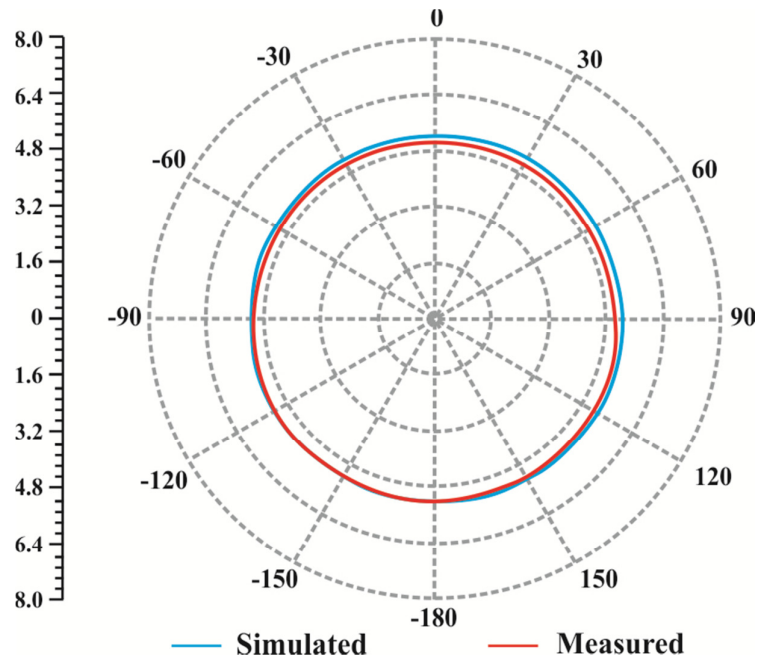


**Fig. 3.8: Radiation Pattern (H-Plane) of RDRA with SMSH at 5.8 GHz**

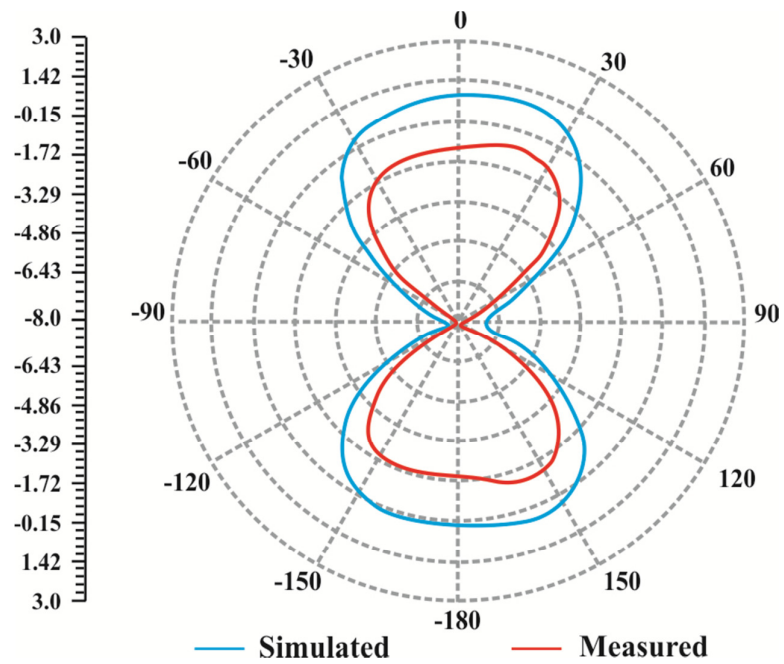


**Fig. 3.9: Radiation Pattern (E-Plane) of RDRA with SMSH at 8.0 GHz**

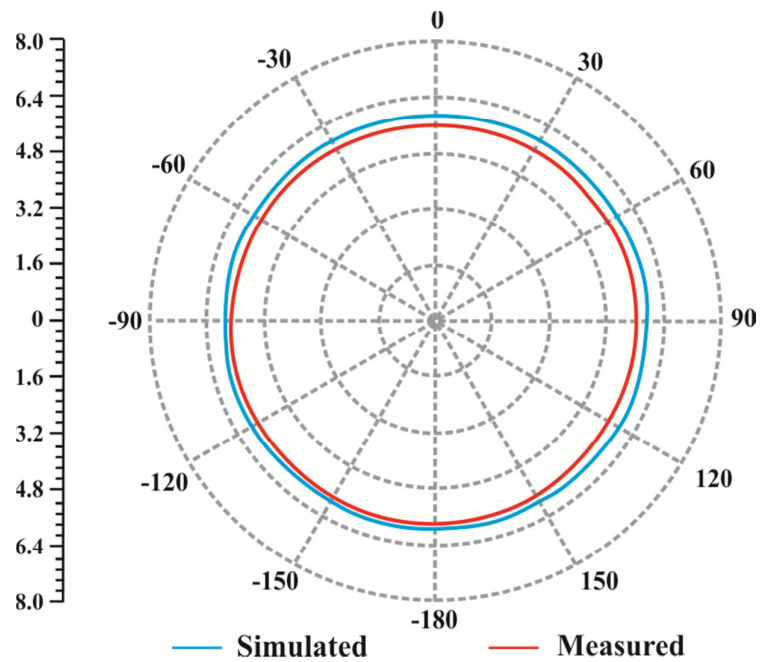


**Fig. 3.10: Radiation Pattern (H-Plane) of RDRA with SMSH at 8.0 GHz**

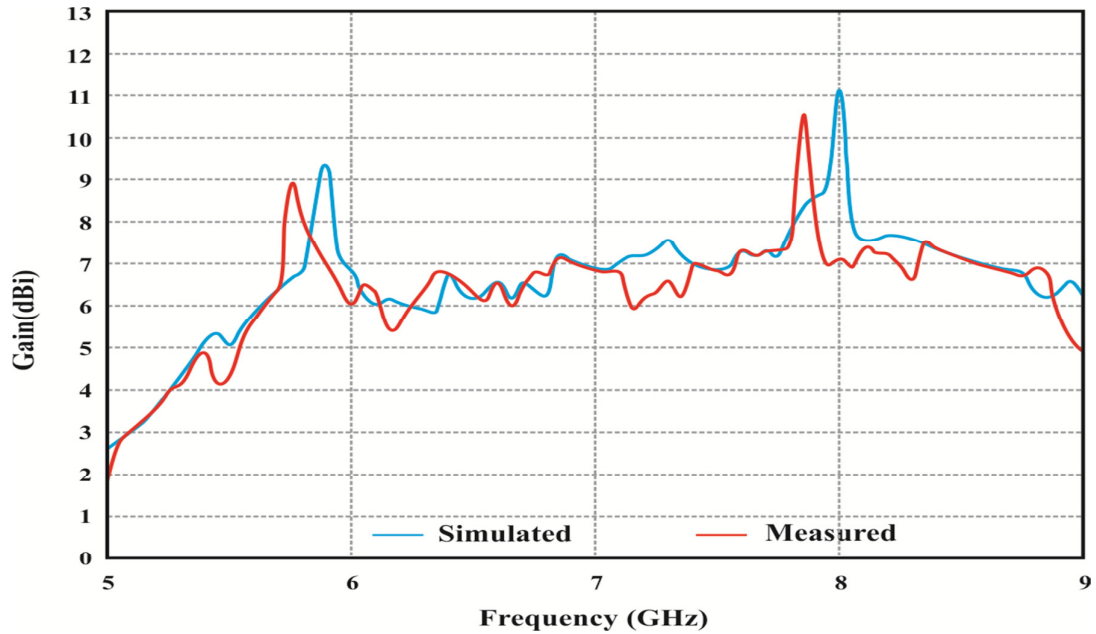


**Fig. 3.11: Gain v/s frequency plot of RDRA with SMSH**

Fig. 3.11 illustrates gain achieved through simulation as well as measured gain for the frequency range 5 GHz - 9 GHz. Simulation results and measured results (with fabricated antenna) for the designed RDRA are shown in Table 3.2.

**TABLE 3.2  
SIMULATION AND MEASURED RESULTS FOR RDRA WITH SMSH**

ATTRIBUTE	SIMULATED RESULT		MEASURED RESULT	
<b>RESONANCE FREQUENCY</b>	5.8 GHz	8.0 GHz	5.75 GHz	7.95 GHz
<b>GAIN</b>	9.3 dBi	11.1 dBi	8.95 dBi	10.65 dBi
<b>BANDWIDTH</b>	380 MHz	440MHz	315 MHz	375 MHz
<b>RETURN LOSS</b>	-23 dB	-25 dB	-21 dB	-23 dB

Marginal differences between the simulation results and measured results (with fabricated antenna) for RDRA with SMSH can be observed from the Table 3.2, which may be due

to the manufacturing tolerances. The gain and bandwidth obtained through simulation are slightly higher as compared to corresponding measured (with fabricated antenna) results. At lower resonance frequency (5.8 GHz) as well as at higher resonance frequency (8.0 GHz), the measured RL (with fabricated antenna) is slightly higher than the RL observed through simulation. However, the bandwidth as well as the highest gain achieved are more, and the return loss is also less in comparison to the results presented in [149]. The measured results of RDRA without SMSH (mentioned in chapter 2) and RDRA with SMSH are compared in the next section.

### **3.5 COMPARISON OF EXPERIMENTAL RESULTS FOR CONVENTIONAL RDRA AND RDRA WITH SMSH**

This section gives a detailed comparison of the measured results related to RDRA fabricated with and without SMSH. Fig. 3.8 shows the comparison of measured gain at lower resonance frequency (5.8 GHz) for conventional RDRA (without SMSH) and also for the RDRA with SMSH. At 5.8 GHz, the measured gain of conventional RDRA is 8.1 dBi, whereas the measured gain of RDRA with SMSH is 8.95 dBi. Fig. 3.9 shows the comparison of measured gain at upper resonance frequency (8.0 GHz) for the conventional RDRA and RDRA with SMSH. At 8.0 GHz, the measured gain of conventional RDRA is 9.05 dBi, whereas the measured gain of RDRA with SMSH is 10.65 dBi. Fig. 3.10 depicts measured gain vs. frequency plot for conventional RDRA as well as RDRA with SMSH for the frequency range 5 GHz - 9 GHz. A comparison of measured results for the conventional RDRA and RDRA with SMSH is shown in Table 3.3.

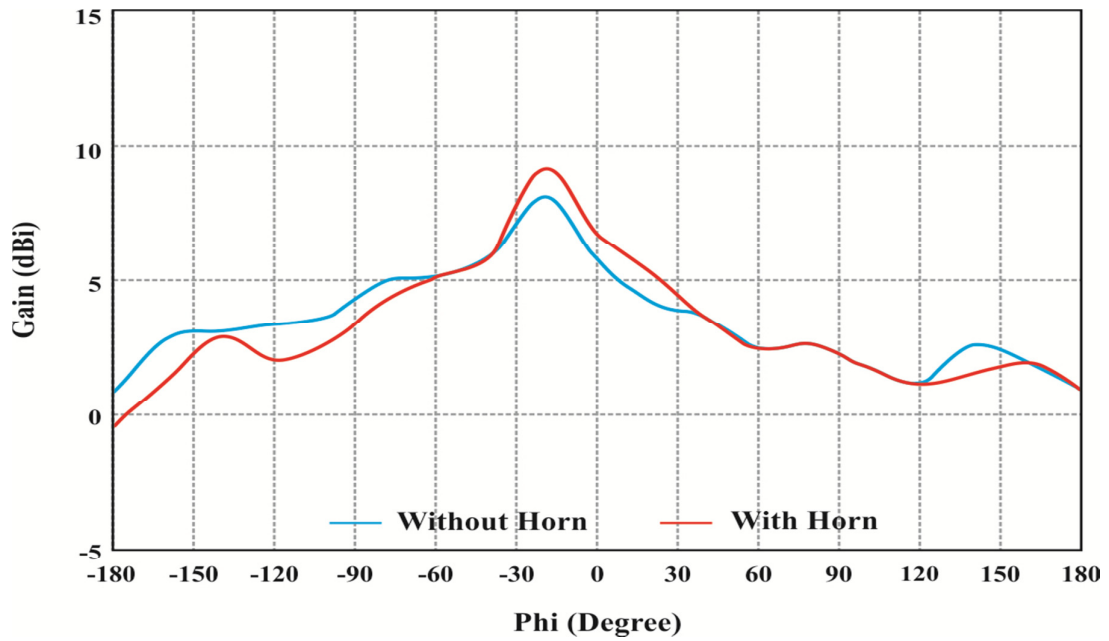


**Fig. 3.12: Measured gain response of RDRA with SSMH and without SSMH at 5.8 GHz**

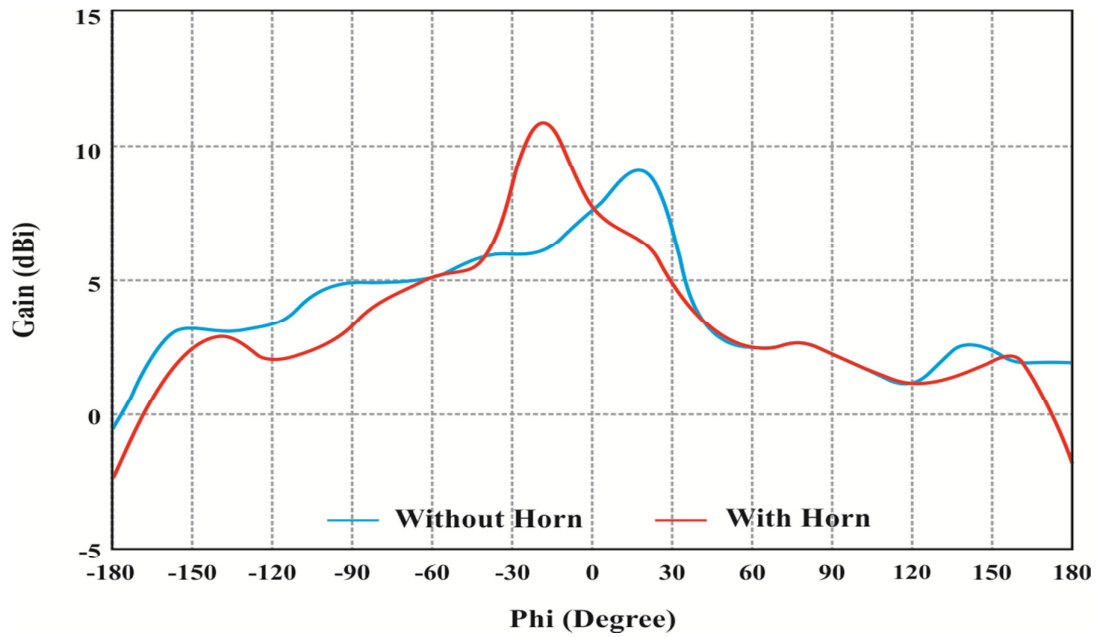


**Fig. 3.13: Measured gain response of RDRA with SSMH and without SSMH at 8.0 GHz**

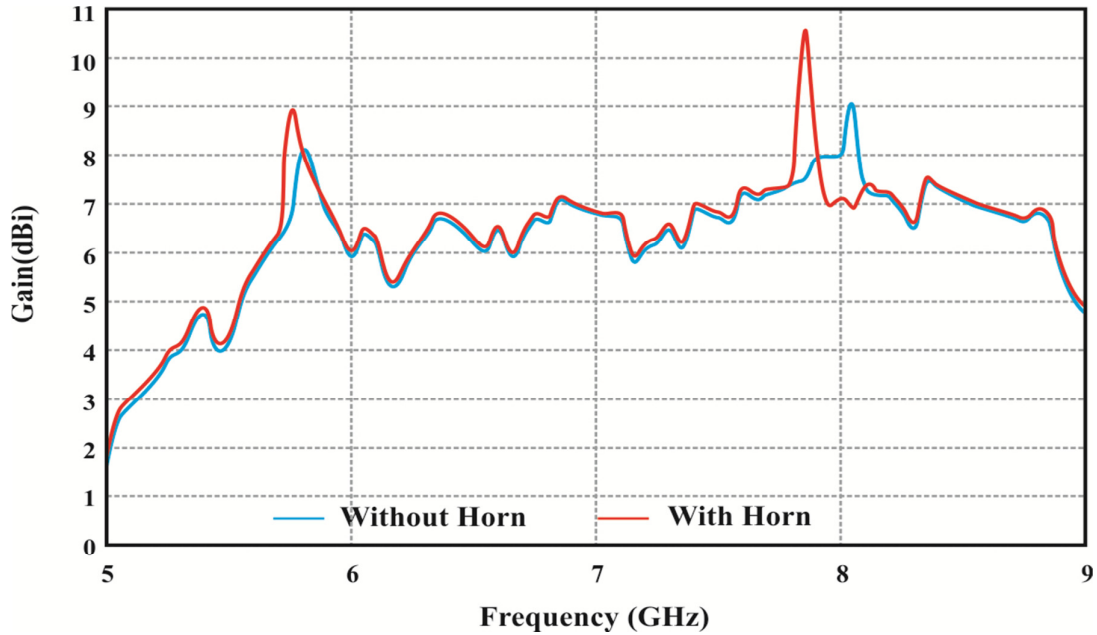


**Fig. 3.14: Measured gain v/s frequency plot of RDRA with SSMH and without SSMH**

**TABLE 3.3**

**COMPARISON OF MEASURED RESULTS FOR CONVENTIONAL RDRA AND RDRA WITH SSMH**

ATTRIBUTE	RECTANGULAR DRA		RECTANGULAR DRA WITH HORN	
	5.80 GHz	7.95 GHz	5.75 GHz	7.95 GHz
<b>RESONANCE FREQUENCY</b>	5.80 GHz	7.95 GHz	5.75 GHz	7.95 GHz
<b>GAIN</b>	8.1dBi	9.05 dBi	8.95 dBi	10.65 dBi
<b>BANDWIDTH</b>	340 MHz	420 MHz	315 MHz	375 MHz
<b>RETURN LOSS</b>	-19 dB	-20.5 dB	-21 dB	-23 dB

It is apparent from Table 3.3 that resonating frequency of RDRA is insignificantly affected by mounting a short horn. However, gain of conventional RDRA is improved by 0.85 dB at lower resonating frequency, whereas it is enhanced by 1.6 dB at upper resonating frequency due to usage of SSMH. The bandwidth of RDRA is marginally decreased at two resonance frequencies because of SSMH. At lower resonance frequency,

the RL is improved by 2 dB, whereas at upper resonance frequency, it is improved by 2.5 dB due to the usage of SMSH.

### **3.6 SUMMARY OF CHAPTER**

In this chapter, a dual-band aperture coupled RDRA (mentioned in chapter 2) has been integrated with an SMSH for its performance enhancement. The designed structure has been fabricated as well as tested. Simulation outcomes have been confirmed by conducting practicals on fabricated antenna. The primary objective is the gain enhancement of RDRA without any adverse effect on the bandwidth. The simulation and measured results (with fabricated antenna) illustrate that the gain of RDRA is enhanced at nearly all the frequencies in range 5 GHz - 9 GHz. The presented antenna (RDRA with SMSH) provides enhanced gain at both the resonance frequencies as compared to the conventional RDRA (without SMSH). The proposed structure is found to be mechanically stable. This dual-band RDRA mounted with short horn has found applications in C- and X-band based communication systems, such as satellite communication and wireless LAN. In this chapter, a dual-band RDRA with SMSH has been designed. However in the next chapter, a hemispherical DRA is designed and its performance is improved by incorporating an electromagnetic band-gap configuration.

**DESIGNING OF HIGH-GAIN HEMISPHERICAL DRA (HDRA)  
WITH ELECTROMAGNETIC BAND-GAP STRUCTURE**

---

Application of electromagnetic band-gap (EBG) structure in gain augmentation of hemispherical dielectric resonator antenna (HDRA) has been investigated in this chapter. It has been demonstrated that performance of dielectric resonator antenna (DRA) can be appreciably enhanced by proficiently restraining the propagating surface-waves. The performance enrichment is due to the transformation of surface-waves into radiations by the cylindrical EBG structure.

Electromagnetic band-gap substrate is based on mushroom-like configuration, which is created by blending of two periodic configurations. First periodic structure consists of three metallic rings. Whereas, second periodic structure is made of vertical grounding metallic vias. These are placed in a particular fashion to form radial and circular periodic configurations. The metal rings are short circuited to the ground through these periodic vias. The periods of both configurations are optimized in terms of gain maximization at operating frequency of antenna. HDRA is excited using a probe-feed and incorporated within a cylinder-type EBG structure to boost antenna gain.

It is apparent that gain of HDRA is enhanced by approximately 3.7 dB due to the usage of cylindrical EBG structure. It is found that the bandwidth is also improved due to incorporation of EBG structure. The designed antenna provides a minimum gain of 6 dBi in the frequency range 3.3 GHz - 5 GHz. HFSS software is employed for the simulation of antenna structure.

## 4.1 INTRODUCTION

In past few years, a lot of emphasis has been given on exploration of DRAs. Dielectric resonator antennas are perfect candidates for antenna applications as these offer numerous advantages over the microstrip patch antennas (MPAs). No conducting parts are there in dielectric resonator antennas, and therefore these offer low dissipation loss. However, the gain offered by DRAs does not suit many of the engineering applications. Numerous attempts have been made to boost gain of dielectric resonator antenna. A DRA utilizing a two-layer configuration with a high dielectric constant has been presented in [58]. This structure provides a trivial gain improvement of approximately 1.2 dB. An alternative paradigm based on offset dual-disk dielectric resonator (DR) structure is explored in [62]. Also, a dielectric resonator antenna using stacked DRs with air-gap in-between patch and DR is described in [133]. However, the proposed topologies may increase size as well as cost of the DRA.

An additional technique to boost the gain of antenna is to diminish the losses due to surface-wave propagation, as these can produce ripples in radiation pattern. Surface-waves are superfluous waves, which are trapped all along substrate. Because of this trapped electromagnetic (EM) energy, efficacy and gain of antenna gets alleviated radically. A substantial extent of EM appears to get trapped inside substrate. This in turn results in the superfluous surface-wave loss. However, antenna gain enhancement can be achieved by removing these surface-waves. Numerous techniques have been projected to trim down the properties of surface-waves [104]-[110]. One of the remedies recommended is synthesized substrate, which reduces effectual permittivity of substrate beneath and around the patch [104]-[105]. In various approaches, different researchers have either used parasitic elements [106]-[107] or incorporated new techniques to reduce surface-waves for gain improvement [108]-[110]. EBG structures, which are also

recognized as photonic crystals [111], are frequently incorporated to perk up antenna efficacy [112]-[118]. By producing EBG structures in the substrate, surface-waves may be effectively removed. These arrangements are capable of opening a band-gap (range of frequencies) in which proliferation of EM waves is prohibited i.e., EBG chunks the surface-waves from spreading in a definite band-gap. Reduction in mutual coupling as well as co-site interference are additional benefits of electromagnetic band-gap structures.

The surface-waves are reduced by the EBG structure, but antenna gain improvement is also because of coupling between DRA and EBG configuration. The efficiency and efficacy of antenna aperture can be considerably enhanced, without escalating antenna dimensions, by properly using these artificial materials (EBG structures). Numerous researchers have publicized that EBG structures can drastically augment its beneficial features like directivity, gain, bandwidth, RL as well as compactness in size etc., when combined with MPAs or DRAs [103]. Due to amalgamation of artificial resonant materials, the surface-waves get radiated along with desired radiations and boosts up antenna gain. It doesn't authorize surface-waves to proliferate in substrate within band-gap, in the region of resonance frequency of the antenna. Consequently, the entire radiations spread up in the vertical path and improve antenna gain. In each blueprint using EBG structure, the antenna is designed with the resonance frequency falling in band-gap of EBG substrate. For the gain improvement, a range of MPAs as well as DRAs have been designed by the researchers in the past few years with EBG substrates.

Boutayeb *et al.* [119] have proposed a novel circularly periodic EBG configuration to enhance gain of the circular MPA. The presented electromagnetic band-gap structure is based on a mushroom-type configuration, which includes two different periodic configurations. First periodic configuration consists of metallic strips. Whereas, second structure consists of vertical metallic vias, which are positioned such that these give rise

to radially and circularly periodic configuration. Square metallic plates, in which various vias are etched, surround an MPA. These metallic plates result in significant reduction of surface-waves generated in the substrate, which in turn enhances the antenna gain. Coaxial probe feeding is used to excite the MPA. The circular MPA is integrated within a cylindrical EBG substrate and is designed to resonate at 2.6 GHz. The designed antenna is matched to frequency range 2.56 - 2.64 GHz, that represents the fractional bandwidth of 3%. However, peak gain of this antenna is 9.33 dBi and gain improvement is approximately 2.9 dB.

Rao *et al.* [67] have further extended the work of Boutayeb [119] to modify gain as well as bandwidth of an MPA. Gain is increased by suppression of surface-wave losses due to the creation of EBG structures by drilling vias in substrate. The bandwidth is improved due to the usage of multi-layer substrate. Both, the bandwidth and patch size, increase with the decreasing value of the size of dielectric. The authors have combined the two substrates to utilize the benefits of both high as well as low permittivity materials i.e., wide bandwidth (due to high dielectric value substrate) and low patch size (due to low dielectric value substrate) respectively. A layer of glass with relative permittivity 4.6 is sandwiched between two silicon layers of relative permittivity 11.9 to form a multi-layer substrate. Two layers of silicon (high permittivity material) provide reduced patch size, whereas a glass layer (low dielectric constant material) provides high bandwidth. Here, silicon is strategically placed beneath the patch for maximum size reduction. Consequently, the size is increased marginally, but bandwidth is enhanced significantly. In proposed design, a periodic structure of EBG (holes in the substrate) is used. Bandwidth increases from 9.5 % to 11 % and the gain increases by 1.769 dB (from 6.887 dBi to 8.656 dBi) by incorporating EBG structure.

Boutayeb *et al.* [119] and Rao *et al.* [67] have successfully enhanced the gain of patch antenna using EBG substrates. But in both the cases, the gain enhancement is not very high (less than 3 dB). Jazi *et al.* [125] have proposed a one-layer traditional mushroom-type EBG configuration to provide higher gain for a single-layer coaxial probe-fed MPA. Three rows of EBG unit cells surround a patch in E-plane as well as H-plane, which form a mushroom-like EBG structure. However, square patch is designed to work in X-band at resonating frequency 9.4 GHz. Both MPA and electromagnetic band-gap configuration are etched on top layer of substrate. The covering of patch in E-plane and H-plane with electromagnetic band-gap results in enhancement of gain of antenna by 3.4 dB. Gain of patch antenna without EBG is 6.4 dBi, and it is enhanced to 9.8 dBi by EBG structure. Further, electromagnetic band-gap surrounding patch, alleviates BRs. Simulation results demonstrate that antenna gain may still be enhanced up to 11 dBi by using larger EBG structure.

Kumar *et al.* [103] have extended the work of Jazi *et al.* [125] to propose three different EBG structures to suppress the surface-waves of an MPA operating at 11 GHz. An MPA, without any artificial material, is composed of a rectangle-type patch put above a substrate with ground plane at bottom, which is fed through a coaxial probe feeding. First EBG structure uses partial substrate elimination method, that boosts antenna gain by 3.06 dB to give 8.7 dBi gain. Second EBG structure uses a mushroom-like EBG to have a band-gap in 8 - 12 GHz range, which has been utilized as a substrate for this antenna. This EBG structure enhances antenna gain by 4.96 dB to give 10.6 dBi gain. Third EBG configuration is based on the dual-grid structure. This structure is simplest in design, which provides better band-gap properties, when utilized as substrate for MPA. It enhances the antenna gain by 3.57 dB to give 9.21 dBi gain. Among three EBG configurations, partial substrate removal method is simplest in design, but gain

improvement is less in comparison to other techniques. Whereas, a mushroom-like EBG structure provides maximum gain enhancement. But, the design and implementation of this structure is most complex among all. Grid-type EBG structure is quite simple, easy to implement and shows good gain improvement.

Jaglan *et al.* [126] have further explored the work presented in [67], [103], [119], [125] for the gain improvement of MPAs by the usage of electromagnetic band-gap substrates, and utilized this to increase the gain of MPA array. The EBG configuration consists of a two dimensional (2-D) lattice of metallic disks, which are conductively attached to ground plane through metallic vias. An electromagnetic band-gap structure is designed to resonate at 5 GHz. Small portion of substrate around patch is left, which prevents shifting of resonance frequency. The patch is excited through probe feeding system. The EBG structure provides 1.29 dB gain enhancement to give 4.56 dBi gain, as compared to 3.27 dBi gain achieved in the case of conventional MPA (without EBG). Along with the improvement in gain, simulation results illustrate improvement in the RL, directivity, F/B ratio as well as antenna efficiency. The lessening of mutual coupling among various antenna components is also analysed.

Hasan *et al.* [127] have proposed a design for the gain enhancement of DRA by using EBG structures. Authors have presented the design of uni-planar compact electromagnetic band-gap (UPC-EBG) millimeter-wave AC-DRA. The simulation outcomes for this antenna with / without UPC-EBG have been detailed in [127] to demonstrate benefits achieved due to usage of UPC-EBG. In the presented antenna, three UPC-EBG periodic configurations are placed symmetrically around dielectric resonator antenna. Coupling from MSL-feed to dielectric resonator antenna is implemented via an aperture. However, aperture dimensions are selected to offer ample excitation to dielectric resonator antenna. Both the proposed antennas, with and without UPC-EBG, have almost

the same resonance frequency (around 62.4 GHz). Here, peak gain is enhanced from 9.7 dBi to 10.4 dBi because of UPC-EBG. BRs are alleviated by approximately 5 dB at an angle of  $150^\circ$  (direction), to a maximum of 11 dB at an angle of  $180^\circ$  (direction). It is clear that, UPC-EBG modifies antenna efficiency and alleviates BR. Thus, final design has benefit of increased antenna efficiency, marginal enhancement in gain, and reduction in BR by suppression of surface-waves.

Hasan *et al.* [127] have enhanced the gain of an AC-DRA using EBG substrate, but the gain enhancement is insignificant (0.7 dB). Denidni *et al.* [128] have presented a novel hybrid DRA to modify its gain as well as impedance BW. The performance of a CDRA is enhanced due to the usage of a cylindrical EBG substrate. CDRA is excited through probe-feed and incorporated in a cylindrical electromagnetic band-gap substrate for gain enhancement. EBG configuration is based on a mushroom-type configuration, which includes a pair of two periodic structures. In this scenario, first configuration consists of metal strips, whereas second configuration is made of vertical metallic grounded vias. These vias are positioned so as to form radial as well as circular periodic configurations. The concentric rings of metal strips are designed on a grounded substrate. For comparison purpose, the reference as well as proposed antennas have been simulated and fabricated. The location of vias is similar to authors' earlier work in [119], where transversal period is kept fixed for every layer. It is observed that gain improvement is maximum, when two periods are dissimilar but close to  $\lambda_0/4$ . Here, simulation resonance frequency is 2.33 GHz, while measured resonance frequency (with fabricated antenna) is 2.31 GHz. The measured bandwidth is approximately 7% at resonating frequency of 2.31 GHz. However, bandwidth obtained through simulation is approximately 6% at resonating frequency of 2.31 GHz. Gain improvement of 3 dB is achieved, which provides maximum gain of 9.84 dBi.

Denidni *et al.* [128] have enhanced the gain of a CDRA using EBG structure, but the gain enhancement (3 dB) is not very high. Coulibaly *et al.* [12] have presented novel hybrid DRA to further modify its gain as well as impedance BW. This structure consists of a dielectric resonator, an intermediate substrate, an aperture coupled feed and an EBG configuration. DR is covered by a circular periodic electromagnetic band-gap structure. The intermediate substrate is inserted between the ground plane and DR. The intermediate substrate alleviates dielectric constant of dielectric resonator antenna, that causes an enhancement in bandwidth. Here, slot is utilized as radiating element as well as coupling device, which couples DR to MSL. The presented mushroom-type electromagnetic band-gap substrate has earlier been designed and analysed in [150]. This hybrid resonating antenna is compared to the reference antenna, which has neither intermediate substrate nor EBG configuration. The EBG substrate consists of metallic rings and grounding vias. Here, concentric rings of strips are designed on the grounded intermediate substrate. Simulation results demonstrate that gain boosting of 6 dB and impedance BW of approximately 24 % are obtained with this new substrate.

Further, Coulibaly *et al.* [151] extended the work presented in [12] to improve the gain of DRA maintaining a large bandwidth. The authors have proposed hybrid antenna based on amalgamation of circular soft surface (EBG structure) and aperture-fed cylindrical dielectric resonator (CDR) to modify its gain as well as impedance BW. However, presented antenna configuration encompasses a dielectric resonator, intermediate substrate, MSL-fed slot and circular soft surface. This cylinder-type soft structure consists of one metal ring, which is short circuited to ground via two sets of periodic vias. The first set is composed of thirty vias and second set consists of twenty vias. An intermediate substrate is inserted between DR and the ground plane of the microstrip. With combination of aforementioned various elements, broad bandwidth and

large-gain are obtained. Moreover, inclusion of intermediate substrate enhances impedance BW of antenna and makes it highly robust. The benefit of ground plane at back of intermediate substrate has been taken to incorporate soft surface made of metal ring and a few grounding vias. For antenna without intermediate substrate and soft surface, a bandwidth of 16% and the gain of around 5.8 dBi is achieved at operational frequency of 5.4 GHz. Therefore, inclusion of an intermediate substrate and a soft surface result in the performance improvement of hybrid antenna. A peak gain of 12.2 dBi is achieved at frequency of 5.3 GHz by providing enhancement of 6.2 dB. This gain achievement is approximately 6 dBi on entire bandwidth. The impedance BW obtained is approximately 24 %.

This chapter is organized as follows. Design and simulation of conventional HDRA have been discussed in section 4.2. Section 4.3 demonstrates the design and simulation of HDRA with cylindrical EBG structure. The simulation results for conventional HDRA (without EBG structure) and HDRA with EBG structure have been illustrated and compared in section 4.4. The concluding remarks are given in section 4.5 for this chapter.

## **4.2 DESIGN AND SIMULATION OF HDRA**

In past three decades, various shapes of DRAs have been investigated. However, cylindrical, rectangular and hemispherical are the most commonly used shapes. These shapes are simple in terms of mathematical formulations and mechanical fabrications. HDRA is advantageous because of the simple spherical interface between free space and itself. The simple structure of HDRA requires no magnetic wall consideration in problem formulation, and therefore more precise solution can be achieved [23]. HDRA has one tunable dimension. Once the resonance frequency of an HDRA is determined by the

radius, everything else is fixed, including the bandwidth. One-dimensional freedom makes HDRAs easy to design.

In this segment, a hemispherical DRA is designed. First, HDRA is designed to work at any arbitrarily selected frequency. Afterwards, cylindrical electromagnetic band-gap structure is designed for gain enhancement of designed HDRA at its operational frequency in the next section. Fig. 4.1 depicts geometry of reference antenna, which comprises of a hemispherical DR located on the grounded substrate. Preliminary values of various dimensions of the proposed antenna, such as radius of hemispherical dielectric resonator ( $R$ ), thickness of dielectric substrate ( $t$ ), length of coaxial probe ( $L$ ) and distance between coaxial probe and the center of HDRA ( $d$ ) are considered arbitrarily. Then, the feed position is adjusted to provide better impedance matching, while keeping values of other dimensions fixed. Table 4.1 demonstrates values of different parameters of proposed antenna. The parametric values of HDRA are reserved same while designing EBG structure (in the next section). The material used for the HDRA is GaAs. The HDRA has radius  $R=18$  mm and dielectric constant  $\epsilon_{dra}=12.94$ . It is placed on substrate (RT Duroid 5880) having a permittivity,  $\epsilon_r = 2.2$  and a thickness,  $t = 3$  mm. Here, feeding is accomplished via a probe-feed of length  $L = 6$  mm located at a distance  $d=5.3$  mm from center of HDRA. However, size of substrate is  $300\text{mm} \times 300\text{mm}$ . The resonance frequency is anticipated to be dependent on the physical attributes of HDRA and substrate. The designed antenna resonates at 4.39 GHz. TM-01 mode is excited in HDRA for excitation. The peak antenna gain is approximately 6.9 dBi. Moreover, gain of the antenna is enhanced by incorporating a cylinder type electromagnetic band-gap structure that has been detailed in next section.

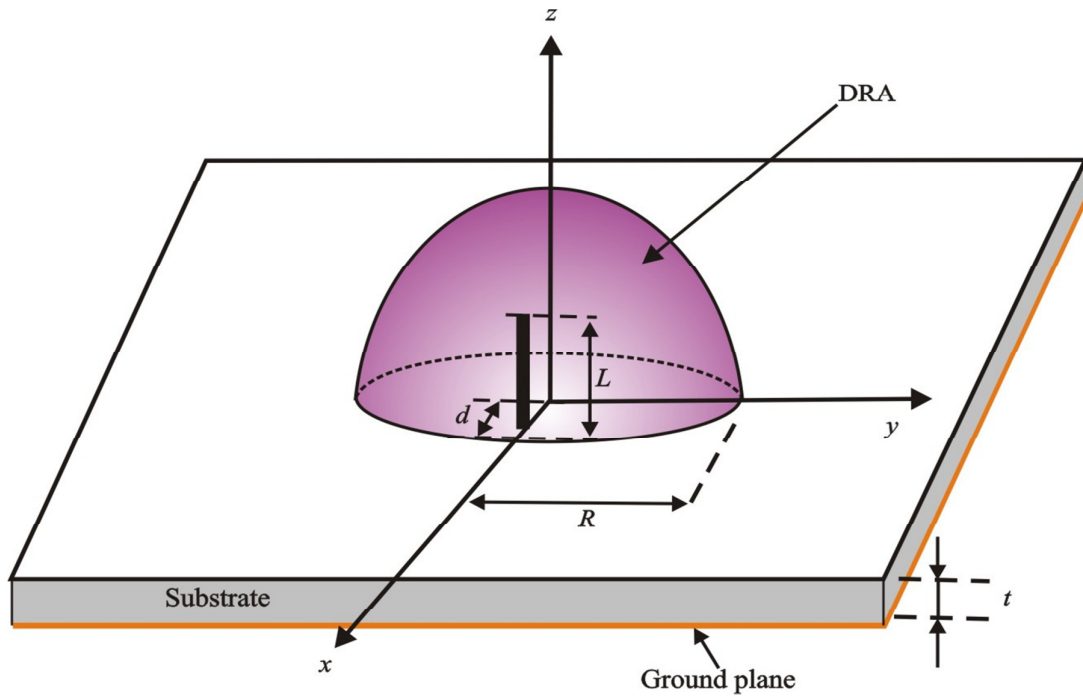


**Fig. 4.1: Geometry of proposed HDRA**

**TABLE 4.1  
PARAMETRIC VALUES OF HDRA**

Parameter	Value
Permittivity of DR (GaAs), $\epsilon_{dra}$	12.94
Radius of DR, $R$	18 mm
Permittivity of grounded substrate (RT Duroid 5880), $\epsilon_r$	2.2
Thickness of grounded substrate, $t$	3 mm
Length of coaxial probe, $L$	6 mm
Distance of coaxial probe from the center of HDRA, $d$	5.3 mm

### 4.3 DESIGN AND SIMULATION OF HDRA WITH CYLINDRICAL EBG STRUCTURE

It has been shown in [103] that the cylindrical mushroom-like EBG structures provide higher gain as compared to the grid-type EBG structures and the EBG structures based on partial substrate removal technique. In cylindrical EBG structures, the holes are drilled in substrate and then these holes are filled with metal. These holes filled with metal look like cylinders. It is the reason that this type of EBG structure is known as cylindrical EBG structure. These metal filled holes (cylinders) are short circuited with the ground, and hence these help in grounding the surface-waves and therefore improve the antenna performance.

This section presents the design of cylindrical electromagnetic band-gap structure to improve gain of HDRA mentioned in last section. Geometry of an hemispherical dielectric resonator (HDR) surrounded by a cylinder-type EBG configuration consisting of metallic rings and grounding (metal) vias is shown in Fig. 4.2. Top view of designed configuration has been explored in Fig. 4.3. The paradigm of presented antenna is based on the fact that capacitive coupling is similar in every radial direction because of circular symmetry of presented electromagnetic band-gap structure. In this, concentric metallic rings have been put on grounded substrate (RT Duroid 5880), with the distance  $g$  between two successive strips. The metal rings are short circuited to the ground through periodic vias.

The radial period of metallic rings is  $P_1$ . The vias have radius  $r$ , transversal period  $P_t$  and radial period  $P_2$ . The location of vias is based on the procedure demonstrated in [119], where transversal period is kept constant for each layer. It has been shown in [119] that the antenna gain enhancement is maximum, when the radial period of metal rings

( $P_1$ ) and the radial period of vias ( $P_2$ ) are different but close to  $\frac{\lambda_0}{4}$ . The value of gap between two successive strips ( $g$ ) is twice the value of  $r$ . The value of radius of vias ( $r$ ) is taken arbitrarily as 1 mm. Hence, the value of  $g$ , which is double the value

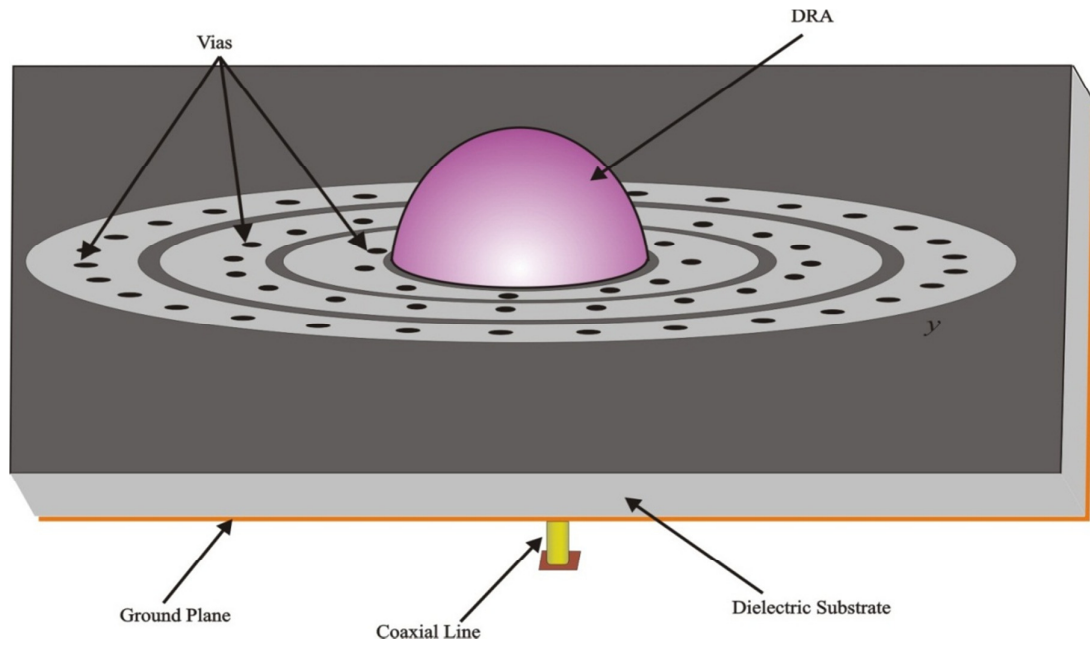


**Fig. 4.2: HDRA surrounded by a cylindrical (mushroom-like) EBG configuration (side view)**

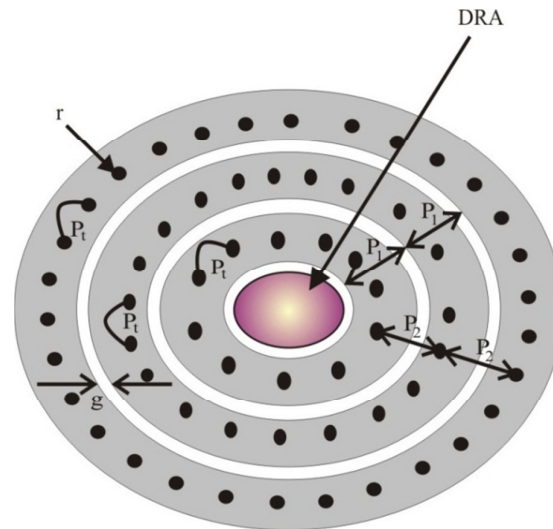


**Fig. 4.3: HDRA surrounded by a cylindrical (mushroom-like) EBG configuration (top view)**

of  $r$ , is taken as 2 mm. The initial values of  $P_1$  and  $P_2$  are calculated using following relations [119]

$$P_2 \approx \frac{\lambda_0}{4} \quad (4.1)$$

where,  $\lambda_0$  is wavelength at resonance frequency.

$$P_1 = \text{slightly less than } \frac{\lambda_0}{4} \quad (4.2)$$

The preliminary value of  $P_t$  is considered arbitrarily. After getting the initial values of radial period of metallic rings ( $P_1$ ) and radial period of metal vias ( $P_2$ ) from Eq. (4.1) and Eq. (4.2), these two parametric values are optimized along with transversal period of vias ( $P_t$ ), to deliver the optimum gain at its resonating frequency. Table 4.2 shows the final parametric values (after optimization) of cylindrical EBG structure. The maximum antenna gain is obtained at the center frequency 4.39 GHz, with the values of  $P_1$ ,  $P_2$  and  $P_t$  fixed as 20 mm, 21 mm and 8 mm respectively. First metallic strip begins at the radius  $R+g$ , and  $n^{\text{th}}$  metallic strip begins at radius  $R+g+(n-1)P_1$ ; where  $R$  is the radius of HDRA. The parametric values of HDRA are kept same, as used in previous section, while designing the conventional HDRA (without EBG structure). The simulation results of conventional HDRA as well as HDRA with EBG structure are presented in next section.

**TABLE 4.2**

**PARAMETRIC VALUES OF CYLINDRICAL EBG STRUCTURE**

<b>Parameter</b>	<b>Value</b>
Radius of vias, $r$	1 mm
Radial period of metal rings, $P_1$	20 mm
Transversal period of grounding vias, $P_t$	8 mm
Radial period of vias, $P_2$	21 mm
Gap between two successive metal rings, $g$	2 mm

#### 4.4 SIMULATION RESULTS WITH PERFORMANCE ANALYSIS

This section presents various simulation results for HDRA and HDRA with EBG structure. The results depicted in Fig. 4.4 shows the RL observed through simulation for two antennas i.e., the conventional HDRA (without EBG structure) and HDRA with EBG structure. It is noteworthy that electromagnetic band-gap configuration slightly improves impedance matching of antenna. The return loss of conventional HDRA is -45 dB, whereas RL of HDRA with EBG structure is -57 dB.

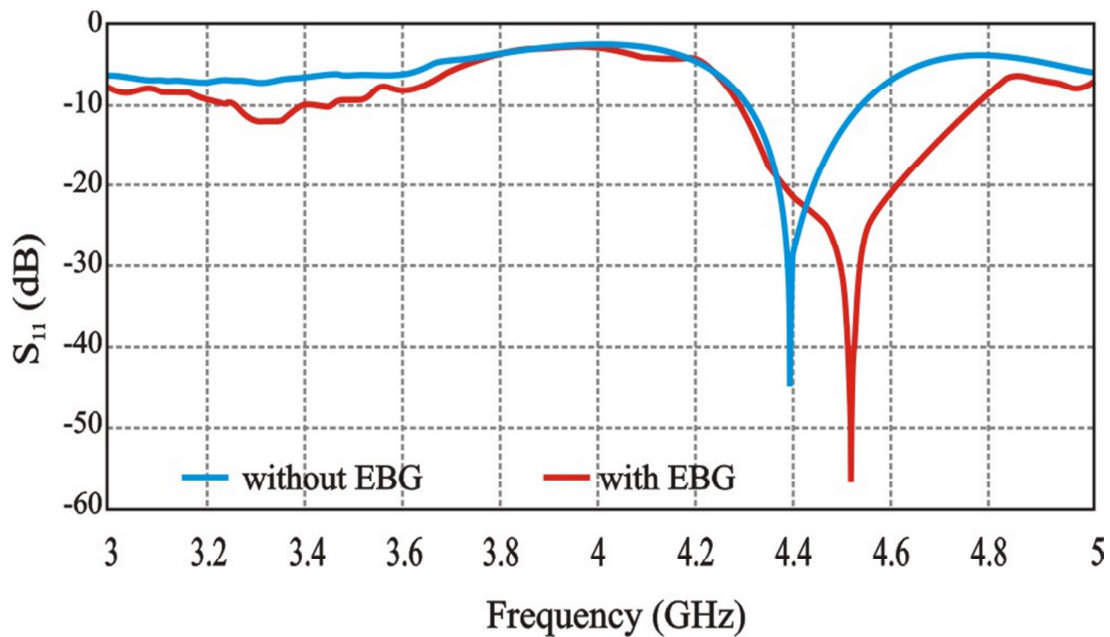


**Fig. 4.4: Frequency response of HDRA (near field measurement)**

Fig. 4.5 shows the gain achieved through simulation as a function of frequency for the two antennas, with and without EBG structure. The electromagnetic band-gap configuration permits us to enhance the gain of antenna around the operating frequency. For conventional HDRA (without EBG structure), the gain achieved and impedance BW are 6.9 dBi and approximately 5.6 % (250 MHz) respectively at the centre frequency of 4.39 GHz. Whereas for HDRA with EBG structure, the gain achieved and impedance BW

are 10.6 dBi and approximately 11.3 % (510 MHz) respectively at centre frequency of 4.51 GHz. Therefore, gain of HDRA is enhanced by 3.7 dB due to the incorporation of EBG structure. The cylindrical EBG structure diminishes the surface-waves, however antenna gain improvement is also because of coupling among DRA and electromagnetic band-gap substrate.

Fig. 4.6 illustrates the radiation pattern (E-plane) of conventional HDRA (without EBG structure) as well as HDRA with EBG structure observed through simulation. Whereas, Fig. 4.7 illustrates the radiation pattern (H-plane) of conventional HDRA (without EBG structure) as well as HDRA with EBG structure observed through simulation.

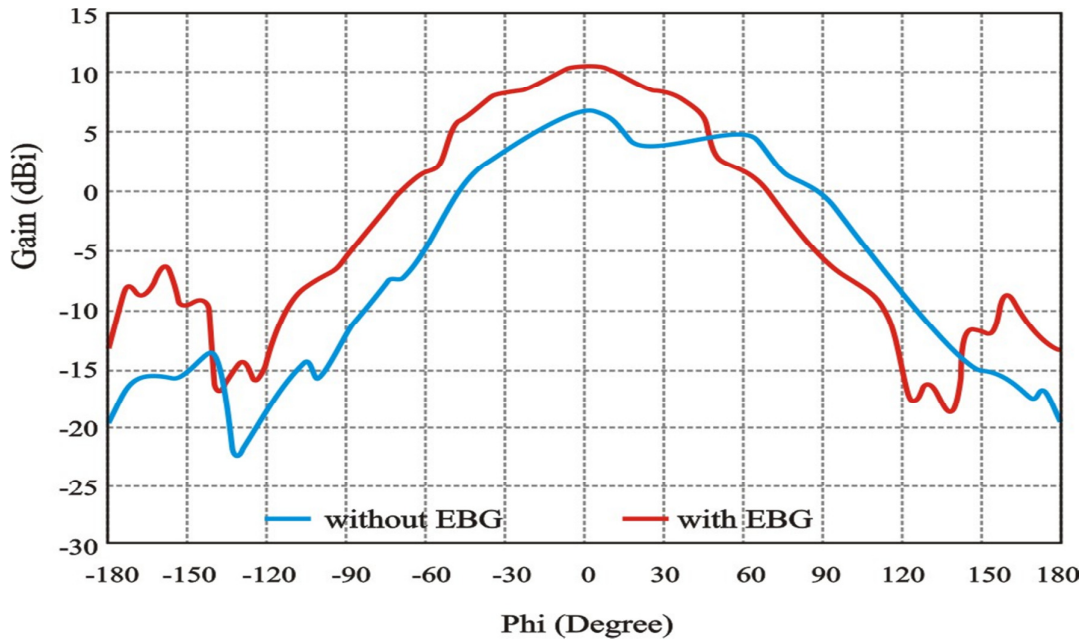


**Fig. 4.5: Gain response of HDRA (far field measurement)**

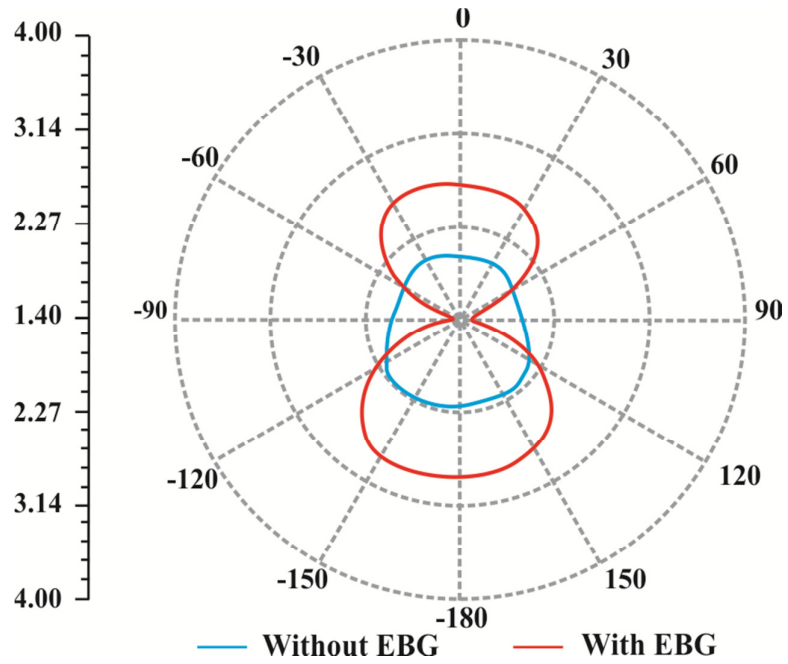


**Fig. 4.6: Radiation Pattern (E-Plane) of HDRA**

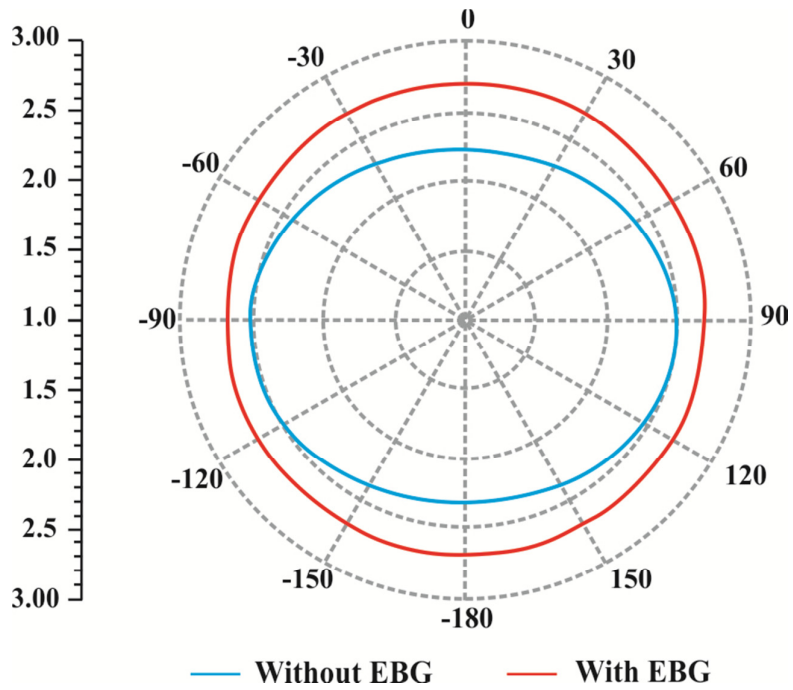


**Fig. 4.7: Radiation Pattern (H-Plane) of HDRA**

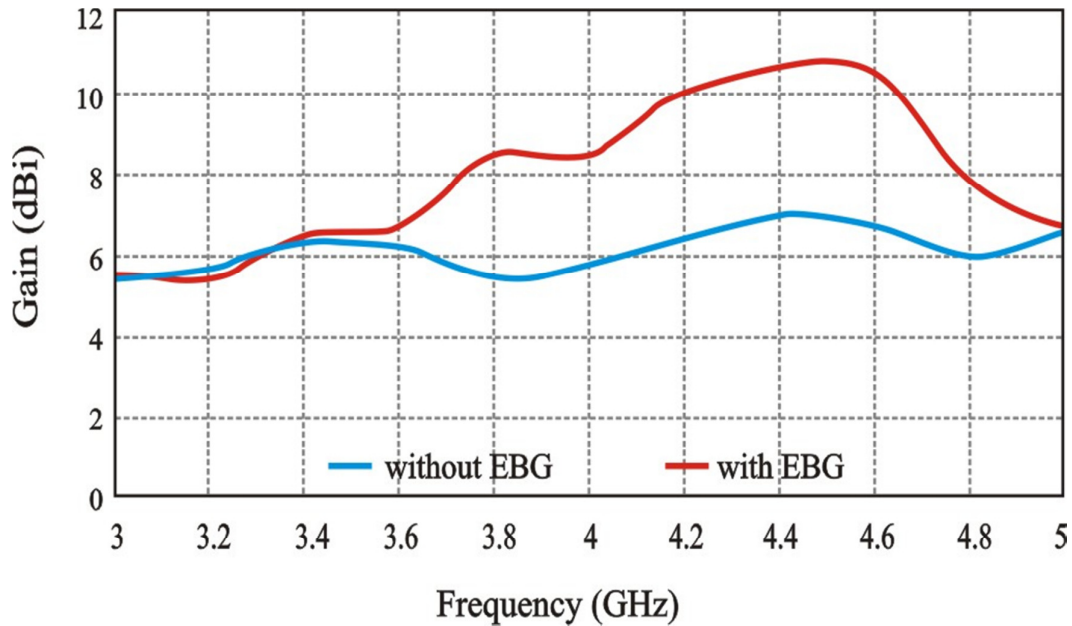


**Fig. 4.8: Gain v/s frequency plot of HDRA**

Fig. 4.8 shows the gain vs. frequency plot for frequency range between 3 GHz to 5 GHz for two antennas i.e., the conventional HDRA (without EBG structure) and HDRA with EBG structure. It is inferred from this figure that designed antenna provides a minimum gain of 6 dB in frequency range of 3.3 - 5 GHz.

**TABLE 4.3**

**COMPARISON OF SIMULATION RESULTS FOR CONVENTIONAL HDRA AND HDRA WITH EBG STRUCTURE**

<b>ATTRIBUTE</b>	<b>CONVENTIONAL HDRA</b>	<b>HDRA WITH EBG STRUCTURE</b>
<b>RESONANCE FREQUENCY</b>	4.39 GHz	4.51 GHz
<b>BANDWIDTH</b>	250 MHz	510 MHz
<b>RETURN LOSS</b>	-45 dB	-57 dB
<b>GAIN</b>	6.9 dBi	10.6 dBi

Further, simulation results for the conventional HDRA and HDRA with EBG structure are shown in Table 4.3. It can be noticed from this table that electromagnetic band-gap substrate slightly improves impedance matching of antenna. Both, gain and bandwidth of designed antenna are enhanced due to incorporation of EBG structure. The return loss is also reduced due to EBG structure. However, the bandwidth, the gain enhancement as well as the highest gain achieved are more, and the return loss is also less in comparison to the results presented in [152].

#### **4.5 SUMMARY OF CHAPTER**

In this chapter, a technique for improving the gain of a probe-fed HDRA has been detailed. With regard to this goal, a cylindrical EBG structure, composed of three concentric rings of metal strip and a periodic structure of grounded (metal) vias, has been used. It is apparent from presented results that efficient suppression of propagating surface-waves leads to substantial improvement in the performance of HDRA. This performance improvement appears because of the transformation of surface-waves into radiated waves due to the usage of cylindrical EBG structure. The simulation results demonstrate that the designed antenna provides a minimum gain of 6 dB in frequency band of 3.3 - 5 GHz. However, gain of HDRA is enhanced by 3.7 dB due to the usage of EBG structure. It is found that due to incorporation of the EBG structure, the bandwidth of HDRA is also enhanced. The designed antenna has found applications in C-band based communication systems, like in wireless local area network (WLAN) applications.

**CONCLUDING REMARKS AND FUTURE SCOPE**

---

**5.1 CONCLUDING REMARKS**

This thesis is an outcome of the studies performed towards enhancement of the gain of dielectric resonator antenna (DRA). The results presented in this thesis constituted three major goals. First aim is the achievement of dual frequency band (C-band and X-band) with an aperture coupled rectangular DRA (RDRA). Second goal is gain enhancement of RDRA in both frequency bands by mounting a quasi-planar surface mounted horn over DRA. Third objective is the designing of a hemispherical dielectric resonator antenna (HDRA) and enhancement of its gain by incorporating electromagnetic band-gap (EBG) structure.

For the last three decades, two classes of antennas i.e., microstrip patch antenna (MPA) and DRA have been under investigation for the modern wireless communication applications. MPAs are attractive due to its light-weight, low-profile planar configuration, conformability and low-cost in comparison to traditional antennas. However, MPAs have various limitations such as narrow bandwidth, significant metal losses (ohmic losses), low-gain and surface-wave excitations etc. Most of the limitations of MPA are removed in dielectric resonator antenna. These DRA configurations have been given high weightage in the past few years for its beneficial applications in the microwave and millimeter-wave communication systems. DRA consists of the dielectric materials in its radiating patch (also known as dielectric resonators) and ground plane (metal) on opposite side of substrate. DRAs offer much wider impedance BW in comparison to MPA because MPA radiates via two slender radiating slots, while dielectric resonator antenna does radiate via its entire surface, except the grounded part. DRA can be

fabricated in various shapes, which allows more flexibility in the antenna design. The most common shapes are rectangular, cylindrical and hemispherical. In comparison to other geometries, the rectangular resonators are more attractive for its fabrication advantages and also because of the existence of two independent aspect ratios (height / length and width / length) for better design flexibility to meet the impedance and radiation requirements. The resulting antenna properties like bandwidth, resonating frequency and radiation pattern, may be conveniently controlled through the adjustment of aspect ratios. The rectangular shaped DRA offers three degrees of freedom, which is one more than cylindrical shaped DRA and two more than hemispherical shaped DRA. The dielectric resonator antennas may be excited through variety of feeding schemes, which include coaxial probes, MSL feed, co-planner feeds and aperture coupling. In comparison to other coupling schemes, aperture coupled feed has an advantage that there is no physical contact between feed and radiator. However, feed network is placed beneath ground plane, which isolates radiating element from any undesired coupling or spurious radiations from feed. The coaxial probe and microstrip line-fed elements are particularly restricted to bandwidth of 2 - 5%. On the other hand, the aperture coupled elements have been showcased with much wider bandwidth.

DRAs offer several advantages. But its gain needs to be enhanced further, as it is not sufficient in many of the engineering applications. Over the years, different investigations have been carried out to improve the gain of DRA by incorporating offset dual-disk dielectric resonators, composite layer dielectric resonators and parasitic overlays. In case of offset dual-disk DRAs, the gain enhancement is moderate. In the domain of composite layer dielectric resonators, it has been observed that the impedance BW reduces with the increasing value of gain of antenna. Due to the usage of parasitic overlays, gain is enhanced, but this configuration is quite long, and therefore unsuitable for compact

antenna applications. As an alternative, the surface mounted horn and EBG structures can be used for boosting antenna gain, while keeping its bandwidth unchanged. Horn is an aperture type antenna, which is excited by the designed RDRA in presented work. Horn improves the gain of antenna by restraining EM field in vicinity of radiating element. Moreover, EBG structures help in reducing the losses due to surface-wave propagation as these waves generate undulations in radiated pattern. The repression of surface-waves results in gain maximization of antenna. In this thesis, we have demonstrated that gain of the conventional RDRA is enhanced by mounting a quasi-planar horn (fabricated using silver metal) at the same resonance frequency, with reduced return loss (RL) and with marginally decreased impedance BW. Whereas, the gain of an HDRA is enhanced by incorporating a mushroom-like EBG structure with reduced RL and enhanced impedance BW.

In this research work, we have first combined the slot antenna and DRA, which has led to the design of a dual-band DRA. The resonance of slot as well as of dielectric configuration gets amalgamated to obtain large bandwidth. However, antenna polarization as well as the radiation pattern is preserved. A compact size of dual-band low-loss AC-DRA is successfully designed, simulated and fabricated. This DRA resonates at two frequencies 5.8 GHz and 8.0 GHz. However, impedance BW obtained through simulation is approximately 6.5 % (380 MHz) and approximately 5.6 % (450 MHz) at the centre frequencies 5.8 GHz and 8.0 GHz respectively. Whereas, measured impedance BW (with fabricated antenna) is approximately 5.8 % (340 MHz) and approximately 5.2 % (420 MHz) at the centre frequencies 5.8 GHz and 7.95 GHz respectively. However, RL values observed through simulation are -20.5 dB and -22.5 dB at two resonating frequencies respectively. Whereas, measured RL values (with fabricated antenna) are -19 dB and -20.5 dB at 5.8 GHz frequency and 7.95 GHz

frequency respectively. The gain achieved through simulation are 8.5 dBi and 9.6 dBi at 5.8 GHz frequency and 8.0 GHz frequency respectively, and the measured gain advantages achieved are 8.1 dBi and 9.05 dBi at 5.8 GHz frequency and 7.95 GHz frequency respectively.

Then, a dual-band AC-RDRA with quasi planar surface mounted horn is successfully designed, simulated and fabricated, which provides enhanced gain as compared to conventional RDRA (DRA without horn). This antenna operates in C-band (WLAN applications) and X-band (military applications, in radiation therapy, and in microwave laboratory experiments). The RL observed through simulation is -23 dB at lower resonance frequency 5.8 GHz and -25 dB at upper resonance frequency 8.0 GHz. However, the measured RL (with fabricated antenna) is -21 dB and -23 dB at 5.75 GHz frequency and 7.95 GHz frequency respectively. There is good matching between two results with RL lower than -10 dB. The gain advantages achieved through simulation are 9.3 dBi and 11.1 dBi at 5.8 GHz frequency and 8.0 GHz frequency respectively, and the measured gain achieved (with fabricated antenna) is 8.95 dBi and 10.65 dBi at 5.75 GHz frequency and 7.95 GHz frequency respectively. The designed antenna has improved power handling capacity in comparison to patch antenna. The simulated impedance BW is approximately 6.5 % (380 MHz) and approximately 5.5 % (440 MHz) at these two resonating frequencies respectively. Whereas, measured impedance BW is approximately 5.4 % (315 MHz) and approximately 4.7 % (375 MHz) at these two resonating frequencies respectively, which showcases good agreement between simulation and measured results.

Subsequently, an HDRA with EBG structure is successfully designed and simulated. This antenna is designed to resonate at 4.39 GHz. It is observed that after incorporating the EBG structure, the gain of antenna is enhanced by approximately 3.7 dB. The RL is

-45 dB for the conventional HDRA (HDRA without EBG structure) and -57 dB for HDRA with EBG structure. For conventional HDRA, the gain achieved and impedance BW is 6.9 dBi and approximately 5.6 % (250 MHz) respectively. Whereas for HDRA with EBG structure, the gain achieved and impedance BW are 10.6 dBi and approximately 11.3 % (510 MHz) respectively. It is found that due to incorporation of the EBG structure, the gain and bandwidth of HDRA are enhanced. The designed antenna provides a minimum gain of 6 dBi in the frequency range 3.3 GHz to 5 GHz.

## **5.2 FUTURE SCOPE**

This thesis has featured novel DRA designs for the applications requiring high-gain and compact antennas. In the light of results illustrated in the thesis, this research effort may be elaborated to design the gain effective antennas using a metallic reflector [55]-[57] in both the designed antennas i.e., with RDRA (mounted with quasi-planar horn) and with HDRA (incorporated with EBG structure) for further gain enhancement. The reflector is a square patch normally centred below the radiation element. It enhances the gain of antenna by reducing its back radiations (BRs). These back radiations are the unwanted radiations, which antenna radiates in the backward direction (opposite to desired direction) in addition to radiations in the desired directions. The metallic reflector of antenna reflects back radiation energy in course of primary radiated energy flux, modifying the antenna gain. Future work could also involve investigations of the novel antenna designs in planar array configurations for radar as well as satellite communications.

For an RDRA, the enhancement in bandwidth is achieved by using the aperture coupling. The same coupling technique can be used with HDRA incorporated with the EBG structure to expand its bandwidth. The gain of HDRA incorporated with EBG structure can be further enhanced by incorporating surface mounting horn in addition to

the EBG structure. Whereas, the gain of RDRA mounted with quasi-planar horn can be further boosted by incorporating an EBG structure in addition to the horn. Future work also includes the fabrication of HDRA incorporated with the EBG structure.

In this thesis, different DRA shapes (first RDRA and second HDRA), different coupling techniques (aperture coupling and coaxial probe-feed) and different gain enhancement techniques (surface mounted horn and EBG structure) have been intentionally used to explore different design techniques and to have variety in the designs. But, it forms only the tip of the iceberg in the domain of antenna and microwave engineering to fulfil the ever increasing demand for high-gain and high-bandwidth, which needs to be investigated further.

## REFERENCES

- [1] A. A. Kishk, Y. Yin, and W. Glisson, "Conical dielectric resonator antennas for wideband applications," *IEEE Trans. Antennas and Propagation*, vol. 50, no. 4, pp. 469-474, April 2002.
- [2] K. M. Luk and K. W. Leung, *Dielectric Resonator Antennas*. U.K.: Hertfordshire, Research Studies Press Ltd., 2002.
- [3] S. A. Long, M. W. McAllister, and L. Shen, "The resonant cylindrical dielectric cavity antenna," *IEEE Trans. Antennas and Propagation*, vol. 31, no. 3, pp. 406-412, May 1983.
- [4] M. W. McAllister and S. A. Long, "Resonant hemispherical dielectric antenna," *Electronics Letters*, vol. 20, no. 16, pp. 657-659, August 1984.
- [5] M. W. McAllister, S. A. Long, and G. L. Conway, "Rectangular dielectric-resonator antenna," *Electronics Letters*, vol. 19, no. 6, pp. 218-219, March 1983.
- [6] R. K. Mongia, A. Ittipiboon, and M. Cuhaci, "Low profile dielectric resonator antennas using a very high permittivity material," *Electronics Letters*, vol. 30, no. 17, pp. 1362-1363, August 1994.
- [7] K. W. Leung, K. M. Luk, E. K. N. Yung, and S. Lai, "Characteristics of a low-profile circular disk DR antenna with very high permittivity," *Electronics Letters*, vol. 31, no. 6, pp. 417-418, March 1995.
- [8] A. A. Kishk, B. Ahn, and D. Kajfez, "Broadband stacked dielectric resonator antennas," *Electronics Letters*, vol. 25, no. 18, pp. 1232-1233, August 1989.
- [9] R. N. Simons and R. Q. Lee, "Effect of parasitic dielectric resonators on CPW/aperture-coupled dielectric resonator antennas," in *Proc. IEEE*, vol. 140, no. 5, pp. 336-338, October 1993.

- [10] Z. Fan, Y. M. M. Antar, A. Ittipiboon, and A. Petosa, "Parasitic coplanar three-element dielectric resonator antenna subarray," *Electronics Letters*, vol.32, no. 9, pp. 789-790, April 1996.
- [11] Nasimuddin, K. P. Esselle, and A. K. Verma, "Gain enhancement of aperture coupled dielectric resonator antenna with surface mounted horn," in *Proc. 28<sup>th</sup> General Assembly Int. Union Radio Sciences(URSI GA05) New Delhi*, pp 1-4, October 2005.
- [12] Y. Coulibaly and T. A. Denidni, "Gain and bandwidth improvement of an aperture coupled cylindrical dielectric resonator antenna using an EBG structure," in *Proc. IEEE Int. Symp. Antennas and Propagation Society (APSURSI '09), Charleston, SC*, pp. 1-4, 1-5 June 2009.
- [13] K. W. Leung, K. Y. Chow, K. M. Luk, and E. K. N. Yung, "Low-profile circular disk DR antenna of very high permittivity excited by a microstrip line," *Electronics Letters*, vol. 33, no. 12, pp. 1004-1005, June 1997.
- [14] A. Petosa,, A. Ittipiboon, Y. M. M. Antar, D. Roscoe, and M. Cuhaci, "Recent advances in dielectric resonator antenna technology," *IEEE Antennas and Propagation Magazine*, vol. 40, no. 3, pp. 35-48, June 1998.
- [15] A. A. Kishk and A. W. Glisson, "Bandwidth enhancement for split cylindrical dielectric resonator antennas," *Progress in Electromagnetics Research*, vol. 15, no. 6, pp. 97-118, April 2001.
- [16] Q. Rao, T. A. Denidni, and A. R. Sebak, "Study of broadband dielectric resonator antennas," in *Proc. Progress Electromagnetic Research Symp.(PIER), Hangzhou, China*, pp. 137-141, 22-26 August 2005.

- [17] M. D. Rotaru and J. K. Sykulski, "Design and analysis of a novel compact high permittivity dielectric resonator antenna," *IEEE Trans. Magnetics*, vol. 45, no. 3, pp. 1052-1055, March 2009.
- [18] M. Verplanken and J. V. Bladel, "The magnetic-dipole resonances of ring resonators of very high permittivity," *IEEE Trans. Microwave Theory and Techniques*, vol. 27, no. 4, pp. 328-333, April 1979.
- [19] R. K. Mongia and P. Bhartia, "Dielectric resonator antennas - a review and general design relations for resonant frequency and bandwidth," *Int. J. Microwave and Millimeter-Wave Computer-Aided Engineering*, vol. 4, no. 3, pp. 230-247, July 1994.
- [20] W. Zheng, "Computation of complex resonance frequencies of isolated complex objects," *IEEE Trans. Microwave Theory and Techniques*, vol. 37, no. 6, pp. 953-961, June 1989.
- [21] R. K. Mongia, A. Ittipiboon, M. Cuhaci, and D. Roscoe, "Radiation Q-factor of rectangular dielectric resonator antennas, theory and experiment," in *Proc. Int. Symp. Antennas and Propagation Society, (AP-S. Digest), Seattle, WA, USA*, vol. 2, pp. 764-767, 20-24 June 1994.
- [22] A. A. Kishk, M. R. Zunoubi, and D. Kajfez, "A numerical study of a dielectric disc antenna above grounded dielectric substrate," *IEEE Trans. Antennas and Propagation*, vol. 41, no. 6, pp. 813-821, June 1993.
- [23] K. W. Leung, K. M. Luk, K. Y. A. Lai, and D. Lin, "Theory and experiment of a coaxial probe fed hemispherical dielectric resonator antenna," *IEEE Trans. Antennas and Propagation*, vol. 41, no. 10, pp. 1390-1398, October 1993.
- [24] K. W. Leung, K. K. Tse, K. M. Luk, and E. K. N. Yung, "Cross-polarization characteristics of a probe-fed hemispherical dielectric resonator antenna," *IEEE Trans. Antennas and Propagation*, vol. 47, no. 7, pp. 1228-1230, July 1999.

- [25] K. W. Leung, K. Y. A. Lai, K. M. Luk, and D. Lin, "Input impedance of aperture coupled hemispherical dielectric resonator antenna," *Electronics Letters*, vol. 29, no. 13, pp. 1165-1167, June 1993.
- [26] A. A. Kishk, G. Zhou, and A. W. Glisson, "Analysis of dielectric resonator antennas with emphasis on hemispherical structures," *IEEE Antennas and Propagation Magazine*, vol. 36, no. 2, pp. 20-31, April 1994.
- [27] A. A. Kishk, A. Ittipiboon, Y. M. M. Antar, and M. Cuhaci, "Dielectric resonator antennas fed by a slot in the ground plane of a microstrip line," in *Proc. 8<sup>th</sup> Int. Conf. Antennas and Propagation, Edinburgh*, vol. 1, pp. 540-543, 30 March- 2 April 1993.
- [28] K. W. Leung, K. M. Luk, K. Y. Chow, and E. K. N. Yung, "Bandwidth enhancement of dielectric resonator antenna by loading a low-profile dielectric disk of very high permittivity," *Electronics Letters*, vol. 33, no. 9, pp. 725-726, April 1997.
- [29] K. W. Leung, W. C. Wong, K. M. Luk, and E. K. N. Yung, "Circular-polarized dielectric resonator antenna excited by dual conformal strips," *Electronics Letters*, vol. 36, no. 6, pp. 484-486, March 2000.
- [30] M. S. Salameh, Y. M. M. Antar, and G. Seguin, "Coplanar-waveguide-fed slot-coupled rectangular dielectric resonator antenna," *IEEE Trans. Antennas and Propagation*, vol. 50, no. 10, pp. 1415-1419, October 2002.
- [31] M. B. Oliver, Y. M. M. Antar, R. K. Mongia, and A. Ittipiboon, "Circularly polarized rectangular dielectric resonator antenna," *Electronics Letters*, vol. 31, no. 6, pp. 418-419, March 1995.
- [32] A. A. Kishk, "Wide-band truncated tetrahedron dielectric resonator antenna excited by a coaxial probe," *IEEE Trans. Antennas and Propagation*, vol. 51, no. 10, pp. 2913-2917, October 2003.

- [33] H. Y. Lo, K. W. Leung, K. M. Luk, and E. K. N. Yung, "Low profile equilateral-triangular dielectric resonator antenna of very high permittivity," *Electronics Letters*, vol. 35, no. 25, pp. 2164-2166, December 1999.
- [34] R. K. Mongia, A. Ittipiboon, P. Bharita, and M. Cuhaci, "Electric monopole antenna using a dielectric ring resonator," *Electronics Letters*, vol. 29, no. 17, pp. 1530-1531, August 1993.
- [35] R. K. Mongia, A. Ittipiboon, Y. M. M. Antar, P. Bhartia, and M. Cuhaci, "A half-split cylindrical dielectric resonator antenna using slot-coupling," *IEEE Microwave and Guided Wave Letters*, vol. 3, no. 2, pp. 38-39, February 1993.
- [36] M. T. K. Tam and R. D. Murch, "Compact circular sector and annular sector dielectric resonator antennas," *IEEE Trans. Antennas and Propagation*, vol. 47, no. 5, pp. 837-842, May 1999.
- [37] G. P. Junker, A. A. Kishk, and A. W. Glisson, "Input impedance of dielectric resonator antennas excited by a coaxial probe," *IEEE Trans. Antennas and Propagation*, vol. 42, no. 7, pp. 960-966, July 1994.
- [38] R. A. Kranenbrug and S. A. Long, "Microstrip transmission line excitation of dielectric resonator antennas," *Electronics Letters*, vol. 24, no. 18, pp. 1156-1157, September 1988.
- [39] R. A. Kranenbrug, S. A. Long, and J. T. Williams, "Coplanar waveguide excitation of dielectric resonator antennas," *IEEE Trans. Antennas and Propagation*, vol. 39, no. 1, pp. 119-122, January 1991.
- [40] J. Y. Wu, C. Y. Huang, and K. L. Wong, "Low-profile, very-high-permittivity dielectric resonator antenna excited by a coplanar waveguide," *Microwave and Optical Technology Letters*, vol. 22, no. 2, pp. 96-97, July 1999.

- [41] J. T. H. S. T. Martin, Y. M. M. Antar, A. A. Kishk, A. Ittipiboon, and M. Cuhaci, "Dielectric resonator antenna using aperture coupling," *Electronics Letters*, vol. 26, no. 24, pp. 2015-2016, November 1990.
- [42] A. Petosa, *Dielectric Resonator Antenna Handbook*, USA: Norwood, Artech House Publishers, January 2007.
- [43] G. P. Junker, A. A. Kishk, A. W. Glisson, and D. Kajfez, "Effect of an air-gap around the coaxial probe exciting a cylindrical dielectric resonator antenna," *Electronics Letters*, vol. 30, no. 3, pp. 177-178, February 1994.
- [44] A. Petosa, R. K. Mongia, A. Ittipiboon, and J. S. Wight, "Investigation of various feed structures for linear arrays of dielectric resonator antennas," in *Proc. IEEE Int. Symp. on Antennas and Propagation, Newport Beach, CA*, vol. 4, pp. 1982-1985, June 1995.
- [45] D. M. Pozar, "A review of aperture coupled microstrip antennas: history, operation, development, and applications," in *Proc. ECS, UMASS, Amherst, MA*, pp 1-12, May 1996.
- [46] L. Wu, "Substrate integrated waveguide antenna applications," Ph.D. Dissertation, University of Kent, Electrical Engg. Dept., UK, August 2015.
- [47] W. O. A. Wahab, S. Safavi-Naeini, and D. Busuioc, "Low cost low profile dielectric resonator antenna (DRA) fed by planar waveguide technology for millimetre-wave frequency applications," in *Proc. 2009 IEEE Radio and Wireless Symp. (RWS 2009), San Diego, CA*, pp. 27-30, 18-22 January 2009.
- [48] W. M. A. Wahab, and S. Safavi-Naeini, "High efficiency millimeter wave planar waveguide fed dielectric resonator antenna (DRA)," in *Proc. 2009 IEEE Antennas and Propagation Society Int. Symp. (RWS 2009), Charleston, SC*, pp. 1-4, 1-5 June 2009.

- [49] Z. C. Hao, W. Hong, A. Chen, J. Chen, and K. Wu, "SIW fed dielectric resonator antennas (DRA)," in *Proc. 2006 IEEE MTT-S Int. Microwave Symp. Digest (RWS 2009)*, San Francisco, CA, pp. 202-205, 11-16 June 2006.
- [50] W. M. A. Wahab, D. Busuioc, and S. Safavi-Naeini, "Millimeter wave high radiation efficiency planar waveguide series-fed dielectric resonator antenna (DRA) array: analysis, design, and measurements," *IEEE Trans. Antennas and Propagation*, vol. 59, no. 8, pp. 2834-2843, August 2011.
- [51] C. A. Balanis, *Antenna Theory: Analysis and Design*, 3rd edition, Hoboken, NJ: Wiley, 2005.
- [52] T. S. Horng and N. G. Alexopoulos, "Corporate feed design for microstrip arrays," *IEEE Trans. Antennas and Propagation*, vol. 41, no. 12, pp. 1615-1624, December 1993.
- [53] A. H. Mohammadian, N. M. Martin, and D. W. Griffin, "A theoretical and experimental study of mutual coupling in microstrip antenna-arrays," *IEEE Trans. Antennas and Propagation*, vol. 37, no. 10, pp. 1217-1223, October 1989.
- [54] J. A. G. Malherbe, "Analysis of a linear antenna-array including the effects of mutual coupling," *IEEE Trans. Education*, vol. 32, no. 1, pp. 29-34, February 1989.
- [55] S. D. Targonski, R. B. Waterhouse, and D. M. Pozar, "Wideband aperture coupled microstrip patch array with backlobe reduction," *Electronics Letters*, vol. 33, no. 24, pp. 2005-2006, November 1997.
- [56] G. S. Kirov and D. P. Mihaylova, "Circularly polarized aperture coupled microstrip antenna with resonant slots and a screen," *Radio Engineering*, vol. 19, no. 1, pp 111-116, April 2010.

- [57] R. B. Waterhouse, D. Novak, A. Nirmalathas, and C. Lim, "Broadband printed sectorized coverage antennas for millimeter-wave wireless applications," *IEEE Trans. Antennas and Propagation*, vol. 50, no. 1, pp. 12-16, January 2002.
- [58] Y. Hwang, Y. P. Zhang, K. M. Luk, and E. K. N. Yung, "Gain-enhanced miniaturized rectangular dielectric resonator antenna," *Electronics Letters*, vol. 33, no. 5, pp. 350-352, February 1997.
- [59] Y. Hwang, Y. P. Zhang, G. X. Zheng, and T. K. C. Lo, "Planar inverted-F antenna loaded with high permittivity material," *Electronics Letters*, vol. 31, no. 20, pp. 1710-1712, September 1995.
- [60] Y. M. M. Antar and Z. Fan, "Theoretical investigation of aperture coupled rectangular dielectric resonator antenna," in *Proc. IEEE Microwaves, Antennas and Propagation*, vol. 143, no. 2, pp. 113-118, April 1996.
- [61] K. M. Luk, K. F. Tong, and T. M. Au, "Offset dual-patch microstrip antenna," *Electronics Letters*, vol. 29, no. 18, pp. 1635-1636, October 1993.
- [62] K. W. Leung, K. Y. Chow, K. M. Luk, and E. K. N. Yung, "Offset dual-disk dielectric resonator antenna of very high permittivity," *Electronics Letters*, vol. 32, no. 22, pp. 2038-2039, October 1996.
- [63] R. Q. Lee and K. F. Lee, "Gain enhancement of microstrip antennas with overlaying parasitic directors," *Electronics Letters*, vol. 24, no. 11, pp. 656-658, May 1988.
- [64] R. Afzalzadm, "Studies on the effects of overlays on microstrip patch antenna and reflection filter," Ph.D. Dissertation, University of Poona, India, December 1990.
- [65] M. Hakkak and H. Ameri, "Gain enhancement of dielectric resonator loaded waveguide antennas with dielectric overlays," *Electronics Letters*, vol. 28, no. 6, pp. 541-542, March 1992.

- [66] A. R. Albino and C. A. Balanis, "Gain enhancement in microstrip patch antennas using ferrite rings," in *Proc. Radio Science Meeting (Joint with AP-S Symp.-2013), USNC-URSI, Lake Buena Vista, FL*, pp. 228-228, 7-13 July 2013.
- [67] N. Rao and K. V. Dinesh, "Performance enhancement of a microstrip antenna by suppression of surface waves using EBG structure in multiple layer substrate," in *Proc. IEEE Conf. on Topical Conference on Antennas in Wireless Communications (APWC), IEEE-APS, Torino*, pp. 935-939, 12-16 September 2011.
- [68] C. H. Lai, T. Y. Hen, and T. R. Chen, "Broadband aperture-coupled microstrip antennas with low cross polarization and back radiation," *Progress in Electromagnetics Research Letters*, vol. 5, pp. 187-197, 2008.
- [69] S. H. Zainud-Deen, H. A. E. Malhat, and K. H. Awadalla, "A single-feed cylindrical super quadric dielectric resonator antenna for circular polarization," *Progress in Electromagnetics Research*, vol. 85, pp. 409-424, 2008.
- [70] M. H. Neshati and Z. Wu, "Rectangular dielectric resonator antennas : theoretical modeling and experiments," in *Proc. IEEE 11th Int. Conf. Antennas Propagation (ICAP 2001), Manchester*, pp. 866-870, 17-20 April 2001.
- [71] D. Yau and N .V. Shuley, "Numerical analysis of an aperture coupled rectangular dielectric resonator antenna using a surface formulation and the method of moments," *IEEE Proc. Microwaves, Antennas and Propagation*, vol. 146, no. 2, pp. 105-110, April 1999.
- [72] R. K. Mongia and A. Ittipiboon, "Theoretical and experimental investigations on rectangular dielectric resonator antennas," *IEEE Trans. Antennas and Propagation*, vol. 45, no. 9, pp. 1348-1356, September 1997.
- [73] R. K. Mongia, "Theoretical and experimental resonant frequencies of rectangular dielectric resonators," in *Proc. IEEE*, vol. 139, no. 1, pp. 98-104, February 1992.

- [74] K. P. Esselle, "A low-profile rectangular dielectric-resonator antenna," *IEEE Trans. Antennas and Propagation*, vol. 44, no. 9, pp. 1296-1297, September 1996.
- [75] P. Rezaei, M. Hakkak, and K. Forooghi, "Design of wide-band dielectric resonator antenna with a two-segment structure," *Progress in Electromagnetics Research*, vol. 66, pp. 111-124, 2006.
- [76] R. Q. Lee and R. N. Simon, "Bandwidth enhancement of dielectric resonator antennas," in *Proc. IEEE Int. Symp. Antennas and Propagation Soc. (AP-S)*, Ann Arbor, MI, USA, vol. 3, pp. 1500-1503, 28 June-2 July 1993.
- [77] K. P. Esselle, "A dielectric-resonator-on-patch (DROP) antenna for broadband wireless applications: concept and results," in *Proc. IEEE Int. Symp. Antennas and Propagation Society (AP-S)*, Boston, MA, vol. 2, pp. 22-25, July 2001.
- [78] K. P. Esselle and T. Bird, "A hybrid-resonator antenna: experimental results," *IEEE Trans. Antennas and Propagation*, vol. 53, no. 2, pp. 870-871, February 2005.
- [79] Z. Aijaz and S. C. Shrivastava, "Effect of the different shapes: aperture coupled microstrip slot antenna," *Int. J. Electron. Engineering*, vol. 2, no. 1, pp. 103-105, 2010.
- [80] D. M. Pozar, "A reciprocity method of analysis for printed slot and slot coupled microstrip antenna," *IEEE Trans. Antennas and Propagation*, vol. 34, no. 12, pp. 1439-1446, December 1986.
- [81] J. F. Zurcher, "The SSFIP: a global concept for high performance broadband planar antennas," *Electronics Letters*, vol. 24, no. 23, pp. 1433-1435, November 1988.
- [82] S. D. Targonski and D. M. Pozar, "Design of wideband circularly polarized aperture coupled microstrip antennas," *IEEE Trans. Antennas and Propagation*, vol. 41, no. 2, pp. 214-220, February 1993.

- [83] F. Croq and A. Papiernik, "Large bandwidth aperture coupled microstrip antenna," *Electronics Letters*, vol. 26, no. 16, pp. 1293-1294, August 1990.
- [84] F. Croq and A. Papiernik, "Stacked slot-coupled printed antenna," *IEEE Microwave and Guided Wave Letters*, vol. 1, no. 10, pp. 288-290, October 1991.
- [85] F. Croq and D. M. Pozar, "Millimeter wave design of wide-band aperture coupled stacked microstrip antennas," *IEEE Trans. Antennas and Propagation*, vol. 39, no. 12, pp. 1770-1776, December 1991.
- [86] S. D. Targonski and R. B. Waterhouse, "An aperture coupled stacked patch antenna with 50% bandwidth," in *Proc. Antennas and Propagation Society International Symp. (AP-S. Digest-1996), Baltimore, USA*, vol. 1, pp.18-21, 21-26 July 1996.
- [87] M. H. Neshati and Z. Wu, "Microstrip-slot coupled rectangular dielectric resonator antenna: theoretical modelling and experiments," in *Proc. 12<sup>th</sup> Int. IEEE Conf. Antennas and Propagation (ICAP 2003), Zahedan, Iran*, vol. 2, pp. 759-762, 31 March-3 April 2003.
- [88] K. P. Esselle, "Circularly polarized higher-order rectangular dielectric-resonator antenna," *Electronics Letters*, vol. 32, no. 3, pp. 150-151, February 1996.
- [89] B. Subudhi, P. K. Ray, S. R. Mohanty, and A. M. Panda, "A comparative study on different power system frequency estimation techniques," *Int. J. Automation and Control (Inderscience-09)*, vol. 3, No. 2/3, pp. 202 – 215, 2009.
- [90] S. Shrivastava, A. Rajesh, and P. K. Bora, "Sliding window Dixon's tests for malicious users' suppression in a cooperative spectrum sensing system," *IET Communications*, vol. 08, no. 7, pp. 1065-1071, May 2014.
- [91] A. Kumar, D. A. Mihovska, R. Prasad, "Spectrum sensing in relation to distributed antenna system for coverage predictions," *Wireless Personal Communications*, vol. 76, no. 3, pp. 549-568, June 2014.

- [92] S. Sharma, S. Attri, and R. C. Chauhan, "Low-power VLSI synthesis of DSP systems," *Integration, The VLSI Journal, Elsevier*, vol. 36. no. 1-2, pp. 41-54, September 2003.
- [93] A. A. Rahman, A. K. Verma, G. S. Kirov, and A. S. Omar, "Aperture coupled microstrip antenna with quasi-planner surface mounted horn," in *Proc. 33<sup>rd</sup> European Microwave Conf., Munich*, pp. 1377-1380, October 2003.
- [94] A. Abdel-Rahman and A. S. Omar, "Improving the radiation and matching characteristics of antenna-arrays for satellite communication with moving vehicles," in *Proc. IEEE Int. Symp. Antennas and Propagation Society, Magdeburg, Germany*, vol. 4, pp. 656-659, 2002.
- [95] A. A. Rahman, A. K. Verma, and A. S. Omar, "High-gain wideband compact microstrip antenna with quasi-planner surface mount horn," in *Proc. IEEE Int. Symp. Microwave Digest (IEEE MTT-S)*, pp. 571-574, June 2003.
- [96] A. A. Rahman, A. K. Verma, and A. S. Omar, "Gain enhancement of microstrip antenna-array using surface mounted horn," in *Proc. 34<sup>th</sup> European Microwave Conf., Amsterdam*, vol. 3, pp.1345-1348, October 2004.
- [97] Y. Ranga, A. K. Verma, K. P. Esselle, and A. R. Weily, "Gain enhancement of UWB slot with the use of surface mounted short horn," in *Proc. IEEE Int. Symp. Antennas and Propagation Society (APSURSI), Toronto*, pp.1-4, 11-17 July 2010.
- [98] W. T. Sethi, H. Vettikalladi, and M. A. Alkanhal , "Millimeter wave antenna with mounted horn integrated on FR4 for 60GHz Gbps communication systems," *Int. J. Antennas and Propagation, Hindawi Publishing Corporation*, vol. 2013, Article ID 834314, pp. 1-5, October 2013.

- [99] Nasimuddin and K. P. Esselle, "High-gain aperture coupled dielectric resonator antenna with surface mounted horn," in *Proc. 9th Australian Symp. on Antennas*, Sydney, Australia, pp 1-5, February 2005.
- [100] Nasimuddin and K. P. Esselle, "A low-profile compact microwave antenna with high-gain and wide bandwidth," *IEEE Trans. Antennas and Propagation*, vol. 55, no. 6, pp. 1880-1883, January 2007.
- [101] Nasimuddin, K. P. Esselle, A. R. Weily, and A. K. Verma, "A low profile microwave antenna with high-gain," in *Proc. 18th Int. Conf. Applied Electromagnetics and Communications (ICECom 2005)*, Dubrovnik, Croatia, vol. 12, pp. 1-3, October. 2005.
- [102] Nasimuddin and K. P. Esselle, "Antennas with dielectric resonators and surface mounted short horns for high-gain and large bandwidth," *IET Microwaves, Antennas and Propagation*, vol. 1, no. 3, pp. 723-728, June 2007.
- [103] A. Kumar, J. Mohan, and H. Gupta, "Surface wave suppression of microstrip antenna using different EBG designs," in *Proc. Int. Conf. Signal Processing and Communication (ICSC-2015) Noida*, pp. 355-359, 16-18 March 2015.
- [104] G. P. Gauthier, A. Courty, and G. H. Rebeiz, "Microstrip antennas on synthesized low dielectric-constant substrate," *IEEE Trans. Microwave Theory and Techniques*, vol. 45, no. 8, pp. 1310-1314, August 1997.
- [105] J. S. Colburn and Y. R. Sammii, "Patch antennas on externally perforated high dielectric constant substrate," *IEEE Trans. Microwave Theory and Techniques*, vol. 47, no. 12, pp. 1785-1794, December 1999.
- [106] D. M. Kokotoff, R. B. Waterhouse, C. R. Britcher, and J. T. Aberle, "Annular ring coupled circular patch with enhanced performance," *Electronics Letters*, vol. 33, no. 24, pp. 2000-2001, November 1997.

- [107] R. G. Rojas and K. W. Lee, "Surface wave control using nonperiodic parasitic strips in printed antennas," in *Proc. IEEE Microwaves, Antennas and Propagation*, vol. 148, no. 1, pp. 25-28, February 2001.
- [108] A. K. Bhattacharayya, "Characteristics of space and surface-waves in a multilayered structure," *IEEE Trans. Antennas and Propagation*, vol. 38, no. 8, pp. 1231-1238, August 1990.
- [109] D. R. Jakson, J. T. Williams, A. K. Bhattacharayya, R. L. Smith, J. Buchleit, and S. A. Long, "Microstrip patch designs that do not excite surface waves," *IEEE Trans. Antennas and Propagation*, vol. 41, no. 8, pp. 1026-1037, August 1993.
- [110] M. Khayat, J. T. Williams, D. R. Jakson, and S. A. Long, "Mutual coupling between reduced surface-wave microstrip antennas," *IEEE Trans. Antennas and Propagation*, vol. 48, no. 10, pp. 1581-1593, October 2000.
- [111] J. Joannopoulos, S. G. Johnson, J. N. Winn, and R. D. Meade, *Photonic Crystals: Molding the Flow of Light*, NJ: Princeton, Princeton University Press, November 2007.
- [112] R. Gonzalo, P. D. Maagt, and M. Sorolla, "Enhanced path-antenna performance by supresing surface waves using photonic-bandgap substrates," *IEEE Trans. Microwave Theory and Techniques*, vol. 47, no. 11, pp. 2131-2138, November 1999.
- [113] D. Sievenpiper, L. Zhang, R. F. J. Broas, N. G. Alexopoulos, and E. Yablonovitch, "High-impedance electromagnetic surfaces with a forbidden frequency band," *IEEE Trans. Microwave Theory and Techniques*, vol. 47, no. 11, pp. 2059-2074, November 1999.

- [114] Y. J. Park, A. Herchlein, and W. Wiesbeck, "A Photonic bandgap (PBG) structure for guiding and suppressing surface waves in millimeter-wave antennas," *IEEE Trans. Antennas and Propagation*, vol. 49, no. 10, pp. 1854-1857, October 2001.
- [115] K. Agi, M. Mojahedi, B. Minhas, E. Schamilogu, and K. J. Malloy, "The effects of an electromagnetic crystal substrate on a microstrip patch antenna," *IEEE Trans. Antennas and Propagation*, vol. 50, no.4, pp. 451-456, April 2002.
- [116] F. Yang and Y. R. Samii, "Microstrip antennas integrated with electromagnetic bandgap (EBG) structures: A low mutual coupling design for array applications," *IEEE Trans. Antennas and Propagation*, vol. 51, no. 10, pp. 2936-2946, October 2003.
- [117] N. Llombart, A. Neto, G. Gerini, and P. D. Maagt, "Planar circularly symmetric EBG structures for reducing surface waves in printed antennas," *IEEE Trans. Antennas and Propagation*, vol. 53, no. 10, pp. 3210-3218, October 2005.
- [118] A. Neto, N. Llombart, G. Gerini, and P. D. Maagt, "On the optimal radiation bandwidth of printed slot antennas surrounded by EBGs," *IEEE Trans. Antennas and Propagation*, vol. 54, no. 4, pp. 1074-1083, April 2006.
- [119] H. Boutayeb and T. A. Denidni, "Gain enhancement of a microstrip patch antenna using a cylindrical electromagnetic crystal substrate," *IEEE Trans. Antennas and Propagation*, vol. 55, no. 11, pp. 3140-3145, November 2007.
- [120] J. R. Sohn, T. H. Sik, J. G. Lee, and J. Hae, "Comparative analysis of four types of high-impedance surfaces for low profile antenna applications," in *Proc. IEEE Int. Symp. Antennas and Propagation Society, Taegu (South Korea)*, vol. 1A, pp. 758-761, 3-8 July 2005.

- [121] C. Jinwoo, V. Govind, and M. Swaminathan, "A novel electromagnetic bandgap (EBG) structure for mixed-signal system applications," in *Proc. IEEE Radio and Wireless Conference, Atlanta(GA)*, pp. 243-246, 19-22 September 2004.
- [122] A. Kumar and D. Kumar, "High performance metamaterial patch antenna," *Microwave and Optical Technology Letters, John Wiley & sons*, vol. 55, no. 2, pp. 409-413, February 2013.
- [123] A. Kumar and D. Kumar, "Novel polarization independent metamaterial and its application to patch antenna," *Microwave and Optical Technology Letters, John Wiley & Sons*, vol. 55, no. 8, pp. 1963-1969, August 2013.
- [124] A. Kumar and D. Kumar, "Performance enhancement of patch antenna using metamaterial as a cover," in *Proc. IEEE Students' Conf. Electrical, Electronics and Computer Science (SCEECS-2014) Bhopal, India*, pp.1-4, 1-2 March 2014.
- [125] M. N. Jazi, E. Erfani, T. A. Denidni, "On the antenna gain enhancement using artificial materials," in *Proc. IEEE Int. Symp. Antennas and Propagation Society (APSURSI-2013), Orlando*, pp. 93-94, 7-13 July 2013.
- [126] N. Jaglan and S.D. Gupta, "Surface waves minimization in microstrip patch antenna using EBG substrate," in *Proc. IEEE int. conf. Signal Processing and Communication (ICSC-2015) Noida, India*, pp.116-121, 16-18 March 2015.
- [127] M. J. A. Hasan, T. A. Denidni, and A. R. Sebak, "A new UC-EBG based-dielectric resonator antenna for millimeter-wave applications," in *proc. IEEE Int. Symp. Antennas and Propagation (APSURSI- 2011), Spokane, WA*, pp.1274-1276., 3-8 July 2011.
- [128] T. A. Denidni, Y. Coulibaly, and H. Boutayeb, "Hybrid dielectric resonator with circular mushroom-like structure for gain improvement," *IEEE Trans. Antennas and Propagation*, vol. 57, no. 4, pp. 1043-1049, April 2009.

- [129] E. A. J. Marcatili, "Dielectric rectangular waveguide and directional couplers for integrated optics," *Bell Labs Technical Journal*, vol. 48, no. 7, pp. 2071-2102, September 1969.
- [130] J. V. Bladel, "on the resonances of a dielectric resonator of very high permittivity," *IEEE Trans. Microwave Theory and Techniques*, vol. 23, pp. 199-208, February 1975.
- [131] A. Karp, H. J. Shaw, and D. K. Winslow, "Circuit properties of microwave dielectric resonator," *IEEE Trans. Microwave Theory Tech.*, vol. 16, pp. 810-828, October 1968.
- [132] K. M. Luk, K. W. Leung, and K. Y. Chow, "Bandwidth and gain enhancement of a dielectric resonator antenna with the use of a stacking element," *Microw. Opt. Technol. Lett.*, vol. 14, no. 4, pp. 215-217, March 1997.
- [133] C. S. Anand and J. S. Sahambi, "MRI denoising using bilateral filter in redundant wavelet domain," in *Proc. IEEE region 10 conf. (TENCON 2008)*, pp. 1-6, November 2008.
- [134] A. N. Gaikwad, D. Singh, and M. J. Nigam, "Application of clutter reduction techniques for detection of metallic and low dielectric target behind the brick wall by sf-cw radar in uwb range," *IET Radar, SONAR and Navigation*, vol. 5, no. 4, pp. 416-425, 2011.
- [135] S. Agarwal, A. Sureka, and V. Goyal, "Open source social media analytics for intelligence and security informatics applications," *Big Data Analytics, Springer International Publishing*, pp. 21-37, December 15.
- [136] M. Rai and R. Tripathi "Performance analysis of a multi access cellular communication network using base site transmitter power control approach," in

- Proc. 7<sup>th</sup> IEEE Int. Conf. Personal Wireless Communications (ICPWC-2005)*, New Delhi, India, pp. 23-25, January 2005.
- [137] B. Sahu, M. Aggarwal, P. Tripathi, and R. Singh, "Stacked cylindrical dielectric resonator antenna with metamaterial as a superstrate for enhancing the bandwidth and gain," in *Proc. IEEE Conf. on Topical Conference on Signal Processing, Computing and Control (ISPCC)*, pp. 1-4, 2013.
- [138] Y. Coulibaly, M. Nedil, Larbi Talbi and T. A. Denidni, "High gain cylindrical dielectric resonator with superstrate for broadband millimeter-wave underground mining communications," *14th Int. Symp. on Antenna Technology and Applied Electromagnetics and the American Electromagnetics Conference [ANTEM-AMEREM]*, pp. 1-4, 2010.
- [139] A. Perron, T. A. Denidni, and A. R. Sebak, "High gain hybrid dielectric resonator antenna for millimeter-wave applications: design and implementation," *IEEE Trans. Antennas and Propagation*, vol. 57, no. 10, pp. 2882-2892, October 2009.
- [140] Y. M. Pan, K. W. Leung, and K. M. Look, "Design of the millimeter-wave rectangular dielectric resonator antenna using a higher order mode", *IEEE Trans. Antennas and Propagation*, vol. 59, no. 8, pp. 2780-2788, August 2011.
- [141] A. Zandieh, S. Jafarlou, B. Biglarbegan, and S. Safavi-Naeini, "CPW-fed chip-scale dielectric resonator antenna for millimeter wave applications", *IEEE Int. Symp. on Antennas and Propagation (APSURSI)*, pp. 1696-1699, 2011.
- [142] C. Gopakumar, "Development and analysis of a novel isosceles trapezoidal dielectric resonator antenna for wireless communication," Ph.D. Dissertation, Cochin University of Science and Technology, Cochin, India, January 2011.

- [143] M. J. Licea, S. V. Beltran, and J. L. Bonilla, "Experimental performance analysis for 2G/3G cellular networks based on mobile terminals," *J. Institution Eng.*, vol. 8, no. 1-2, pp. 25-38, July 2011.
- [144] E. M. Ashmila, S. S. Dlay, and O. R. Hinton, "Adder methodology and design using probabilistic multiple carry estimates," *IEEE Proc. Computer, Digit. Tech.*, vol. 152, no. 6, pp. 697-703, November 2005.
- [145] V. M. DaSilva and E. S. Sousa, "Fading-resistant modulation using several transmitter antennas," *IEEE Trans. Commun.*, vol. 45, no. 10, pp. 1236-1244, October 1997.
- [146] G. F. Gerard, R.J. Potter, M.D. Smith, K. Rosenthal, G. Dhariwal, J. Lee, and D. Chatterjee, "The role of template-primer in protection of reverse transcriptase from thermal inactivation," *Nucleic Research*, vol. 30, no. 14, pp. 3118-3129, Jul. 2002.
- [147] S. Suseela, M. Urdaneta, and P. Wahid, "Use of magnetic nanoparticles in microwave ablation," in *Proc. IEEE Int. Conf. 16th Annual Wireless and Microwave Technology, WAMICON*, Article number 7120415, June 2015.
- [148] U. Nanda, D. P. Acharya, and S. K. Patra, "Design of a low noise PLL for GSM application," in *Proc. Int. Conf. Circuits, Controls and Communications (CCUBE-2013), Bengaluru, India*, pp. 1-4, 27-28 December 2013.
- [149] Nasimuddin, and K. P. Esselle, "Gain enhancement of a dielectric resonator antenna with use of surface mounted short horn," *Microwave and Optical Technology Letters*, vol. 49, no. 5, pp. 1162-1166, May 2007.
- [150] H. Boutayeb, T. A. Denidni, K. Mahdjoubi, A. C. Tarot, A. R. Sebak, and L. Talbi, "Analysis and design of a cylindrical EBG-based directive antenna," *IEEE Trans. Antennas and Propagation*, vol. 54, no. 1, pp. 211-219, January 2006.

- [151] Y. Coulibaly, M. Nedit, T. Denidni, and L. Talbi, "Design of a single circular soft surface applied to an aperture fed dielectric resonator antenna for gain and bandwidth improvement," in *Proc. IEEE Int. Symp. Antennas and Propagation (APSURSI-2011) Spokane, WA*, pp. 1692-1695, 3-8 July 2011.
- [152] Y. Coulibaly, H. Boutayeb, T. A. Denidni, and L. Talbi, "Gain enhancement of a dielectric resonator antenna using a cylindrical electromagnetic crystal substrate," in *Proc. IEEE Int. Symp. Antennas and Propagation Society (2007 IEEE)*, pp. 1325-1328, 2007.